Author:
Liu, Guang Ning

Title:
Vulnerability and integrity of nonlinear dynamic structures

Vulnerability and Integrity of Nonlinear Dynamic Structures

Guang Ning Liu

A Thesis Submitted in Partial Fulfillment

of the Requirements for the Degree of

Doctor of Philosophy

in

Civil Engineering

March 2008

Abstract

The response of a nonlinear dynamic structure can be sensitive to its initial conditions or parameters. In order to ensure its safety and robustness, an understanding of the global structural responses is necessary. This requires performing a parameter study. However, this is extremely difficult due to the complexity arising from nonlinearities and the associated computational costs. Hence, it is highly desirable to have new methods to tackle these difficulties.

The aims of this research are to develop an efficient method to assess vulnerability of a nonlinear dynamic structure, and to formulate approaches to obtain reduced models that qualitatively capture the important dynamics of a nonlinear structure, making them suitable for parameter studies. For this purpose, a statistical feature space formed by applying Proper Orthogonal Decomposition (POD) analysis to response time histories of nonlinear dynamic structures, is used.

Firstly, a new method to assess the vulnerability of nonlinear dynamic structures is proposed. A POD feature space is sensitive to changes in the form of a structure and the excitation. The resulting weighted change in the space basis due to damage, is proposed as a quantitative measure of the consequence of the damage. The application of the method to a truss shows that it is able to identify critical failure scenarios.

Secondly, two novel approaches for constructing reduced models of a nonlinear dynamic structure in a POD space, are proposed. The first one uses load-deflection pairs obtained from nonlinear static finite element analyses. The second one employs response time-histories obtained from nonlinear dynamic finite element analyses. Model reductions are performed by transforming these responses into the POD space. The latter method can handle more types of nonlinearities than the former but requires more computation. A particular benefit of these two methods is any commercial FEM package or experimental

data can be utilised directly. Once the reduced models are fully specified, a parameter study for the global behaviour can be conveniently carried out.

The proposed methods are tested on nonlinear elastic structures, including a fully clamped beam, a portal frame and a cantilever with one side stop. The resulting reduced models qualitatively capture the dynamics of these nonlinear structures. A study of global behaviour shows the sensitivity of the system to parameter changes.

Acknowledgments

First and foremost, my heartfelt thanks to my supervisor, Dr. Jitendra Agarwal for his constant guidance and encouragement throughout the course of my research.

I would like to thank many friends of mine: Dr. X. Xie, Dr. J. Zhang, Dr. X. Liu, Dr. Y. Ying, Dr. Z. Qin, Dr. Y. Chen, Dr. W. Jiang, at Engineering Faulty for their inspired discussions and suggestions. I also would also like to express my gratitude to Mr. O. Oddbjornsson for his help regarding the use of Dynamics Solver and his program of conducting parameter studies, and Dr. N. Alexander for his valuable advice on least-squares analysis. Special thanks are due to Mr. Chris Hawkins for his computer support during this work.

My most sincere thanks to my parents, my wife, Dan, and my son, Danwei, for their unflagging support both financially and mentally, without which this work would not have been possible.

Finally, the financial support of the Engineering Physical Science Research Council, UK (EPSRC), and Overseas Research Students Awards, UK (ORS) is gratefully acknowledged.

Declaration

The author declares that, except for commonly understood and accepted ideas, or where specific reference is made to the work of other authors, the contents of this thesis are his own work and include nothing that is the outcome of work done in collaboration. This thesis has not been previously submitted, in part or in whole, to any University or Institution for any degree, diploma or other qualification.

SIGNED:

Contents

List of Figures

List of Tables

Chapter 1

Introduction

1.1 Motivations

Structures are designed to ensure that the demands placed upon them do not exceed their capacity, with appropriate allowances reserved for uncertainties and associated risks. Design procedures for static loads within linear elastic material behaviour are well established, although they sometimes may not lead to a robust solution. At the extremities of dynamic loading, the response of a structure becomes nonlinear and complex. For example, small changes in its initial conditions or parameters might lead to large changes in the response. These highly nonlinear behaviours cannot be explained by linear theory [1], as the principle of linear superposition is not generally applicable to nonlinear structures. Thus, a global analysis of dynamic behaviours of the nonlinear structures is necessary to ensure their safety and robustness.

The advancements in nonlinear dynamic system theory provide many valuable concepts and techniques to investigate global behaviour of highly nonlinear structures. However, most of the work in nonlinear dynamics is based upon simplified models, often low-dimensional models. Nevertheless, how to apply these concepts and techniques, in particular parameter study, to examine nonlinear structures with complex geometry, is an important and challenging problem as the real structures are high-dimensional. There are two important factors to be addressed with respect to a parameter study. Firstly, such study involves all types of uncertainties, such as modelling uncertainties and computational errors that cannot be eliminated by the most accurate analysis [2]. Secondly, the sensitivity of nonlinear systems amplifies the influence of these uncertainties and degrades the quality of any predictive models. Therefore, the main objective of a parameter study is to understand the global behaviour of the nonlinear structures, rather than fulfil a code-specified safety threshold.

Finite element method (FEM) is a well-established numerical method for dynamic analysis of nonlinear structures and is capable of determining the dynamic response of nonlinear structures with complex geometry. FEM relies on localised interpolation basis functions (shape functions) to approximate the solution to a nonlinear system. This characteristic offers FEM the power to approximate various nonlinear problems and model very complex structures. However, it has a disadvantage in that it often requires a very large number of degrees-of-freedom (DOF) to accurately model the structure [3] and it produces a large number of equations that must be solved simultaneously for each time step. Thus, the computational demand is extremely high, even for a simple nonlinear structure. It is difficult to obtain global dynamics of a nonlinear dynamic structure directly using FEM. Hence, new practical approaches are needed for modelling and studying global behaviour nonlinear dynamic structures.

Model reduction techniques can be used to decrease the computational costs of the qualitative analyses of highly nonlinear structures [4]. It is based on the assumption that if the dynamic information of a system is available either from experimental or simulation data, then some mathematical patterns can be extracted from this data and a reduced model can be reconstructed to approximate the dynamics of the system. This idea can drastically decrease the computational cost, without significantly compromising the quality of the computational results [5]. However, unlike linear systems, no complete theory of model reduction for nonlinear systems exists and most of the steps for model reduction are still a subject of research for nonlinear models.

1.2 Model reduction

One of the model reduction techniques utilises the idea of space transformation. The number of states required to approximate the important dynamics of a system is a function of the response, not of the discretisation of the full order system [6]. Hence, it is possible to identify a feature space in which the dynamics of the system can be represented using a low-dimensional model, with a minimal loss in overall accuracy over the parameter range of interest. This reconstructed model can be used to fully explore the global behaviour of the nonlinear dynamic structure. Thus, the term 'model reduction' is used to describe the reduction of a complex physical model to mathematical models requiring less computation.

The new model can be either in a physical coordinate space or a generalised coordinate space. A reduced model is expressed by the equation of motion in terms of the space coordinates. Typical model reduction methods such as static condensation [53], dynamic condensation [7] and hybrid methods, such as Component Mode Synthesis (CMS) [8], employ physical coordinate spaces. One of the difficulties of these model reduction approaches is the need to modify the original FEM code, which is impractical in reality and prevents the use of powerful commercial FEM packages. The methods based upon modal basis [9], and Ritz basis [10], in generalised coordinate spaces have been extensively used. However, these methods still require the knowledge of mass and stiffness matrices, even though they are more efficient. This limits their application to complex nonlinear structures.

A model reduction method, based upon feature extraction techniques, may be more efficient. The feature extraction techniques can identify the dominant patterns that are hidden in the response data. The dominant patterns characterise global dynamics of the nonlinear dynamic structure. This extracted feature can be used to form a generalised coordinate space in which a more efficient model reduction can be performed as statistical features rather than physical features are considered. Proper Orthogonal Decomposition (POD) is a feature extraction technique. This technique describes the spatial distribution of physical variables in terms of a set of proper orthogonal modes (POMs). The time-dependent characteristics of the physical variables are given by the time varying coefficients of POMs.

In this thesis, to overcome the difficulty of studying global behaviour of nonlinear dynamic structures with large DOF, two methods are proposed. The proposed methods combine the efficiency of a statistical feature space and the power of commercial FEM packages.

1.3 Objectives

The overall aim of the research presented in this thesis is to develop new methods to investigate the vulnerability and integrity of nonlinear dynamic structures. These methods rely on POD to determine a statistical feature space that efficiently represents the dynamics of the system obtained from numerical simulations. The primary objectives are as follows:

- To analyse the implications of nonlinear dynamic system theory for safe design of structures and to review the modelling of nonlinear structures, the purpose of which is to search for practical ways to study the robustness of nonlinear dynamic structures;
- To review the existing model reduction methods for nonlinear structures aimed at identifying an efficient solution to study vulnerability and integrity of nonlinear dynamic structures;
- To propose new methods to investigate vulnerability of nonlinear dynamic structures by studying the changes of POMs after member failures;
- To introduce a new strategy for investigating integrity of nonlinear dynamic structures by using POD-based reduced models to perform a parameter study, which provides new techniques for engineers to understand the global behaviour of nonlinear elastic structures;
- To propose a method of constructing reduced models in a POD feature space for geometrically nonlinear structures by using nonlinear static FEM analysis and a parameter identification technique in combination;
- To propose a new method for extracting a reduced model in a POD feature space for nonlinear elastic structures by using Harmonic Balance Method and a parameter identification technique in combination;
- To demonstrate the proposed methods with a set of examples throughout the thesis.

1.4 Outline

The thesis is organised as follows:

Chapter 2 begins with an introduction to the qualitative behaviour of nonlinear structural systems and key techniques for detecting qualitative dynamics. Then it moves to a discussion of safety of the nonlinear dynamic structures. Finally, various nonlinearities in structural dynamics and modelling of nonlinear structural dynamics are reviewed.

Chapter 3 gives an overview of the existing mode reduction techniques, including physical and generalised coordinate space based model approaches. The properties of generalised space based model reduction methods are discussed. The mathematical foundations for POD and its application in structural dynamics are reviewed. A scheme for the construction of a reduced model in a POD feature space, and the study of global dynamics using the reduced model is proposed.

Chapter 4 presents a new approach to analyse the dynamics and nonlinearities in structural vulnerability theory using POD analysis. Firstly, an introduction to structural vulnerability theory is given and it is demonstrated through an example. Then the procedure for vulnerability assessment using POMs is presented. A planar truss is used to examine the effectiveness of this approach.

Chapter 5 proposes a new method for extracting a reduced model of structural systems with geometric nonlinearity, based upon a full finite element model. The proposed approach identifies the stiffness terms of a reduced model in a POD feature space using nonlinear static finite element simulations and least squares techniques in combination. A clamped beam and a two dimensional portal frame are used to demonstrate this method.

Chapter 6 proposes a new method for extracting a reduced model of a nonlinear elastic structure with nonlinearities. It uses a set of numerical simulation data obtained from a commercial FEM package. The identification of the stiffness terms of a reduced model in a POD feature space using the Harmonic Balance Method (HBM) and a least-squares analysis in combination, is explained. A cantilever with one-side stop is used to demonstrate this method and a parameter study using the resulting reduced model is carried out.

Finally, in Chapter 7, conclusions and some issues for future research are given.

Chapter 2

Nonlinear Structural Dynamics

2.1 Objectives

- To review the basic concepts and techniques of nonlinear dynamic system theory
- To analyse its implications for safe design of structures
- To review modelling approaches for nonlinear structures

2.2 Introduction to nonlinear structural dynamics

A fundamental aspect of nonlinear dynamics is a nonlinear system's extreme sensitivity to initial conditions or system parameters. A small change in their initial conditions or parameters might lead to significant changes in their behaviour. Systems behaving in this manner are called chaotic. Besides, a complex system consisting of nonlinear components, may give rise to collective behaviour, which is not simply the sum of the individual components but results from their interaction. These two aspects, are the sources of un-predictability in nonlinear systems.

2.2.1 Qualitative behaviour of nonlinear structural systems

Sensitivity

A nonlinear deterministic structure with no random inputs may produce an apparently chaotic motion, which has a sensitive dependence on initial conditions [11]. When a

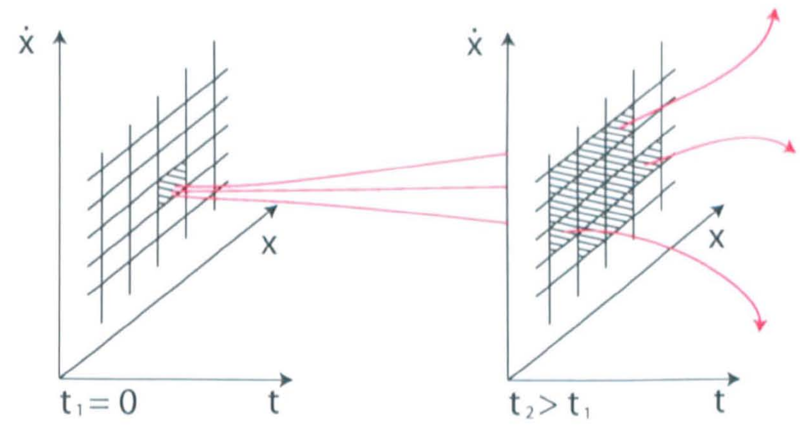

Figure 2.1: Condition sensitive nonlinear systems

nonlinear but non-chaotic deterministic system starts to evolve from two nearby initial conditions, its trajectories keep close to one another in its phase space, which is a plane composed of its displacement, $x(t)$ and its velocity, $\dot{x}(t)$. Thus, their future values can be predicted and the behaviour of the system is largely known given any initial conditions. However, if the system is chaotic, its trajectories evolve exponentially away from each other after a short time, as illustrated in Figure 2.1, and therefore its behaviour cannot be predicted. This characteristic of nonlinear dynamic systems is further explained in Figure 2.2 where trajectories of a nonlinear system, Duffing's oscillator, with two initial conditions are shown. This complexity of the behaviour is due to internal rather than external dynamics.

This natural feature of nonlinear dynamic structures makes it impossible to use typical superposition-based approaches in structural dynamics, for example natural frequencies and modal shapes, to explore their behaviour. In other words, the occurrence of new and unexpected phenomena associated with nonlinear systems, are not predicted, or even hinted at by the linear theory [12]. Some early surveys on nonlinear dynamic systems from the engineers point of view are provided by Moon [13]. Virgin [14] used experimental data gathered from mechanical models to explain the basic theory of nonlinear systems and chaos. Thompson and Stewart [11] provided a comprehensive introduction to this field.

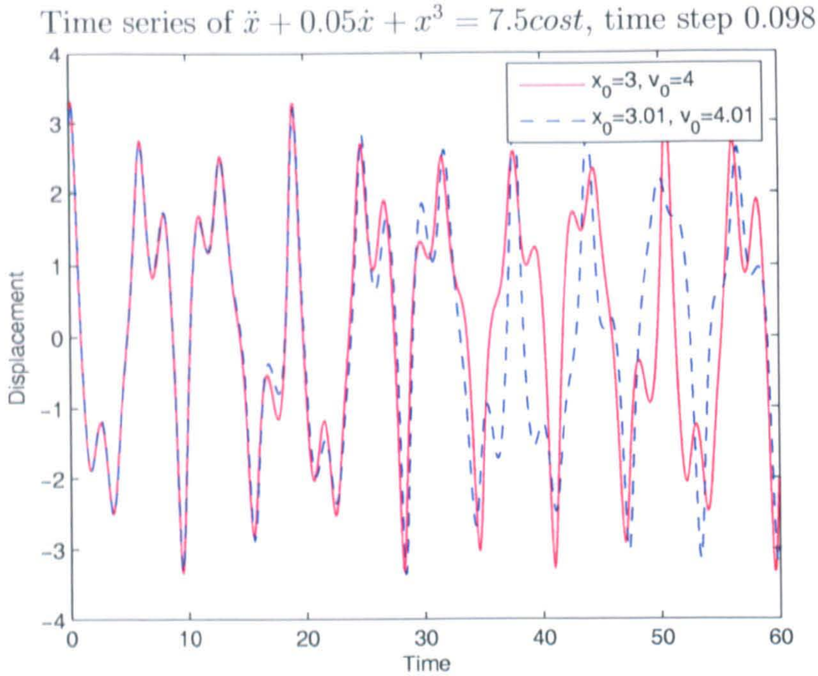

Figure 2.2: Sensitivity of Duffing's equation to initial conditions

Basins of attraction

For a nonlinear system, different initial conditions may lead to different attractors (including equilibrium, periodic motions and chaotic motions). Each attractor has a region to attract the trajectories to itself, which is called a basin of attraction. Basins of attraction are also functions of the system parameters. To understand structural behaviour of a nonlinear dynamic structure, one needs to investigate how these basins of attraction change with the system parameters. Motions of a Duffing's oscillator [11] are governed by

$$\ddot{x} + 0.05\dot{x} + x - x^2 = f sin(\omega t) \tag{2.1}$$

where x is the state variable, f is the amplitude of the external excitation, ω is the circular frequency and a dot denotes differentiation with respect to time t. By sweeping f from 0.01 to 0.3 and ω from from 0.1 to 1, an investigation of how the system evolves as the parameters change was conducted in a tool [15]. The result of this parameter study are shown in Figure 2.3. In this figure, different colours represent different numbers of loading cycles the system can survive before its displacement is beyond an allowable threshold

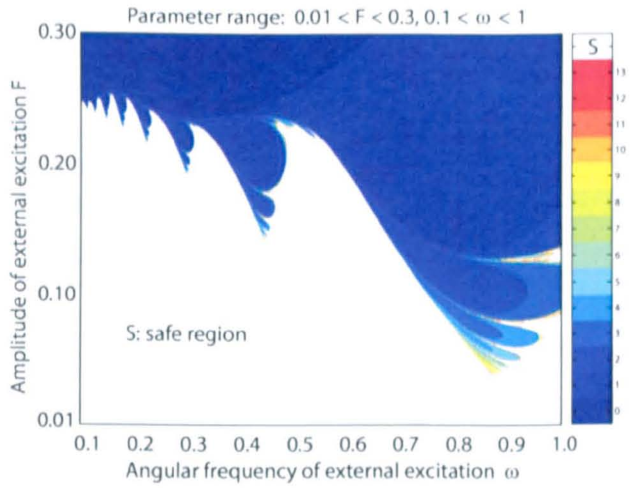

Figure 2.3: Integrity diagram produced by parameter study of system governed by Equation 2.1

and the safe region is determined. The safe region is assumed after 13 cycles. The information about basins of attraction is very useful to the safe design of structures because it provides a global picture of structural behaviour in parameter space. Even though the basin boundaries are fractal,a safe region can be identified considering proximate loading conditions.

2.2.2 Tools to characterise qualitative dynamics

Nonlinear dynamic theory provides many geometric ways to characterise dynamic behaviour by tracking motion of a dynamic system. Some main methods include time history, phase space, Poincaré section and Fourier frequency spectrum. They are illustrated through an oscillator with piecewise linear stiffness, studied by Wagg [16]. Its normalised motion of equation can be represented as follows

$$\ddot{y} + 2\zeta\dot{y} + g(y) = fcos(\omega t) \tag{2.2}$$

where y is the non-dimensional state variable, ζ is the non-dimensional damping, f is the non-dimensional amplitude of excitation, ω is the non-dimensional circular frequency, t is the non-dimensional time, a dot at present denotes differentiation with respect to non-dimensional time t and the stiffness $g(y)$ is defined by

$$g(y) = \begin{cases} -1 & \text{for } y < -1 \\ y & \text{for } -1 < y < 1 \\ 1 & \text{for } y > 1 \end{cases} \tag{2.3}$$

Parameter values, ζ and ω, in Equation 2.2, were taken as 0.05 and 1.0, respectively. All simulations of the oscillator were conducted in Dynamic Solver [17] using Dormand-Prince method, a member of the class of Runge-Kutta methods, to demonstrate three basic ways of detecting nonlinearities in structural dynamics: phase space, Poincaré section and Fourier frequency spectrum. These three tools can also be used to verify if two models are similar in terms of their dynamic behaviour. Other methods, such as Lyapunov Exponents and fractal dimensions in [14], and [11], are also used but these result in a value.

Phase space

The phase space, also called phase plane, is a geometric method of representing the relationship between two state variables such as displacement and velocity in structural dynamics. From the shape of the path and direction of motion of a structural node over time, some conclusions regarding the qualitative character of the nonlinear system can be drawn. Phase space is the simplest method for distinguishing a periodic motion from an aperiodic motion.

A remarkable feature of the phase space is its ability to represent a complex behaviour in a geometric and therefore comprehensible form. As shown in Figure 2.4, periodic motions reveal themselves as closed orbits in the phase space, whereas chaotic and quasi-periodic motions both fill up a part of its area. A closed orbit crossing itself, as the double loop in Figure 2.4.b, is an indicator of subharmonic motion. In other words, the fundamental frequency of the oscillation is lower than the frequency of external excitation. This motion is called a period-2 orbit, as it takes two oscillation to return to any point on the curve.

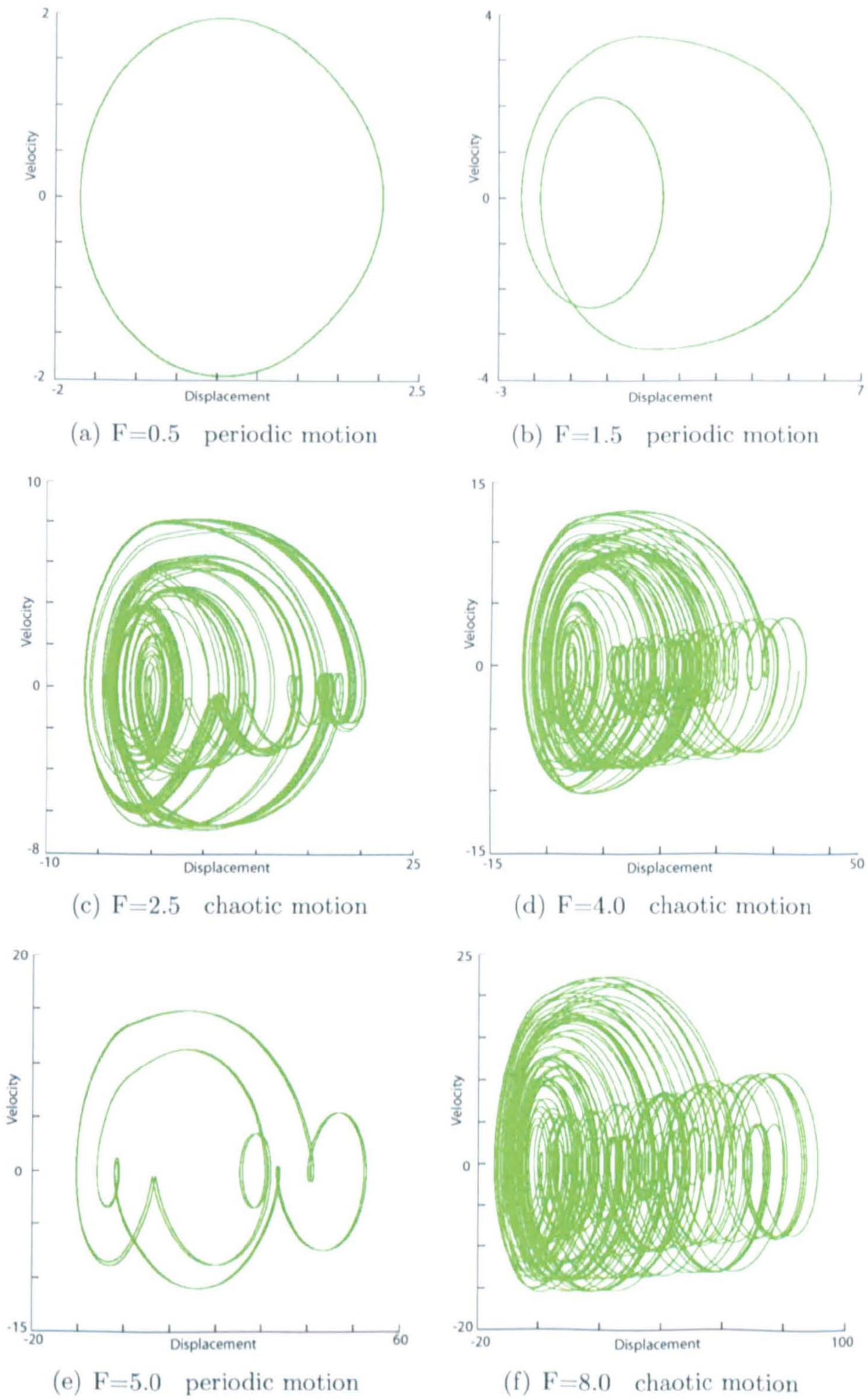

(a) F=0.5 periodic motion

(b) F=1.5 periodic motion

(c) F=2.5 chaotic motion

(d) F=4.0 chaotic motion

(e) F=5.0 periodic motion

(f) F=8.0 chaotic motion

Figure 2.4: Phase space of an oscillator (Equation 2.2) with piecewise stiffness. Force amplitude F: (a) 0.5, (b) 1.5, (c) 2.5, (d) 4.0, (e) 5.0, (f) 8.0

Poincaré section

A Poincaré section is a stroboscopic view of the phase space plot of velocity against displacement. It consists of a large number of discrete points, with reference to a specified set of systematic parameters, at a constant time interval, which is the period of external excitation in the case of forced periodic vibration.

Figure 2.5 shows Poincaré sections of the oscillator, given by Equation 2.2, for the different loading conditions. Periodic motions always show up as a finite number of points, depending on the period and sampling rate. In Figure 2.5a, there are two points, indicating period-one motion because the sampling rate used is half of the period of the external excitation. An infinite number of points filling up a closed curve stand for a quasi-periodic motion, and an infinite number of distributed points stand for a chaotic motion. A chaotic motion usually forms a geometric pattern in the Poincaré section, which makes it easier to distinguish chaotic motions from random motions, shown in Figure 2.5c,d,f.

Fourier frequency spectrum

Figure 2.6 shows the Fourier frequency spectrum in terms of log-amplitude for the oscillator with piecewise stiffness. A periodic motion always shows up as a discrete frequency spectrum (e.g. Figure 2.6a,b). A chaotic motion appears as a continuous broadband spectrum, shown in Figure 2.6c. However, a nonlinear structure consisting of many nonlinear components can also produce a continuous spectrum because there are many frequencies involved in the response.

2.3 Safety of nonlinear dynamic structures

The essence of a safe design is to ensure that the capacity of the structure exceeds the demands placed upon it, with appropriate allowances being made for uncertainties and associated risks. Design procedures for static loads within linear elastic material behaviour are well established though these may sometimes not lead to a robust design. At the extremes of dynamic loading, the response of a structure becomes nonlinear and complex. The complexity may be exemplified in the form of emergent behaviour and sensitivity to initial conditions or parameters as discussed in Section 2.2.1. The effects of phenomena

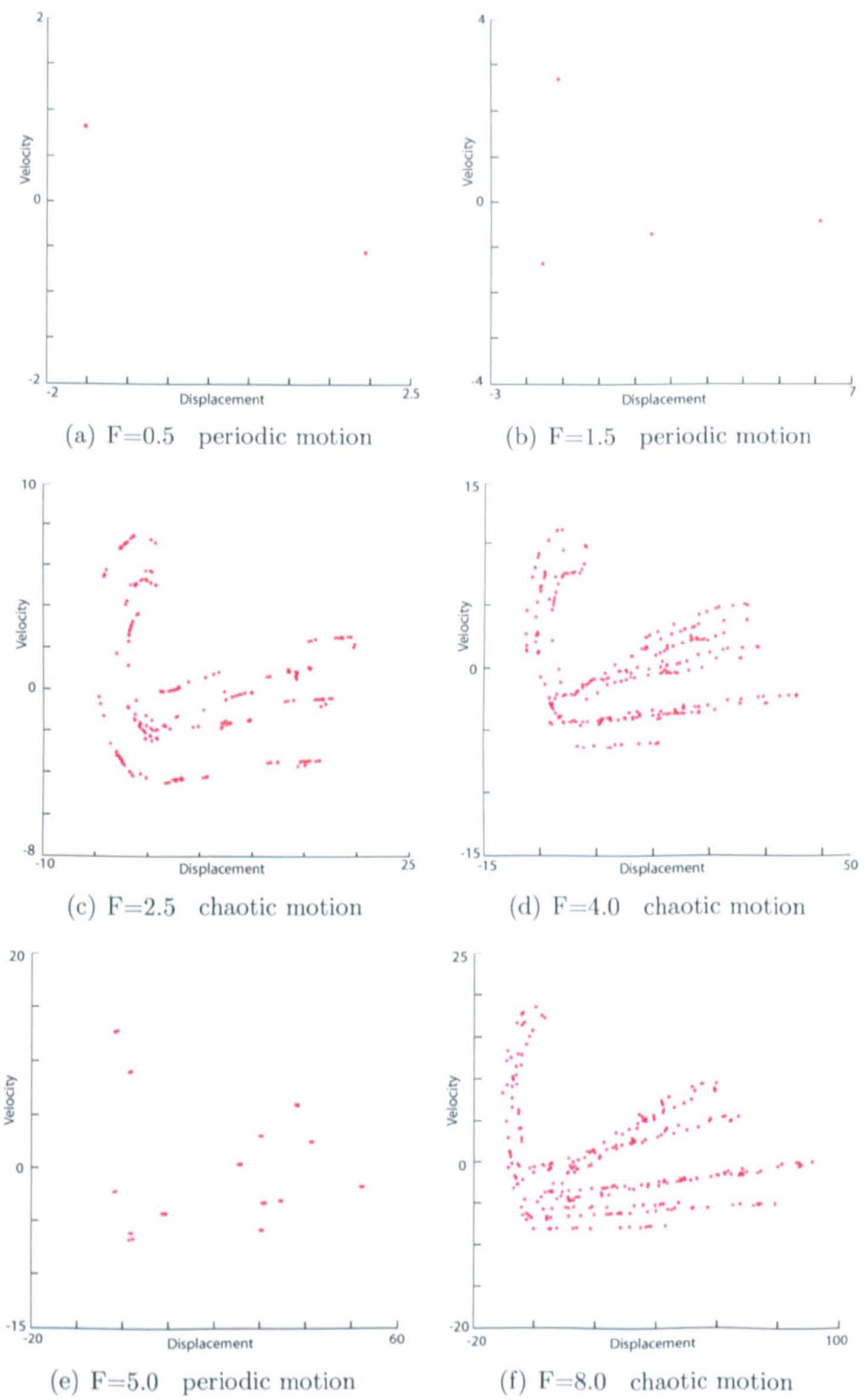

(a) F=0.5 periodic motion

(b) F=1.5 periodic motion

(c) F=2.5 chaotic motion

(d) F=4.0 chaotic motion

(e) F=5.0 periodic motion

(f) F=8.0 chaotic motion

Figure 2.5: Poincaré section of an oscillator (Equation 2.2) with piecewise stiffness. Force amplitude F: (a) 0.5, (b) 1.5, (c) 2.5, (d) 4.0, (e) 5.0, (f) 8.0

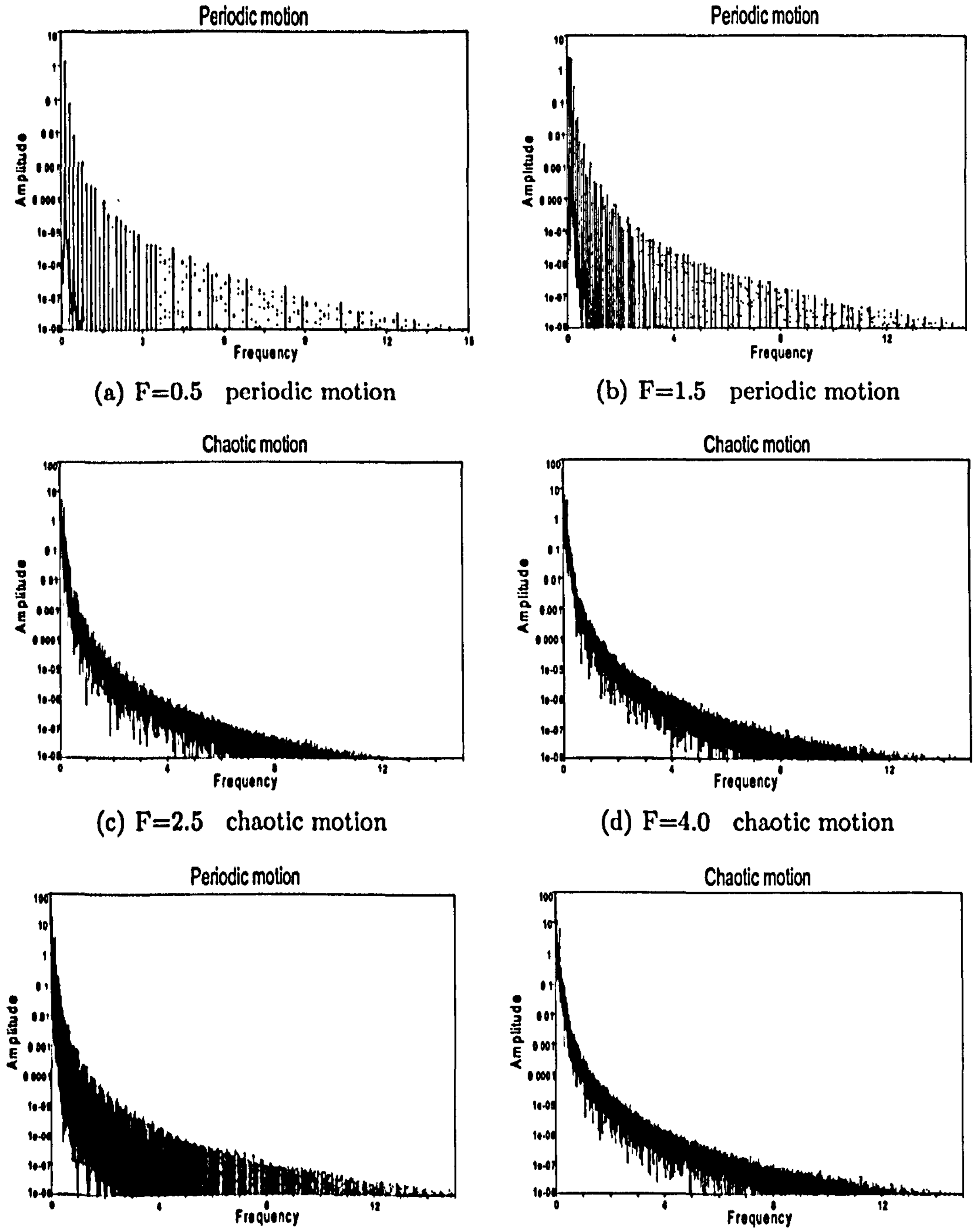

(a) F=0.5 periodic motion

(b) F=1.5 periodic motion

(c) F=2.5 chaotic motion

(d) F=4.0 chaotic motion

(e) F=5.0 periodic motion

(f) F=8.0 chaotic motion

Figure 2.6: Fourier frequency spectrum of an oscillator (Equation 2.2) with piecewise stiffness. Force amplitude F: (a) 0.5, (b) 1.5, (c) 2.5, (d) 4.0, (e) 5.0, (f) 8.0

such as bifurcations and chaos in the dynamic response are yet to find their way into the design process and until then some structures may remain vulnerable. Excessive vibrations of the Millennium Bridge, London [18] is an example of unintended consequences and vulnerability. From a design point of view, it is important to examine the global dynamics to enable an understanding of the vulnerability and integrity of nonlinear dynamic structures.

Most of the work in nonlinear dynamic structures is based on simplified models, often a single degree-of-freedom (DOF) model, such as that given by Equation 2.2. In a finite element model of a structure, described in Section 2.5.3, it is common to have a large number of degrees-of-freedom. Exploring the global dynamics of a large DOF system is not an easy task, computationally. New tools and techniques are needed for modelling the global response with the least effort and for analysing the implications of resulting behaviour for the robustness of the structure.

2.3.1 Safety of nonlinear structures

Structural design is followed by an analysis of the likely hazards which might threaten the success of a proposed structure. The hazards may be physical causing defined limit states to be exceeded, they may be random external events such as fires or floods, or they may be human errors. To deal with physical hazards, the loads are estimated, the response of the structure to these loads is obtained, and the safety of the structure is examined. Of these, structural response analysis has been studied extensively. Sophisticated methods such as the finite element technique have been developed [19]. Probabilistic methods account for the variation in loading and material properties. To deal with the time varying nature of loading, stochastic methods are being developed [20]. However, all these methods assume a unique response a-priori which can no longer be depended on for nonlinear systems. A nonlinear system can have more than one outcome for a given set of control parameters. Each outcome is associated with its basin of attraction i.e. the set of initial conditions leading to that particular outcome. In many nonlinear systems, the basin boundaries are found to be fractal under certain parameter ranges causing unpredictability in response. Generally, a system is designed to operate near to one stable dynamic equilibrium state. However, during its operation it may experience conditions which tend to change its equilibrium state. A design which is sensitive to these conditions, whether initial conditions or control parameters, can lead to a different state and possibly failure (for example, seismic pounding of adjacent buildings). Studies of building frames [21], showing counter-intuitive behaviour, further highlight the importance of complex global dynamics for structural performance under seismic loads.

2.3.2 Practical examples

During the last two decades, several studies have been made to identify and describe chaotic phenomena and investigate the fundamental nature of nonlinear systems (e.g. ([13, 11]). A few studies of practical structures such as an elasto-plastic beam [22], suspension cables [23], and shallow spherical shells [24], demonstrate the existence of chaotic motion, but the implications of such complex behaviours for the design of structures have not been sufficiently addressed. Among the few studies which consider safety Thompson et. al. [25] have analysed global integrity in engineering dynamics, Hogan [26] has considered a rocking rigid-block and Agarwal et al. [27] have done a preliminary study of spring-mass systems using a massively parallel Connection Machine. The implications of such studies for structures are immense, as many of them have some degree of nonlinearity, which are described in Section 2.4.

Most of the previous studies were carried out with a simplified model of the system where the system was analytically reduced to a single DOF system (SDOF) with a bilinear or cubic nonlinearity in the stiffness term. Amongst other studies, Lee et. al. [28] have reported richer dynamics with a two DOF model of an elasto-plastic beam as compared to SDOF used by Poddar et. al. [22]. Moorthy et. al. [29] have used a finite element model of a beam with nonlinear boundary conditions and compared the results against experimental findings of Moon and Shaw [30]. However, the question of complex models reproducing the same results as a highly simplified model has remained unaddressed. For a safe design, it needs to be examined whether an approach can be found to take advantage of the power of complex finite element models to produce similar dynamic response both qualitatively and quantitatively.

2.3.3 Hierarchical modelling and simulation

The mathematical theory of nonlinear systems is quite complex and closed form solutions are available only either for very simple systems or after making drastic simplifications. Laboratory experiments may represent the behaviour of a system more closely but the effort required to study dynamics would be quite substantial. In this thesis, computer simulations using reduced models will be carried out to obtain the time-histories of a structure for different sets of parameters. A structural system such as a beam or multi-storey building can be modelled at different levels of definitions, which are discussed in Section 2.5. Most physical systems have very intricate spatial and temporal evolution properties. To study the temporal evolution of a system, it may sometimes be sufficient to model the system as a single DOF system or at most a few DOF. However, to understand the spatial behaviour of a system, a high-dimensional model is required. Turbulence in fluids is a common example of the spatio-temporal dynamics, where the dynamics are governed by Partial Differential Equations (PDEs). Similar problems exist in the dynamics of structures. Spatial dimensions become more important in thin structures e.g. plates and shells. Coupled differential equations bridge the gap between a continuous space-time system and a discrete space-time system. These are used to model a system which is continuous in time and can be discretised in space. The space discretisation depends upon the nature of a problem. For example, a multi-storey building can be modelled as a one-dimensional chain of masses and springs with nearest neighbour coupling. A more complex example of space discretisation is that using a finite element technique.

A finite element model of a real structure may contain thousands of DOF, and model reduction techniques [31] can be used to reduce the computational effort. The philosophy of model reduction is to reduce the dimensionality of the system, by a co-ordinate transformation, while retaining its intrinsic properties. Proper Orthogonal decomposition, discussed subsequently in Chapter 3, provides an efficient way to reconstruct reduced order models from a time series data of a full system [32]. Because a chaotic system is sensitive to changes in parameters or initial conditions, it is quite possible to get different behaviours with the different models of the same structure. To investigate the vulnerability of response, it is necessary to simulate the response for a range of parameters and more importantly, to examine the dependability of the response as the model or the parameters are perturbed.

2.3.4 Vulnerability and dependability of response

A structure is vulnerable if damage from any action produces consequences that are disproportionately large in comparison with that damage [33]. A structure may be acceptable under one kind of demand (e.g. normal loading) but unacceptable under some other kind (e.g. accidental lateral loading). If a structure is vulnerable in any single way, it is not robust. The term vulnerability conveys a susceptibility to a disproportionately large consequence from a relatively small amount of damage or perturbation. However that susceptibility derives from a characteristic of the system within a given context. For dynamic systems, nonlinearities have the potential to make a system vulnerable.

A typical structure has many DOF and its dynamic behaviour is reflected in the time-histories corresponding to all the DOF. To study qualitative behaviour, it is necessary to vary parameters. A continuous variation in a parameter would help to locate the bifurcation points. In structural systems, the important parameters which may be varied are the forcing amplitude, forcing frequency and structural damping for a given nonlinearity. A control over initial conditions is also needed. For some sets of parameters a nonlinear system may exhibit more than one type of dynamic motion, depending on its initial state [27]. Thus, to obtain the global behaviour of a system and the dependable regimes, simulations need to be carried out for a range of initial conditions as well as the control parameters. While it is desirable that responses be explored for a large range of initial states, some of them may lie far away from the normal state of a system and may only occur infrequently. Hence, a rational choice of the space of initial condition is needed. It is of interest also, to examine the vulnerability of the structural response to different forms or levels of nonlinearity. For some structures, a periodic form of excitation gives the worst response. It helps to maintain the vibrations and understand the long term dynamics of a system with minimum complexity.

2.4 Nonlinearities in structural dynamics

In theory, nonlinearity exists in a system whenever there are products of dependent variables and their derivatives in the equations of motion, boundary conditions and/or constitutive laws. These may also arise due to discontinuities or jumps in the system. Ehrich and Abramson [12] summarised different nonlinearities encountered during vibrations. Among these, geometric and boundary nonlinearities are commonly observed. Nayfeh [34] explained various types of nonlinearities and corresponding structural modes in detail along with examples. A nonlinear system is said to be 'characterised' when the location, type and functional form of all the nonlinearities throughout the system are known [35]. Different nonlinearities in structural systems can be broadly classified into the following categories:

- *Damping* is essentially a nonlinear phenomenon. Linear viscous damping is an idealization. Coulomb friction, hysteretic damping, etc. are examples of nonlinear damping.

- *Geometric* nonlinearity exists in systems undergoing large deformations or deflections. This nonlinearity arises from the potential energy of the system. In structures, large deformations usually result in nonlinear strain-displacement and curvature-displacement relations. This type of nonlinearity is presented, for example, in the equation governing the large-angle motion of a simple pendulum, in the nonlinear strain-displacement relations due to mid-plane stretching in strings, and because of nonlinear curvature in cantilever beams.

- *Inertia* nonlinearity derives from nonlinear terms containing velocities and/or accelerations in the equations of motion. It should be noted that nonlinear damping, which has similar terms, is different from nonlinear inertia. The kinetic energy of the system is the source of inertia nonlinearities. Examples include centripetal and coriolis acceleration terms. It is also presented in the equations describing the motion of an elastic pendulum (a mass attached to a spring) and those describing the transverse motion of an inextensional cantilever beam.

- When the constitutive law relating the stresses and strains is nonlinear, it is called *material* nonlinearity. Rubber is the classic example.

- Nonlinearities can also appear in the *boundary* conditions. A nonlinear boundary condition exists, for instance, in the case of a pinned-free rod attached to a nonlinear torsional spring at the pinned end.

- Many other types of nonlinearities exist, like the ones in systems with impacts, with backlash or play in their joints, etc.

Worden [36] also summarised the most common types of nonlinearities encountered from dynamic experiments. These include polynomial stiffness and damping, clearances, impacts, and friction. According to the modelling characteristic, the structural nonlinearities can be divided into two categories viz. distributed and concentrated [37]. A nonlinearity caused by large deformation belongs to the distributed category, and friction and contacts are examples of the concentrated nonlinearity.

However, real nonlinear structures are very complex and hence it is difficult to know the nature of any nonlinearity from a knowledge of the behaviour of the material and the layout of structural members.

2.5 Modelling of nonlinear structural systems

The behaviours of nonlinear dynamic structures are governed by partial differential equations (PDEs). The finite dimensionality of the global attractors of those PDEs suggests that the dynamics of the attractors can be captured by a system of ordinary differential equations (ODEs). Hence the long-term dynamics of the PDEs is equivalent in some sense to the dynamics of a suitable system of ODEs. Three approaches can be used to build up these PDEs or ODEs:

- Closed form methods

- Lumped-component modelling methods

- Direct discretisation using the finite element method (FEM), the finite difference method (FDM), or the meshless method

2.5.1 Closed form methods

Analytical solutions for nonlinear structural problems are only possible for special cases when only weak nonlinearity exists or a simple geometry is involves. These nonlinear, constant parameter, second order ODEs such as the Duffing's equation governed by Equation 2.1, even though simple, do not provide any analytical solutions. Thus, to solve realistic nonlinear structures two ways are possible: a lumped-component modelling or a numerical approach such as the finite element method or the finite difference method.

2.5.2 Lumped-component modelling methods

The lumped-component method is the most straightforward approach to create a compact model for nonlinear structural systems. In this method, the structure is partitioned into a few small parts that have simple geometrical shapes or even a few nodes with concentrated mass connected by springs and dampers. By approximately assembling all lumped components, the overall nonlinear structural model of the original system can be built up. However, due to the omission of the complex geometry of the actual structure, simulation results from such a model may be inconsistent with those from a detailed element-based model. In addition, generally speaking, there is not a universal lumped-component method that can analyse all nonlinear structural systems. When the nonlinearities are known, lumped-component modelling method can be used to approximate the original structure. Perturbation methods and nonlinear normal modes, described below, belong to this category. However, it is often difficult to construct accurate lumped-component models for continuous systems, especially when arbitrary geometries are involved.

Perturbation methods

The majority of physical systems belong to the class of weakly nonlinear (or quasi-linear) system. For certain phenomena, these systems exhibit a behaviour only slightly different from that of their linear counterparts. In addition, they also exhibit phenomena which do not exist in the linear domain. Therefore, for weakly nonlinear structures, the usual starting point is still the identification of the linear natural frequencies and mode shapes. Then, in the analysis, the dynamic response is usually described in terms of its linear natural frequencies and mode shapes. The effect of the small nonlinearities is seen in the equations by applying small nonlinear perturbations to the above linearised solutions. The methods using this strategy, are called perturbation methods [38]. In order to explain this concept, an illustrative nonlinear system is considered as follows:

$$\ddot{x} + x = \epsilon x^3, x = x(t) \tag{2.4}$$

where x is the state variable and a function of time, t, and $\epsilon(\epsilon \ll 1)$ is a small parameter indicating that the nonlinear term, ϵx^3 is assumed to be weak, compared to the linear term, x. By a straightforward expansion, the solution of Equation 2.4 can be written in terms of the small parameter, ϵ:

$$x(t;\epsilon) = x_0(t) + \epsilon x_1(t) + \epsilon^2 x_2(t) + \cdots \tag{2.5}$$

where $x_i, i = 1, 2, \ldots$ are unknown functions. Substituting Equation 2.5 into Equation 2.4, a polynomial in ϵ is obtained. The sum of all coefficients of each polynomial term is equal to zero as x_i is independent of ϵ, which results in a series of algebraic equations in different orders. Based upon this approach, the unsolved variables are represented in terms of powers of some parameter which is considered small, and the coefficients of the particular choice of the perturbation parameter are determined later on.

The three common perturbation methods for approximately solving nonlinear systems are: Multiple Scales Method, Averaging Method and Harmonic Balance Method (HBM) [39]. In Multiple Scales Method, the expansion of the solution is

$$x(t;\epsilon) = x_0(t_0, t_1, t_2, \ldots) + \epsilon x_1(t_0, t_1, t_2, \ldots) + \epsilon^2 x_2(t_0, t_1, t_2, \ldots) + \cdots \tag{2.6}$$

where $t_i, i = 0, 1, \ldots$ are independent time scales. In the Averaging method, the expansion of the solution is

$$x(t;\epsilon) = acos(t + \varphi); a = a(t), \varphi = \varphi(t) \tag{2.7}$$

where a is the amplitude and φ is the phase. Both a and φ are the function of time, t. Similarly, the expansion selected in HBM is a Fourier series. A simple procedure to solve

ODE equations using HBM [40] is as follows:

- Assume a solution in the form of a truncated Fourier series with a finite number of harmonics
- Substitute the assumed solution into the equation of motion
- Arrange the results in terms of frequencies
- Balance each harmonic term by setting the coefficients of each frequency term on both sides of the equation to be equal
- Solve the resulting set of algebraic equations and determine the Fourier coefficients of the assumed solution

The accuracy of perturbation methods typically decreases for growing amplitude of motion and hence they cannot be directly used in strongly nonlinear systems. It is noted that HBM can be used to gather important information from a time series. Yasuda et al. ([41], [42]) identified parameters of nonlinear systems by taking advantage of this characteristic of HBM. In Chapter 6, this idea is used to deduce a reduced model of a nonlinear system.

Nonlinear normal modes

For nonlinear dynamic systems, it is possible to extend the idea of a linear modal analysis to nonlinear modal analysis. The concept of nonlinear normal modes was first developed by Rosenberg [43] and further developed by Shaw and Pierre [44]. The nonlinear normal modes are defined as the motions of a nonlinear system occurring on invariant manifolds, which define the constraint relationships between the master modes and slave modes. The manifolds are generally tangent to the corresponding eigenvectors of the the linearised system, at the equilibrium position, and can be obtained analytically in a series form by different perturbation methods described above [45]. Once these relationships are obtained, the system dynamics can be only approximated by the master modes. However, the method requires a-priori knowledge of nonlinearities, which is not available in most cases. Moreover, the method still leads to coupled modal equations, so their application in obtaining a model to conduct parameter studies is impractical.

2.5.3 Finite element method

Mass, stiffness, and damping are the main physical terms simulated in many computational models. The time-dependent characteristics of these terms determine the state variables such as displacement, stress, and kinetic energy. In structural engineering for example, displacements are very important state variables which determine the behaviour of the structure.

Typically, mass, stiffness and damping are described by a set of partial differential equations, defined over a specified spatial domain and over a specified time period. One of the prominent modeling tools for dynamic behaviour of structures is the Finite Element Method (FEM). In FEM, the motion of the structure is described by discretising the spatial and temporal domain of the governing equations. The FEM models provide the simulation data of the state variables at every discretised spatial domain and at every time step.

In FEM models, the relevant spatial domain is discretized into very small elements. FEM relies on localised interpolation basis functions (shape functions) to approximate the solution to a nonlinear system. These local basis functions are generated by meshing the domain of interest and parameterizing the desired solution locally on each mesh element. This parameterized solution converts a continuous Partial Differential Equation (PDE) problem to a coupled system of ODEs that can be integrated in time. These characteristics provide FEM with the power to solve any nonlinear problem. These characteristics also result in a set of equations with large DOF as each element might have several variables. These equations must be solved simultaneously at every time step. For every element, the governing mass, momentum, and energy equations are assumed to hold. Hence, for every partial differential equation, a set of discretised equations equal to the number of elements has to be solved.

In general, the system of equations of the finite element formulated structural vibration problem can be written

$$\mathbf{M}\ddot{\mathbf{x}} + \mathbf{C}\dot{\mathbf{x}} + \mathbf{K}\mathbf{x} = \mathbf{f} \tag{2.8}$$

where $\mathbf{x}$ contains the displacements, $\mathbf{M}$ is the mass matrix, $\mathbf{C}$ is the viscous damping matrix, $\mathbf{K}$ is the stiffness matrix and $\mathbf{f}$ is the nodal force vector. This system can be solved using two different approaches. The first approach uses direct integration, based on a time stepping technique, for example the Newmark scheme [19, 46]. In the second approach, assuming harmonic excitation, a steady-state solution is sought, where the force and corresponding response are expressed as harmonic functions,

$$\mathbf{f} = \hat{\mathbf{f}}e^{i\omega t} \tag{2.9}$$

$$\mathbf{x} = \hat{\mathbf{x}}e^{i\omega t} \tag{2.10}$$

where $\hat{\mathbf{f}}$ and $\hat{\mathbf{x}}$ are the complex force and displacement amplitudes respectively, and ω is the angular frequency. Inserting these expressions into Equation 2.8, and suppressing the time dependance $e^{i\omega t}$, the equation of motion in the frequency domain becomes

$$\mathrm{D}(\omega)\hat{x} = \hat{\mathbf{f}} \tag{2.11}$$

where the dynamic stiffness matrix $\mathrm{D}(\omega)$ is

$$\mathrm{D}(\omega) = -\omega^2\mathrm{M} + i\omega\mathrm{C} + \mathrm{K} \tag{2.12}$$

Despite the fact that FEM models have been proven to be reliable representations of various nonlinear dynamic structures, such models are generally too slow and too large to conduct parameter studies. In addition to the large dimension, FEM models also have to take nonlinearities into account which may be present in the models due to the variable-dependent parameters such as temperature-dependent material. Consideration of the nonlinearities and the fact that the mass, momentum, and energy balances are coupled, substantially add to the complexity of FEM models.

Although FEM simulations generate accurate results, dynamic FEM models are in general computationally intensive, especially in the case of highly nonlinear structures with relatively long transient responses. Thus, the computational demand is extremely high even for a simple nonlinear structure and it is not sufficient to only employ FEM to conduct parameter studies.

It would be beneficial to have a simpler model (in the sense that it comprises less numbers of equations) which approximates the original FEM model and provides the estimates of state variables in a fast and reliable manner. It is also desirable to derive such models through an automated and integrated procedure, so that without the requirement of a-priori physical insights, a simpler model can be derived from the high resolution FEM models. Furthermore, it is also desired, that the simpler models are capable of taking the original physical relationship into account.

Of the three approaches described above, finding a closed-form solution is usually very difficult to achieve and sometimes impossible [47]. The second approach requires the knowledge of nonlinearities, in explicit form to some extent. However, for systems with complex nonlinearities, it may be very difficult or impossible to implement the method. Moreover, the method is only suitable for nonlinear systems of one or a few DOF. Highly nonlinear systems with large DOF, cannot be obtained using this approach because of the existence of nonlinear coupling. The third method, i.e. direct numerical simulations, seems to be the only feasible method for large nonlinear systems. However, when conducting parameter studies, it is usually extremely time-consuming even using powerful computers, because the method involves the time integration of a large number of DOF for any set of parameters.

2.6 Conclusion

Nonlinear dynamic systems are known to have responses such as chaotic and unpredictable behaviour. In order to ensure the safety of a nonlinear dynamic structure, it is important to perform a parameter study to draw a global picture of its dynamic behaviour.

However, it is difficult to obtain a proper model to conduct the parameter study because of the existence of nonlinearities and the limits of computational power. Although direct numerical simulation using FEM, seems to be the only feasible solution to conduct a parameter study with complex nonlinearities, it is usually extremely time-consuming and impractical. Hence, an alternative approach which takes advantage of FEM capabilities but does not require lots of computational effort is needed. A reduced model becomes necessary to conduct the parameter study and is crucial to the understanding of global behaviour of nonlinear structures.

Chapter 3

Model Reduction Methods in Structural Dynamics

3.1 Objectives

- To review model reduction methods, with the aim to examine their suitability for exploring global dynamics
- To present the essential details of generalised space based model reduction methods
- To introduce proper orthogonal decomposition, as a feature basis to model nonlinear systems
- To describe the strategy of constructing a reduced model in a POD feature space and of conducting parameter studies

3.2 Introduction to model reduction methods

As described in Chapter 2, techniques for analysing nonlinear dynamic systems, based on geometric methods, are well developed. However, efforts in understanding the behaviour of nonlinear structures have particularly focused on nonlinear systems with a few degrees-of-freedom (DOF). In contrast, real structures have large DOF, particularly when FEM is employed to obtain responses. A fine discretisation in FEM leads to a large number of equations which need to be solved simultaneously at every time step. Besides, FEM models are very slow and numerically intractable. Nonlinearities can substantially add to the complexity of FEM models. All these characteristics of FEM make it impossible to employ directly, to study qualitative nonlinear dynamics.

Naturally, it is desirable to combine the two approaches described above taking advantage of their individual merits to investigate the vulnerability and integrity of nonlinear dynamic structures. The research in this thesis takes advantage of the power of FEM, to extract a global index or a reduced model which can represent the global behaviour of original nonlinear dynamic structures. Thus, it should be possible to have a simplified model which approximates the original FEM model and which is able to predict the behaviour of the structure using techniques from nonlinear dynamics. Generally speaking, the simplified models can be obtained based upon physical insights or the study of response data collected from simulations or experiments.

In many cases of structural dynamics, high order, complicated numerical models, created by means of many commercial FEM codes, accurately represent the problem at hand, but are unsuitable for system-level modelling, which can provide qualitative understanding of nonlinear structural systems, including an understanding of the bifurcation structure of these systems. A simplified approach is to perform system-level modelling using a mass-spring system with a few degrees-of-freedom, known as lumped-component methods. However, obviously this oversimplified model neither preserves necessary information, nor provides useful information that can be translated to element-level modelling of original structural system. This gives rise to a big gap between system-level and element-level modelling.

Model reduction methods can overcome these limitations and fill in the gap [4]. They decrease the number of DOF in the original structure by capturing important structural characteristics of the original nonlinear structure. For linear systems, this approach had worked well [48] and has been attempted for nonlinear systems as well [49]. It is well known that the asymptotic behaviour of high dimensional or even infinite dimensional dissipative systems can often be described by the deterministic (possibly chaotic) flow on a low dimensional attractor [50]. Certain dissipative partial differential equations posses finite dimensional inertial manifolds, which means that the long-term dynamics described by the partial differential equation is completely governed by a finite dimensional ordinary differential equation, without error [4].

More importantly, model reduction methods, based up statistical feature extraction, are global in nature and therefore provide a potential approach to interpret computational data from highly precise simulations.

Hence, they are computationally efficient for exploring the global dynamics of a large-scale nonlinear structural system. The premise that motivates model reduction is that complex systems can have a relatively simple dynamic behavior which only depends on a relatively small number of essential variables in a generalised space. The challenge for constructing low-dimensional models for complex physical systems is the choice of basis vectors and an identification of the modes that should be preserved in the reduced model [48].

3.3 Classification of model reduction methods

Parametric studies of nonlinear dynamic structures are hampered by a lack of appropriate models. The model reduction methods provide a potentially practical solution to perform such studies and quickly assess the influence of systematic parameter. A reduced model can be formed either in the physical coordinate space or in the generalised coordinate space (Fig. 3.1).

Physical coordinates The structural analysis is based upon the coefficients in matrices of the system, obtained by spatial discretisation. The advantage of this approach is its physical insight, because of the manipulation of mass, damping and stiffness coefficients. It gives a solution which will always be physically meaningful. Typical model reduction methods such as static and dynamic condensations, described in Section 3.3.1, are physical-insight based, as they require the knowledge of stiffness and mass matrices of nonlinear dynamic structures.

Although the reduced system based upon the physical coordinate space, is more accurate, than that based on the generalised coordinate space, the latter is more popular than the former, because of the inefficiently in computing time and unreliable solution accuracy of the condensation methods [51].

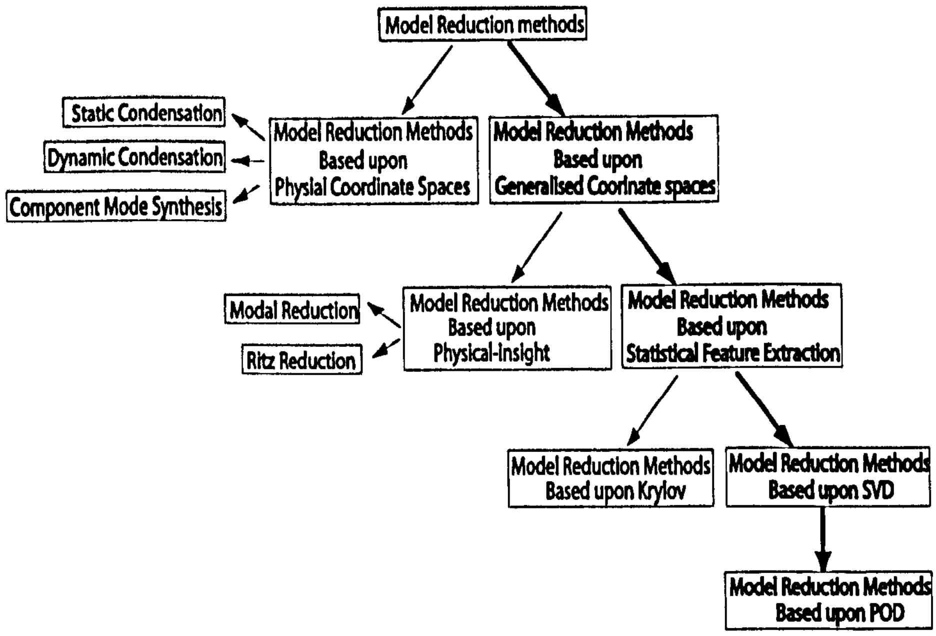

Figure 3.1: Classification of model reduction methods in structural dynamics

Generalised coordinates The structural analysis is carried out in the generalised space, based upon the generalised coordinates. Usually, a relatively small number of modes are required to regenerate the response of the system, which greatly reduces the computational cost involved. In addition, the introduction of statistical modelling approaches mentioned before, reduces the algebraic burden even more.

Its main limitation, is that the responses in the generalised space have little physical meaning. Although the direct matching techniques between the physical space and a generalised space exist, approaches at conciliation between reduced models and original models are not available all the time. More often than not, introducing a statistical approach leads to impossible physical arrangements.

3.3.1 Physical space based model reduction methods

FEM, described in Section 2.5.3, can be used to approximate structures with arbitrary complexity using geometrically piecewise solutions on each element. Model reduction methods seek to build an approximation with base vectors that are defined over the whole model or one of its components. The base vectors are called global basis. It is assumed that the true response of a structure can be approximated within a restricted subspace using this global basis. The size of the subspace governs the quality of the approximation but it is usually much smaller than that of using a FEM model.

In Equation 2.8, DOF, x, are physical because they represent motion at a particular node. From the point of view of model reduction methods, these DOF are coefficients describing the structural motion, as a linear combination of base shapes. In other words, the base shapes or vectors can be regarded as primary DOF. Based upon these base vectors or generalised DOF, model reduction methods conduct space transformations between physical DOF and generalised DOF. They eliminate a number of unimportant primary DOF, thus, producing a good approximation of the original structural dynamics. However, if the the primary DOF are not selected properly, the accuracy of the reduced system can not be guaranteed.

Static and dynamic condensation In structural dynamics, model reduction methods have been widely used [52], by straightforwardly removing part of the original system of equations with all DOF. The removed DOF are those that contribute little to the dynamic behaviour of the system. The remaining part is a crucial subset of the original full model. Usually, the DOF in the structure are split into subsets, one external set, which contains a small number of the original DOF, usually only the nodes where loads or boundary conditions are applied, and one internal set which controls the geometric configuration of the structure. The system of equations (3.1) is partitioned into master DOF, $\mathbf{x}_m$, which are retained, and slave DOF, $\mathbf{x}_s$, which are to be condensed, as (when neglecting damping)

$$\begin{bmatrix} \mathbf{M}_{mm} & \mathbf{M}_{ms} \\ \mathbf{M}_{sm} & \mathbf{M}_{ss} \end{bmatrix} \begin{bmatrix} \ddot{\mathbf{x}}_m \\ \ddot{\mathbf{x}}_s \end{bmatrix} + \begin{bmatrix} \mathbf{K}_{mm} & \mathbf{K}_{ms} \\ \mathbf{K}_{sm} & \mathbf{K}_{ss} \end{bmatrix} \begin{bmatrix} \mathbf{x}_m \\ \mathbf{x}_s \end{bmatrix} = \begin{bmatrix} \mathbf{f}_m \\ 0 \end{bmatrix} \tag{3.1}$$

The boundary conditions and external forces are applied at the physical DOF of the reduced model. Such model reduction methods are also called physical coordinate reduction methods.

Static condensation One of the oldest and most popular reduction methods is static condensation or Guyan Reduction [53]. In this method the inertia terms associated with the discarded DOF are neglected.

$$\begin{bmatrix} \mathbf{K}_{mm} & \mathbf{K}_{ms} \\ \mathbf{K}_{sm} & \mathbf{K}_{ss} \end{bmatrix} \begin{bmatrix} \mathbf{x}_m \\ \mathbf{x}_s \end{bmatrix} = \begin{bmatrix} \mathbf{f}_m \\ 0 \end{bmatrix} \tag{3.2}$$

The displacements can thereby be expressed using the master DOF, $\mathbf{x}_m$ (the slave DOF, $\mathbf{x}_s$, are eliminated)

$$\begin{bmatrix} \mathbf{x}_m \\ \mathbf{x}_s \end{bmatrix} = \begin{bmatrix} \mathbf{I} \\ -\mathbf{K}_{ss}^{-1}\mathbf{K}_{sm} \end{bmatrix} \mathbf{x}_m = \Phi_{sc}\mathbf{x}_m \tag{3.3}$$

Introducing this equation as the change of base, the system of equations is reduced to

$$\mathbf{M}_{sc}\ddot{\mathbf{x}}_m + \mathbf{K}_{sc}\mathbf{x}_m = \mathbf{f}_m \tag{3.4}$$

where

$$\mathbf{M}_{sc} = \Phi_{sc}^T \mathbf{M} \Phi_{sc}, \ \mathbf{K}_{sc} = \Phi_{sc}^T \mathbf{K} \Phi_{sc} \tag{3.5}$$

The choice of master DOF has a large influence on the frequency limit where the reduced model ceases to be valid. This limit in frequency is at the point when the dynamic effects of the condensed DOF become important. As a simple measure, the reduced model is valid up to the lowest natural frequency of the model with the master DOF constrained. More details in relation to methods of choosing master degrees are given in [54] and [55].

While exact for a static model, when applied to a dynamic model, this scheme is not exact and often lacks the required accuracy.

Dynamic condensation In order to partially or fully consider the inertia effect, dynamic condensation methods have been developed [7]. These methods alleviate the limitations of the static condensation method [52]. In these methods, in general, some extra terms are added to the static reduction to make allowance for the inertia effect. The dynamic stiffness matrix $\mathbf{D}(\omega)$, in Equation 2.12, can be partitioned into master and slave DOF

$$\begin{bmatrix} \mathbf{D}_{mm} & \mathbf{D}_{ms} \\ \mathbf{D}_{sm} & \mathbf{D}_{ss} \end{bmatrix} \begin{bmatrix} \mathbf{x}_m^\omega \\ \mathbf{x}_s^\omega \end{bmatrix} = \begin{bmatrix} \mathbf{f}_m^\omega \\ 0 \end{bmatrix} \tag{3.6}$$

where $\mathbf{x}_m^\omega$ and $\mathbf{x}_s^\omega$ are master and slave displacements in frequency domain, respectively. Thus, the displacements can be represented only using the master DOF

$$\begin{bmatrix} \mathbf{x}_m^\omega \\ \mathbf{x}_s^\omega \end{bmatrix} = \begin{bmatrix} \mathbf{I} \\ -\mathbf{D}_{ss}^{-1}\mathbf{D}_{sm} \end{bmatrix} \mathbf{x}_m^\omega = \Phi_{dc}\mathbf{x}_m \tag{3.7}$$

and the system of equation is reduced to

$$\mathbf{D}_{dc}(\omega)\mathbf{x}_m^\omega = \mathbf{f}_m^\omega \tag{3.8}$$

where

$$\mathbf{D}_{dc}(\omega) = \Phi_{dc}^T\mathbf{D}\Phi^T = \mathbf{D}_{mm} - \mathbf{D}_{ms}\mathbf{D}_{ss}^{-1}\mathbf{D}_{sm} \tag{3.9}$$

The advantage of static and dynamic condensation methods is their physical insight, because of the direct manipulation of mass, damping and stiffness matrices. However, static and dynamic condensation methods require the direct operation of the stiffness matrix of FEM models and cannot take advantage of powerful commercial FEM codes.

Component mode synthesis The Component Mode Synthesis (CMS) method, as a hybrid reduction method, has been proposed to develop a dynamic model for the overall structure by taking advantage of the dynamic properties of the substructures. This approach [8] combines the exact static reduction with a limited number of the lowest eigenmodes in such a way that the reduced model is able to represent both static and dynamic behaviour satisfactorily. In this method, a given domain is divided into components, and each component is described by a set of displacement modes. For the ith component of a system, the equation of motion is

$$\mathbf{M}_i\ddot{\mathbf{x}}_i + \mathbf{K}_i\mathbf{x}_i = \mathbf{f}_i \tag{3.10}$$

where $\mathbf{M}_i$, $\mathbf{K}_i$, $\ddot{\mathbf{x}}_i$ and $\mathbf{f}_i$ are the mass matrix, the stiffness matrix, the displacement and the force vector of this ith component. Equation 3.10 can be partitioned into boundary (master) DOF, $\mathbf{x}_m$, and internal (slave) DOF, $\mathbf{x}_s$

$$\begin{bmatrix} \mathbf{M}_{mm} & \mathbf{M}_{ms} \\ \mathbf{M}_{sm} & \mathbf{M}_{ss} \end{bmatrix} \begin{bmatrix} \ddot{\mathbf{x}}_m \\ \ddot{\mathbf{x}}_s \end{bmatrix} + \begin{bmatrix} \mathbf{K}_{mm} & \mathbf{K}_{ms} \\ \mathbf{K}_{sm} & \mathbf{K}_{ss} \end{bmatrix} \begin{bmatrix} \mathbf{x}_m \\ \mathbf{x}_s \end{bmatrix} = \begin{bmatrix} \mathbf{f}_m \\ \mathbf{f}_s \end{bmatrix} \tag{3.11}$$

This ith displacement, $\mathbf{x}_i$, can be defined in terms of a set of basis

$$\mathbf{x}_i = \mathbf{z}_i \boldsymbol{\phi}_i \tag{3.12}$$

where $\boldsymbol{\phi}_i$ is the set of modes for this component, and $\mathbf{z}_i$ is the corresponding modal amplitude. Thus, Equation 3.10 can be transformed into

$$\boldsymbol{\phi}_i^T \mathbf{M}_i \boldsymbol{\phi}_i \ddot{\mathbf{z}}_i + \boldsymbol{\phi}_i^T \mathbf{K}_i \boldsymbol{\phi}_i \dot{\mathbf{z}}_i = \boldsymbol{\phi}_i^T \mathbf{f}_i \tag{3.13}$$

The assembly of all the components is conducted using a Lagrange multiplier [19]. However, how to consider the coupling between substructures continues to be a major challenge for computational vibration analysis [56].

The component mode synthesis method has been used extensively in the dynamic analysis of complex structures during the last three decades [57]. This method uses the same sub-structuring of the internal and external DOF as for static reduction and some dynamic condensation methods. But in addition to retaining the external DOF, some allowance for the inertial forces on the internal (slave) DOF is provided through an extra set of so called generalized DOF. This is a set of eigenvectors of the first (lower) eigenmodes of the internal to the structure that are calculated with the external DOF blocked. In this way, the level of dynamic excitation of the internal modes of the structure is used as an extra set of DOF, and the dynamic behaviour of the structure is described more accurately than with the static reduction.

3.3.2 Generalised space based model reduction methods

There are usually two approaches, shown in Figure 3.1, for formulating a generalised space:

Physical-insight based approach

Using physical insight, an initially complex model can be transformed into a simpler one by making some assumption. For example, the FEM model of a frame can be replaced by a lumped-component model which assumes that the frame is composed of mass-springs whose relationships are ruled by structural mechanics. This assumption leads to a simpler model since the original FEM model can be approximated by a smaller number of ordinary differential equations (ODEs). The disadvantage of this approach is that detailed physical insight is required. In addition, this approach cannot model distributed nonlinearities in structures.

Some efforts have focused on reconstructing a reduced model through coordinate transformation and truncation in a modal space, e.g. [9], [58]. In these approaches, the reduced model is still obtained by transforming the original system of equations with full DOF to a smaller set. However, all operations associated with model reduction are performed in a generalised space, not in the original physical space. This concept is also called the Rayleigh-Ritz procedure. In this procedure, it is assumed that the motion of the system can be described using a reduced set of basis vectors, or modes,

$$\mathbf{x} = \phi_1 z_1 + \phi_2 z_2 + \ldots + \phi_m z_m \tag{3.14}$$

where $\phi_1, \phi_2, \ldots, \phi_m$ are the mode shapes and $z_1, z_2, \ldots, z_m$ are the corresponding modal coordinates. A key point in this procedure is that the number of introduced modes m is much smaller then the total number of DOF, n. Substituting Equation 3.14 in Equation 2.8, leads to

$$\Phi^T \mathbf{M} \Phi \ddot{\mathbf{z}} + \Phi^T \mathbf{C} \Phi \dot{\mathbf{z}} + \Phi^T \mathbf{K} \Phi \mathbf{z} = \Phi^T \mathbf{f} \tag{3.15}$$

It is noted that $\phi_1, \phi_2, \ldots, \phi_m$ can be any suitable vector. Consequently, these methods are also called generalised coordinate reduction methods. At the simplest level it is a matter of replacing a local spatial representation (as constructed from FEM or finite difference method) with a global spatial representation. A relatively small number of global modes give an accuracy in the solution comparable to that obtained from a local spatial grid with a corresponding very large number of DOF. However, the local spatial grid model is essential to construct the global modes. This feature greatly reduces the computational cost involved.

The modal space and the Ritz space are two types of frequently used generalised spaces e.g. [46], [59]. Modal reduction, is one of the classical methods of the generalised coordinate reduction. The dynamic response of a n DOF model in the original physical space can be expressed in terms of the modal coordinates in modal space.

Modal space For a system with n DOF, the eigenvalue problem, can be solved and n normal modes can be calculated, which describe all possible movements of the system. In an analysis it is however often only necessary to include m number of the lowest modes, where $m < n$, based on two assumptions:

- The dynamic force only excites the modes included
- The FEM model introduces a frequency limit above which the model ceases to be valid, the modes over this limit being nonphysical.

Also, when only a limited number of modes are needed, in structural dynamics, it is traditional to retain those modes associated with the lowest frequencies [9]. Using the normal modes to reduce the system in Equation 3.15, the mass and stiffness matrices are reduced to two diagonal matrices. With mass-normalised normal modes the system can be rewritten as

$$\mathbf{I}\ddot{\mathbf{z}} + \mathbf{\Phi}^T\mathbf{C}\mathbf{\Phi}\dot{\mathbf{z}} + \mathbf{K}(\mathbf{z}) = \mathbf{\Phi}^T\mathbf{f}(t) \tag{3.16}$$

where $\mathbf{I}$ is the unity matrix, and $\mathbf{\Phi}$ the eigenvectors, or normal modes. With general damping, the modal damping matrix becomes fully populated. Using simplified damping descriptions (either proportional Rayleigh damping or hysteretic damping), the damping matrix becomes diagonal thus resulting in an uncoupled system of equations [46].

By employing a modal space, the idea of generating reduced models based upon FEM results has been studied extensively in ([60]- [66]). In all these methods the reduced model is constructed in modal spaces using parameter identification techniques, and nonlinear functions are assumed to be functions of many modal modes. However, these methods can cause difficulties for systems with many modes of interest and require complex procedures to be employed in order to determine which of the modes really contribute to the nonlinearity. Additionally, when performing parameter identification of the assumed model, such methods would lead to a very complex unknown nonlinear model structure, with too many parameters to determine for a large number of modes preserved [67].

Ritz space The use of an orthogonal set of specially selected Ritz basis is shown to be very effective in reducing the cost of dynamic analysis by modal superposition [10]. The construction of the Ritz space is generally computationally more efficient than the modal space as the Ritz vectors take into account the influence of loads. However, the equations of motion of the reduced model derived from Ritz reduction are generally coupled while those obtained from modal reduction are usually uncoupled. In addition, convergence speed of a basis is crucial to achieve a reduced model with a desired accuracy. The number of basis terms one needs to retain in the reduced model is an important issue.

The calculation of Ritz vectors requires the knowledge of the mass and stiffness matrix and the procedure, following [68], is as follows

1. Generate force vector $\mathbf{f}$
2. Factorise the known stiffness matrix: $\mathbf{K} = \mathbf{LU}$
3. Generate the first Ritz vector
   - Solve for the first Ritz vector: $\mathbf{Kx_1} = \mathbf{f}$
   - Normalise the Ritz vector in term of the known mass matrix: $\mathbf{x}_1^{norm} = \frac{x_1}{\sqrt{(\mathbf{x}_1^T\mathbf{M}\mathbf{x}_1)}}$
4. Repeat the same procedure to determine the other Ritz vectors
   - A product of mass matrix and previous Ritz vector is assumed to be a force vector
   - Solve for Ritz vector x_i: $\mathbf{Kx}_i = \mathbf{M}\mathbf{x}_{i-1}^{norm}$
   - Use Gram-Schmidt orthogonalisation procedure: $\mathbf{x}_i = \mathbf{x}_i - \sum_{j=1}^{i-1}(\mathbf{x}_j^T\mathbf{M}\mathbf{x}_i)\mathbf{x}_j$

- Normalise the Ritz vector in term of the known mass matrix: $\mathbf{x}_i^{norm} = \frac{\mathbf{x}_i}{\sqrt{(\mathbf{x}_i^T \mathbf{M} \mathbf{x}_i)}}$

It is noted that modal reduction, Ritz reduction and POD reduction (explained in Section 3.5) all conduct a similar space transformation from an original physical space to a generalised space. The advantage of these space transformation reduction methods is the effectiveness of the deduced models. The first two approaches require physical-insights such as mass and stiffness matrices. The POD reduction is based upon statistical feature extraction and thus does not require knowledge of physical-insights. However, reduced models obtained from the POD reduction have little physical meaning.

3.3.3 Statistical feature extraction based approach

Since structural systems are becoming more and more complex, with highly nonlinear characteristics, it is difficult to evaluate the global dynamics of the structural systems from the raw response data directly. Feature extraction techniques, which transform this raw data from the original physical space into the feature space, are thus needed, to identify the dominant patterns that are hidden in the raw data. The dominant patterns characterise global dynamics of the structural system. With the advent of these techniques, such as the Proper Orthogonal Decomposition (POD) [69] and Independent Component Analysis (ICA) [70], empirical models can be derived from the simulation data. The geometric pattern of this data has fundamental implications for understanding the behaviour of structures. System identification techniques, such as Wavelet [71], Harmonic Balance Method (HBM) [41] and POD [72] can be used to determine coefficients of the empirical models obtained above. The advantage of this approach is that there is no detailed physical insight required. However, the physical interpretation of the original model is often lost. More details are given in Section 3.4.

Dynamic behaviour of a nonlinear system can be captured by FEM or other numerical methods in the form of time series or response histories. A global feature of the system would represent the general behaviour of a response time series and be able to explain most geometric patterns. It could be a one dimensional variable that contains all the information necessary for the pattern identification. Typical examples, include the temporal mean, variance, the maximum and minimum of a response time series. Unfortunately, it is rare to find a feature extraction problem that can be solved by using these naive feature variables because many totally different time series may have similar values for these feature variables. These feature variables are influenced by multiple factors that control the evolution of the system, most of which are not linked to the feature extraction problem and therefore obscure different values in the different time series.

More advanced features deal with the concept of information, for example mutual information and the definition of entropy for time series, for instance the Kolmogorov-Sinai entropy [73]. However these features are very complex and very sensitive to noise. In addition, they are difficult to construct, even for mathematical models.

It is feasible to use a finite number of feature variables rather than only one variable to represent the time series. A set of basis functions are selected as global features which are extracted from the response time series. The central idea here is that the basis functions decompose a time series into different components and therefore potentially extract the most important information in the time series. Fourier series, POD, and wavelet decomposition represent a time series through a linear combination of their basis functions. Similarly, the basis functions can be used as assumed modes to project PDEs of a nonlinear system into a series of ODEs in modal coordinates. Usually only a few of the assumed modes are active, hence a truncated series of equations can be used to approximate the original system.

In fluids, it is common to use nonlinear reduced models. Dowell and Hall [74] summarised two distinct approaches to model nonlinearities in fluids. In the first one, called the time-linearisation model, a fully nonlinear solution for the steady flow about a body is determined (assumed stationary), and then a small dynamic perturbation on the nonlinear solution is considered. The approach naturally leads to a reduced model. In the other, called the nonlinear dynamic model, an attempt is made to determine a fully dynamic nonlinear solution with the help of the Finite Difference Method (FDM).

There are three common approaches for obtaining a nonlinear dynamic model in fluid flows.

- Balance Method: Here the basic idea is to utilise information from both the inputs and outputs of a dynamic system to deduce its reduced model. It is performed using the controllability and observability grammians from control fields. Some details can be found in [75] and [76].

- System Identification Methods: By considering a small number of inputs and outputs, a nonlinear input/output relationship in the form of a transfer function, can be determined numerically. Such a system identification technique uses simulation results to arrive at a relatively small number of equations. Worden [36] provided a detailed explanation of the entire realm of nonlinear system identification.

- Eigenmode Computational Methods: In many problems, a relatively small number of eigenmodes are dominant. This suggests a way to construct an efficient computational model using these and that is to find an orthogonal set of eigenfunctions which span the data in an optimal way. POD is one of these methods.

In fact, these approaches can be applied in solid structures as well. The time-linearisation modelling approach has some similarity with perturbation methods described earlier in Section 2.5.2. The nonlinear dynamic modelling approaches, in particular, the combination of system identification methods and eigenmode computational methods, offer considerable promise for building up a model to perform parameter studies. However, the combined approach will be a semi-black-box modelling technique whose disadvantage is the loss of all physical interpretations of the original model.

Nayfeh et al. [77] explained that the aim of eigenmode methods is to obtain a transformation from the physical coordinates of the system to a set of new generalised coordinates associated with the eigenfunction corresponding to the lowest eigenvalues. They classified the methods into two groups viz. node methods and domain methods, according to the way transformation was obtained.

Lucia et al. [49] reviewed reduced order modelling techniques and emphasised Volterra series representations (based on system identification method), POD and HBM. These three methods share a common reliance on existing numerical techniques. POD is the only one that can be easily incorporated into existing commercial codes.

3.4 Properties of generalised spaces based on statistical feature extraction

Some important properties of generalised spaces based on statistical feature extraction are described in this section.

3.4.1 Decomposition

The concept of model reductions has been developed as a mixture of linear algebra and statistical analysis by means of decomposition or transformation techniques [48]. The decomposition technique, by virtue of providing an alternative representation, often reveals key features of a signal that are difficult or impossible to discern in the original domain. A decomposition can unveil the composition of a signal in terms of the elemental blocks, or basic functions. For instance, the well known Laplace transformation can decompose a function into a weighted combination of a set of basic functions e^{st}

$$x(t) = \int_{-\infty}^{\infty} X(s)e^{st}ds \tag{3.17}$$

where the weight $X(s)$ is the Laplace transform of $x(t)$ and s is the complex frequency. Similarly, using wavelets, the original signal can be separated into its contribution at different regions of the time-scale space by projecting on the corresponding wavelet basis functions. This concept of decomposition can be extended into a general state matrix X, which can be transformed, using a transformation matrix $\mathbf{P}_n \in R^{n \times n}$ as follows:

$$\mathbf{X} = \mathbf{P}_n \cdot \mathbf{Y} \tag{3.18}$$

where $\mathbf{Y}$ is a re-representation of $\mathbf{X}$ in terms of generalized coordinates expressed by the transformation matrix $\mathbf{P}$, which is also, from the geometry point of view, a rotation and a stretch that transforms $\mathbf{Y}$ into $\mathbf{X}$. While $\mathbf{X}$ has the spatial and physical meanings as a state matrix, $\mathbf{Y}$ has neither. Rather, $\mathbf{Y}$ is a vector of multiplication factors for the 'global shape functions', given by the columns of matrix $\mathbf{P}_n$, which can be approximated by a reduced matrix $\mathbf{P}_m (m \ll n)$, preserving most of the information of the nonlinear structural system.

By using discretisation methods, the state vector $\mathbf{x}$ over the whole domain is approximated as a linear combination over the elements:

$$\mathbf{x} = \sum_{\Omega_1} a_k^1 \mathbf{N}_k^1 + \cdots + \sum_{\Omega_e} a_k^e \mathbf{N}_k^e, \qquad k = 1, \cdots n \tag{3.19}$$

where n is the number of coefficients a_k in each element (which can be the nodal displacements for example) and e is the total number of elements. A property of each local shape function $\mathbf{N}_k$ is that it is the one at the kth node and zero outside the finite element. Within the element, $\mathbf{N}_k$ can linearly decay between one and zero. The only way to directly reduce a system based on Equation 3.19 is to coarsen the mesh, i.e. to choose the shape functions which cover several elements. This, however, results in a significant loss of precision.

On the other hand, each column of matrix $\mathbf{P}_n$ in Equation 3.18 can be seen as a linear combination of the local shape functions, i.e. as a global shape function over the whole interested domain. Thus it is possible to truncate some of the generalized coordinates and therefore reduce the dimension of the system represented by Equation 3.18 without losing much accuracy.

$$\mathbf{X} \approx \mathbf{P}_m \cdot \mathbf{Y} \tag{3.20}$$

Both ways of capturing crucial information have their advantages and disadvantages. By coarsening the mesh, one preserves the physical nodes, but looses the precision, whereas by performing a mathematical model order reduction, one looses the physical nodes, but preserves high accuracy.

3.4.2 Orthogonal basis

Two basis vectors $\mathbf{v}_1$ and $\mathbf{v}_2$ are orthogonal if $< \mathbf{v}_1, \mathbf{v}_2 >= 0$ (i.e. dot product is equal to zero) and orthonormal if $< \mathbf{v}_1, \mathbf{v}_2 >= 0$ and $< \mathbf{v}_1, \mathbf{v}_1 >=< \mathbf{v}_2, \mathbf{v}_2 >= 1$. A set of vectors $\mathbf{x}_i, i = 1, 2, \ldots, n$ is orthogonal if

$$< \mathbf{x}_i, \mathbf{x}_j >= c\delta_{ij} \tag{3.21}$$

where c is a constant and the Kronecker Delta

$$\delta_{ij} = \begin{cases} 0, & i \neq j \\ 1, & i = j \end{cases}$$

These vectors are orthonormal if $c = 1$. When two vectors are orthogonal, they have no correlation, that is, the projection between any single pair of vectors is zero. Let $\mathbf{v}_i$ be a set of orthonormal vectors that span the n-dimensional space, then any $n \times 1$ vector x is a linear combination of the $\mathbf{v}_i$

$$\mathbf{x} = \sum_{i=1}^{n} < \mathbf{x}, \mathbf{v}_i > \mathbf{v}_i \tag{3.22}$$

If $\mathbf{v}_i$ is not orthonormal, $\mathbf{x}$ can still be expressed as linear combination of v_i, but the coefficients of $\mathbf{v}_i$ are no longer simple inner products of $< \mathbf{x}, \mathbf{v}_i >$. By employing the knowledge of orthogonal decomposition, one vector can be decomposed into a combination of independent parts, because of the property of orthonormal basis vectors. The truncation of some orthogonal components will not affect the others, which is crucial for the POD. Now let

$$\tilde{\mathbf{x}} = \sum_{i=1}^{m} < \mathbf{x}, \mathbf{v}_i > \mathbf{v}_i, \; m \ll n \tag{3.23}$$

where parts of the vectors, $\mathbf{v}_i, i = m+1, m+2, ..., n$ are truncated to deduce a reduced representation of the system. In other words, $\tilde{\mathbf{x}}$ is one approximation of $\mathbf{x}$ in terms of the reduced set of vectors $\mathbf{v}_i, i = 1, 2, \ldots, m$, as a result, the truncation of the basis provides a way to find lower dimensional approximations of the given vector.

3.4.3 Basis determination

The main issue in model reduction is the determination of basis, i.e. how to truncate the obtained basis functions. The principle of model reduction methods is that if the basis vectors are chosen appropriately, the relevant high-dimensional systematic dynamics can be captured with a greatly reduced number of states. The reduced model should be chosen so that it contains all the features of the states encountered during the simulation of structures. In other words, the reduced model $\hat{\mathbf{x}}$ should be the best approximation of the original vector $\mathbf{x}$ in the least squares sense

$$\|\mathbf{x} - \hat{\mathbf{x}}\|^2 \leq \|\mathbf{x} - \tilde{\mathbf{x}}\|^2 \tag{3.24}$$

3.4.4 Types of basis

Based on the concepts of decomposition and orthogonality, model reduction methods can be turned into a mathematical problem in linear algebra viz. how to handle the top or bottom eigenvectors of special matrices constructed from experimental or numerical data. Any reduced model has two main elements. One is a set of basis that helps to group structural behaviours of dynamic systems. The other is the projection of the original system onto the subspace constructed by the set of basis.

There are many bases that can be used for model reduction methods, including Lagrange basis, Hermite basis, Taylor basis, Galerkin basis and snapshot basis. Antoulas and Sorensen [48] reviewed model reduction methods for large-scale systems in which model reduction methods are classified as the SVD-based, the Krylov-based, the SVD-Krylove-based approximation methods, shown in Table 3.1.

SVD-based approximation method The method has its roots in the singular value decomposition (SVD) and the resulting solution of the approximation of matrices is by means of matrices of lower rank, which are optimal in the 2-norm (or more generally in unitarily invariant norms). The quantities which are important in deciding to what extent a given finite-dimensional operator can be approximated by one of lower rank, are the so-called singular values; these are the square roots of the eigenvalues of the product of the operator and its adjoint.

Krylov-based approximation method This method does not rely on the computation of singular values and instead is based on moment matching. The method has been very influential in iterative eigenvalue computations and more recently in model reduction. Its drawbacks are that the resulting reduced models have no guaranteed error bound, stability is not necessarily preserved, and some of them are not automatic.

In the field of pattern analysis, graph-based methods have recently emerged as a

Approximation methods for dynamic systems		
SVD		Krylov
Nonlinear Systems	Linear Systems	
POD method Empirical grammian	Balanced truncation Hankel approximation	Realization Interpolation Lanczos Arnoldi
SVD-Krylov		

Table 3.1: Approximation methods for dynamic methods

powerful tool for analysing high dimensional data that has been sampled from a low dimensional submanifold. They share a similar structure, which includes computing nearest neighbours of the input patterns, constructing a weighted graph based on these neighbourhood relationships, deriving a matrix from this weighted graph, and producing an embedding from the top or bottom eigenvectors of this matrix. The latest of which is the principle of SVD-based or Krylov-based approximation method.

3.4.5 Several common basis

The idea to derive a reduced model originates from the opportunity of representing a variable in a suitable, data based coordinate system, consisting of orthogonal basis functions such as Fourier, wavelet and POD basis functions.

The transformation of a vector or matrix into an orthonormal set of basis vectors is a simple but effective inner product operation in linear algebra. This important property results in a typical model reduction method which has three steps. Firstly, construct an orthonormal basis, secondly conduct truncation, and finally, project nonlinear dynamic systems onto the reduced space. The approximation quality of the resulting reduced model depends highly on the choice of the basis vector [78].

In the context of structural dynamics, the model reduction of linear systems is performed by the decomposition of their modal modes in which a small number of these modal modes with the lowest frequencies, are retained to represent the dynamics of the system, whereas all other basis are discarded. Or, due to the existence of the physical meanings of these modes, a reduction criterion is available by comparing frequency content of the loadings with eigenfrequencies of the modes [78]. Idelsohn and Cardona [79] showed that frequent changes of the basis can change the dynamic behaviour of the model and even lead to numerical stability. These linear modal basis are constant against any excitation. Therefore, if the nonlinearity is weak, the linear modal basis has the great advantage of involving model reduction.

From the numerical point of view, it is generally the best choice to use an orthonormal basis for ansatz and test space. Then the resulting system of equations will be well conditioned [80]. An overview is available in [81] and [82]. In the following only the bases that are used most frequently, are described.

Fourier transformation method, the discrete wavelet method and POD, reconstruct a reduced model based upon an orthonormal basis, and share a common reliance on existing numerical techniques. All of them require data sampling and can take advantage of high-fidelity simulation tools. All these three bases are global in nature.

However, it is important to realise that the modal decomposition alone does not provide enough information to decide upon a good reduced model. What is additionally necessary is a method of deciding which modes should be preserved in the model [6]. POD is superior to the Fourier transformation method and the discrete wavelet method in term of the performance of model reduction, as POD

- is potentially more efficient [83].
- has a reduction criterion, which is described in Section 3.5.4.

Fourier decomposition

According to Fourier, any periodic function $f(t)$ can be expanded in terms of discrete sine or cosine functions as

$$f(x,t) = \frac{1}{2}a_0 + \sum_{n=1}^{\infty}(a_n cos(\omega_n t) + b_n sin(\omega_n t)) \tag{3.25}$$

For Fourier decompositions, the basis functions are dilations of cosine and sine components (each component spanning the entire time interval).

Proper orthogonal decomposition

For POD, the basis functions are eigenfunctions. Thus, when a function can be decomposed into two parts: the mean part and the oscillation part, its oscillation can be represented as follows

$$f(x,t) = \sum_{n=1}^{\infty} a_i \phi_i(x) \tag{3.26}$$

where ϕ_i is the ith proper orthogonal mode (POM) and a_i is the corresponding time dependent coefficient. This is further explained in Section 3.5.

Wavelet decomposition

The idea behind Fourier decomposition is to extract a frequency component from a time series, and the idea behind POD is to ensure non correlation between the coefficients. Thus there are two ways to select the components that account for the most variance. Wavelet decomposition focuses on localised characteristics of a time series at chosen time scales.

For wavelet decompositions, the basis functions are different translations and dilations of one function, called the mother function, along with a scale function (each spanning a fixed subinterval).

3.5 Proper orthogonal decomposition (POD)

Proper Orthogonal Decomposition (POD) is a simple procedure that provides an optimal linear basis for the representation of sampling data. The data may come from experiments or, from numerical simulations, as in this work. POD is also known as Karhunen-Loéve, principal component analysis (PCA) and empirical orthogonal function [84]. The method is either a variance maximization technique, or a least-mean-squares technique [85]. POD has been developed as a popular method of obtaining basis vectors for structural systems with large DOF. Holmes et al. [86] have used this for the modelling of turbulence.

In this section, basic concepts of POD are introduced and its mathematical theory is presented.

3.5.1 Basic concepts of POD

The proper orthogonal decomposition (POD) is a multivariate analysis technique to deduce a set of orthonormal basis, by finding a transformation between the original set of variables and a new set of uncorrelated variables, called principal components or proper orthogonal modes (POMs), which are linear combinations of the original variables [69]. All the principal components are orthogonal to each other so there is no redundant information. The principal components as a whole construct an orthogonal basis for a state space. Usually, the first few principal components can capture most of the variance, Var, in the state space so that they can be used as a reduced model of this space.

The principal components are determined by minimizing the average squared distance between the original model and its reduced model which still retains important variables affecting the behaviour of a structural system. When applying the approach to high dimensional systems, covariance measures from statistics are used to represent the linear relationship between two variables in a state matrix, which make it possible for POD to identify a small number of global vibration modes of a dynamic structural system. Glosmann and Kreuzer [87] give a clear description of the mathematical concepts associated with POD.

3.5.2 POD basis

A vector $\mathbf{x}$ spanned by ϕ_i can be written in the following form

$$\mathbf{x} = \sum_{i=1}^{m} a_i \phi_i \tag{3.27}$$

where the basis, ϕ_i, is the spatial POD information and a_i, is the temporal POD information and the time dependent coefficient of the corresponding basis. Using the optimal orthonormal basis, ϕ_i, POD seeks to represent a state ensemble, $\mathbf{X}$, either from experimental or numerical simulation in a subspace. This subspace can be formed by a projection operator, $\mathbf{P}$, which maps vectors in R^n onto the space spanned by ϕ_i. The condition for the optimality of the basis ϕ_i can be satisfied by minimizing the norm of difference, Err, between the state ensemble $\mathbf{X}$, and its projection in a subspace defined by the projection operator, **P**

$$\text{Err} = MIN\sum_{k=1}^{m} \| \mathbf{X} - \mathbf{P} \cdot \mathbf{X} \| \tag{3.28}$$

where the projection operator, $\mathbf{P} = \Phi\Phi^T$ $(\Phi^T \cdot \Phi = 1)$. The definition of the norm is the minimised expression in Equation 3.28 which is conventional Euclidean L_2 term, although other norms can be selected as well. The minimization problem is analogous to a problem of maximizing the projection of **X** onto the span Φ, under the condition of a normalization criteria, $\Phi^T \cdot \Phi = 1$

$$\text{Var} = MAX(\sum_{k=1}^{m} \frac{\langle(\mathbf{X}, \Phi)^2\rangle}{\| \Phi \|^2}) \tag{3.29}$$

where $(\cdot,\cdot)$ indicates an inner product and $\langle\cdot\rangle$ stands for an average. When the L_2 norm is selected, this constrained optimization in Equation 3.29 can be solved by a standard Lagrangian technique as follows

$$J(\Phi) = \sum_{k=1}^{m} \langle(\mathbf{X}, \Phi)^2\rangle - \lambda(\| \Phi \|^2 - 1) \tag{3.30}$$

where λ is a Lagrange multiplier to integrate the constraint on the norm of the basis Φ. Assuming $\mathbf{X} = \mathbf{x}_1, \cdots, \mathbf{x}_m$, the differentiation of Equation 3.30 with respect to Φ generates

$$\frac{d}{d\Phi}J[\Phi] = 2\mathbf{X}\mathbf{X}^T\Phi - 2\lambda\Phi \tag{3.31}$$

Letting Equation 3.31 equal to zero, leads to a eigenvalue problem

$$(\mathbf{X}\mathbf{X}^T - \lambda\mathbf{I})\Phi = 0 \tag{3.32}$$

which can be transferred into

$$\mathbf{X}\mathbf{X}^T\Phi = \lambda\Phi \tag{3.33}$$

where Φ are the proper orthogonal modes (POMs) and λ are the proper orthogonal values (POVs).

3.5.3 Method of snapshots

To reduce computational cost in Equation 3.32, Sirovich [88], [89], [90] put forward an elegant method called the snapshots method. Using the snapshots method, the determination of the POD basis is linked to the Singular Value Decomposition (SVD) of the state ensemble **X**, which can be represented as

$$\mathbf{X} = [\mathbf{x}_1 \cdots \mathbf{x}_m] = \begin{pmatrix} x_{11} & \cdots & x_{1m} \\ \cdots & \cdots & \cdots \\ x_{n1} & \cdots & x_{nm} \end{pmatrix} \tag{3.34}$$

where n is the number of samples at different times, and m the number of the measurements at different locations. In other words, each column in the matrix **X** is called one snapshot, which naturally leads to another name of the matrix **X**: the snapshot matrix, in relevant literature. It is noted that each column in the state ensemble **X** represents a modified state variable time series rather than a directly recorded state variable time series. This modification is performed to generate a zero-mean time series whose mean is subtracted from the original recorded time series. If the number of data sampling, m, is large enough, and the data is zero mean, a reliable approximation of the covariance matrix, S, of snapshot matrix **X** can be obtained as

$$\mathrm{S} = \lim_{n\to\infty} \hat{\mathrm{S}} = \lim_{n\to\infty} \frac{1}{n}\mathbf{X}^T \cdot \mathbf{X} \tag{3.35}$$

The POMs and POVs are thus determined by the eignsolutions of the covariance matrix, S. Since the POD does not use the snapshots as basis themselves, in order to take an ensemble of snapshots which leads to a good approximation of the full order FEM solution, one natural solution to capture the characteristics of the original physical system is to take a sufficiently large number of snapshots.

Model reduction, employing the POD basis, is accomplished by truncating the bottom eigenvectors obtained from the SVD computation of the covariance matrix, S.

$$\mathrm{S} = \mathbf{U}\Sigma\mathbf{V}^T \tag{3.36}$$

where the columns $\mathbf{u}_i$ of $\mathbf{U}$ are the proper orthogonal modes POMs, the columns $\mathbf{v}_i$ of $\mathbf{V}$ are the proper orthogonal coordinate (POC) times series, corresponding to each POM, and Σ is a diagonal matrix whose diagonal element, λ_i are the proper orthogonal values (POVs), corresponding to each POM. The POC time series indicate the amplitude modulation of each POM and the POVs indicate the relative energy level of each POM in the covariance matrix, S, and provides a quantitative measure of the contribution of each POM to this covariance matrix. Thus this covariance matrix can be represented as a summation of POMs and corresponding POC time series as follows

$$\mathbf{S} = \Sigma_{i=1}^{m} \lambda_i \mathbf{u}_i \mathbf{v}_i^T \tag{3.37}$$

where m is the number of POMs remained after the mode truncation. This truncation of the optimal basis provides optimal low dimensional approximation of the given data [91]. Other POD calculation methods can be found in [32].

3.5.4 POD reduction criterion

In practical problems, the determination of the number of proper orthogonal modes relies on the knowledge that, beyond a certain value of m, an increase of the number m should not have any influence on the qualitative behaviour of the phenomenon considered. This knowledge is a main idea of the identification of the combination form of the basis that should be preserved in the reduced model [84]. A quantitative measure of the relative importance of these POMs with regard to the energy of the system captured by the POD is as follows:

$$\frac{\sum_{i=1}^{r} \lambda i}{\sum_{i=1}^{m} \lambda i} \gg 0.96 \tag{3.38}$$

where λ_i stands for the ith proper orthogonal value. The equation states that the top rth proper orthogonal models contain 96% of the total energy of the structural system considered. This chosen threshold on the right side of Equation 3.38 determines the number of the remained POMs, m, in Equation 3.37.

3.5.5 POD quality

POD theory implies that the error of a POD basis is analogous to the sum of the truncated POD eigenvalues according to Equation 3.35. This error definition only provides a measure of how closely the reduced POD basis can represent an element from the snapshot space. However, this error does not supply a reliable indication to the ability of the resultant reduced model in representing the original model if the snapshot data does not contain necessary information about a particular systematic characteristic. In other words, a POD model, as a linear reconstruction, will only be able to represent phenomena snapshots can capture.

As a statistical method, the quality of POD mainly depends on the quality of the original data, which should capture dynamics of interest in numerical format. This is related to two factors:

- the reliable data generator – without practical tools capable of capturing dynamics of nonlinear systems in numerical format, further improvement in constructing a reduced model will ba hampered. Commercial FEM codes provides a reliable way of achieving this requirement for complex nonlinear structures.

- the total sampling number – the overwhelming factor that influences the accuracy of POD is the total sampling number [92], which represents how many nodes are present in one snapshot. Unfortunately, there is no way to know *a priori* how many nodes will yield the best results, although the convergence test of natural frequencies or POMs might help.

The first step in the construction of a POD model is the gathering of appropriate sampling records. The snapshots are sampling records representing state variables with other parameters of interest such as the amplitudes and frequencies of external excitation. These could be snapshots at a number of instances in time for a dynamic analysis. The important factors that affect the POD computations are the number of snapshots and the spacing between them [93].

3.5.6 POD Applications in nonlinear structural dynamics

Feeny and Kappagantu [94] identified that POMs converge to the linear normal modes of vibration in undamped or lightly damped systems, which fit dynamic structures in civil engineering. Kerschen and Golinval [95] provided some insights into the physical interpretation of POMs using SVD.

Azeez and Vakakis [93] used POMs in a Galerkin reconstruction process to obtain lower dimensional models for a beam and a rotor. Kerschen et al. [96] extended the model reconstruction of a cantilever by means of POMs and showed that the reduced model accurately captured the bifurcation diagram.

Kerschen et al. [32] demonstrated the utility of POD for dynamic characterization and order reduction of linear and nonlinear mechanical systems. Solar et al. [97] and Carassale et al. [98] provided a state-of-the-art description and some prospects on POD, in particular its application in wind engineering.

POD application in nonlinear structural dynamics can be considered along two lines (*a*) the direct analysis of POMs to estimate the behaviour of nonlinear structural systems, and (*b*) the model reconstruction in terms of POMs. In the former, Aschheim et al. [99] applied POD to displacement response data for a 12-story frame building, and concluded that the POD modes provide an unambiguous and simple description of the 'predominant' mode of structures responding to earthquake ground motions. Gutirrez and Zaldivar [100] commented that POD is a flexible method and can be applied to examine the data either as a complete event, or sub-events of the complete process history, and also suggested that it can be used as a sequential monitoring method.

The latter can be further classified into two types: the first includes the generation of a reduced model, based upon POD and the second uses POD as an identification tool. Some examples of the latter include [101], [72] and [102].

3.5.7 Advantages and disadvantages of POD

Rathinam and Petzold [91] summarised two main advantages of using POD:

- POD is completely data dependent and does not assume any prior knowledge of the process that generates the response data. This property is advantageous in situations where *a priori* knowledge of the underlying process is insufficient to warrant a certain choice of basis [91]. It also helps in exploring patterns in data that may reveal some insight into the underlying process that generates it.

- Combined with the Galerkin projection procedure, POD provides a powerful method for generating lower dimensional models of dynamic systems that have a very large or even infinite dimensional phase space. The fact that this approach always looks for linear (or affine) subspaces, instead of curved submanifolds, makes it computationally tractable. However, it must be noted that POD does not neglect the nonlinearities of the original vector-field. This is so because, if the original dynamic system is nonlinear, then the resulting POD reduced order model will also typically be nonlinear.

POD, as a multivariate statistical method can disclose relevant but unexpected structure hidden in the sampling records. POD is versatile in the sense that the sampling records it uses can originate from different numerical or experimental recourses, and that the way it handles the records requires no prior knowledge of the physical phenomena of interest.

The POD method relies on a set of basis vectors, or modes, extracted from a time-series solution representing the dynamics of that problem. Unlike the eigensolution basis, the POD basis is extracted from the dynamics of response time histories; it thus contains more essential information of the system. Unlike the element-based finite element basis, the POD basis spans the whole spatial domain of computation; it contains information at various time stations; as a result, this basis does not need to be updated as with the eigensolution basis computed from a traditional linearisation of the full FEM model.

The POD forms a reduced basis for the structural system from its response records instead of directly extracting information from the system itself. This makes it quite suitable for large, complex systems. POD can avoid some of the computational difficulties associated with a large number of state variables when using direct approaches.

Rathinam and Petzold [91] also illustrated two potential inadequacies of POD:

- Even capturing 100% of the energy of a globally attracting low dimensional trajectory may still lead to a reduced model with the wrong dynamics. The author attributed the cause of the inadequacy to two reasons: (a) a set of trajectories alone do not carry all the information about the dynamics; (b) the projection operator on a given subspace may not result in a stable model.

- The sensitivity of POD to the data trajectory may lead to qualitatively different reduced models, in particular, POD results may be very sensitive to slight perturbations in the data when $\lambda_k \approx \lambda_{k+1}$. This inadequacy is avoided if only a few of POMs are used. Chelidze and Zhou [103] introduced a differential operator matrix to generate smooth POD to overcome this deficiency.

In structural dynamics, the second inadequacy of the POD is that POMs might change if the external excitation or the initial conditions of dynamic systems change, that is, POMs are not always optimal in the parameter space of the system. However, POMs are still the most robust orthogonal models to generate a reduced model of the system over the parameter range of interest. In addition, this limitation can be overcome by using combined POMs [104] or predefined POD [105]. Based upon the fact that, the structural response to an initial condition is expressed as a weighted summation of the proper orthogonal modes and the corresponding proper orthogonal coordinate histories, shown in Equation 3.37, Allison et al. [106] proposed a method to consider the influence of changes in initial conditions by adjusting the weight of each mode in the response.

3.6 Model reduction using POD

POD is a powerful technique for extracting features from the response data sets. POMs obtained using POD are global in nature and suitable for exploring the global behaviour of nonlinear structures because of the simplicity and generality of POD. In this thesis, a reduced model is constructed with dominant POMs and its strategy is outlined as follows.

3.6.1 Formulation of reduced models

In order to construct a reduced model to study global behaviour of a nonlinear dynamic system, a reduced model can be assumed, in a generic form, in a generalised feature space as

$$\mathbf{f}_{re} = h(\mathbf{z}) \tag{3.39}$$

where $\mathbf{z}$ and $\mathbf{f}_{re}$ are the low-dimensional state vectors, and the corresponding load vector in the generalised space, respectively, and $h(\mathbf{z})$ postulates the relationship between $\mathbf{z}$ and $\mathbf{f}_{re}$. $h(\mathbf{z})$ is an unknown explicitly nonlinear function of $\mathbf{z}$ and needs to be identified.

The identification of the reduced model can be achieved by taking advantage of a known relationship in the physical space

$$\mathbf{f} = H(\mathbf{x}) \tag{3.40}$$

where $\mathbf{x}$ and $\mathbf{f}$ are the high-dimensional state vector and the corresponding loading vector in the physical space, respectively, and $H(\mathbf{x})$ defines the relationship between $\mathbf{x}$ and $\mathbf{f}$. $H(\mathbf{x})$ is an implicitly nonlinear function of $\mathbf{x}$ and is represented in the form of the numerical load-response data. Due to the existence of nonlinear coupling, it is difficult to utilise $H(\mathbf{x})$. However, this difficulty can be overcome by applying a space transformation operator, B,

$$\begin{aligned} \mathbf{z} &= B(\mathbf{x}) \\ \mathbf{f}_{re} &= B(\mathbf{f}) \end{aligned} \tag{3.41}$$

to Equation 3.39, which results in

$$B(\mathbf{f}) = h(B(\mathbf{x})) \tag{3.42}$$

Equation 3.42 states that the relationship, $H(\mathbf{x})$, in the physical space, is transformed into the generalised space in the form of numerical data and the relationship, $h(\mathbf{z})$, can be identified using the transformed numerical data. The effectiveness of the reduced model mainly depends on the selection of the generalised space.

A POD feature space is by far the best choice for a standard Galerkin approximation, because the contribution of the higher POMs decays most rapidly [50]. Consequently, in this thesis, a POD feature space is selected as a generalised feature space to conduct a model reduction, i.e. the space transformation operator, B, is determined by the dominant POMs. A reduced model constructed in the POD feature space can satisfy the following specifications in conducting a parameter study

- Generic, repeatable for other physical processes or engineering designs. A generic procedure means that detailed physical insight is not required when deriving a reduced order model.
- Able to approximate the original physical system within a subspace of its parameter space in terms of dynamics of interest.
- Computationally efficient and tractable.

3.6.2 Determination of a POD feature space

Following the basic concepts of POD, described in Section 3.5, a POD feature space is constructed as follows.

1. Conduct dynamic analysis of a nonlinear structure using a FEM code (or other numerical code).
2. Record all of the time series of the nodes selected and form a response ensemble using the snapshot method, explained in Section 3.5.3 (each column and each row of this ensemble matrix collect the displacement time series of one node and all nodal displacements at a snapshot).
3. Calculate the mean of each nodal displacement time series, $\bar{\mathbf{x}}$.
4. Subtract the mean from the response ensemble obtained in step (1) to form a modified response ensemble, $\mathbf{X}$, using Equation 3.34.
5. Calculate the covariance matrix, S, using Equation 3.35.

6. Conduct an SVD calculation of the the covariance matrix, S, using Equation 3.36 to obtain POMs and POVs.

7. Determine the number of POMs preserved, using the POD reduction criterion presented in Equation 3.38.

8. Form a POD feature space using the remaining POMs.

POM is an optimal basis which contains more information than any other ones and can also be applied in computations with different parameters or initial conditions. In other words, the reduced model obtained at one parameter value simulation can be performed for a range of parameter values, if dominant POMs do not change over a range of parameters of interest. Hence, a reduced model in a POD feature space can be used in lieu of the original model, to conduct the parameter study within a subspace of the parameter space of the original system. However, this application has to be considered with caution. Even if the same bifurcation patterns is found, simulations of the original system in a range of parameter values may be necessary [50].

3.6.3 Determination of a reduced model

One of the most widely used methods for model reduction of general dynamic systems is to apply a POD to the state space, and use Galerkin projection to construct the reduced system [6]. However, a disadvantage of the method is that the original full order equations of motion must be available to construct the reduced order model. This requirement is not satisfied when a system is modelled using a commercial code, or only some measurement data of the structure are available. Additionally, Samaio and Soize [107] used six continuously nonlinear examples to demonstrate that POMs are no more efficient than the linear modal bases when both of the bases are used to construct a reduced model as a predictive model for any expiation, using Galerkin projection directly. System identification methods have been proposed to overcome these difficulties [36].

Practical system identification begins with experiment design or numerical simulation to collect the data that we will use it to identify a system. This is followed by choosing a model structure, applying functional expansion to approximate the nonlinearity, and then implementing least-squares or optimization algorithms to estimate the parameters. The original data sets from experiments or simulations are very important. The designed experiments should excite all necessary conditions and contain all dynamics that we are interested in and which eventually will be expressed in the identified model. To identify a system in the time domain, a large amount of data may be needed, and the noise level must be considered. In the frequency domain, one must be careful if the actual input is fed back from the output, since spectral and correlation analysis may not be reliable. It is necessary to choose a proper excitation to the system so the measured response reflects all the dynamics needed.

In this thesis, an explicit form of $h(\mathbf{z})$ is assumed in a POD feature space with unknown coefficients. To determine all of these unknown coefficients of the assumed reduced model, a parameter identification technique must be used which can take output and/or input data from an input-output source represented by Equation 3.40. Lucia et al. [49] provide a comprehensive review of reduced modelling methods based upon parameter identification.

Parametric identification methods can be classified as parametric and non-parametric:

- Parametric identification methods assume a specific mathematical form of the system, for example, a SDOF system, and the aim is to identify the parameters included in the assumed model. The nonlinearities are represented by an explicit analytical function. When the parameters appear implicitly, a complicated model with coupling terms for example, a FEM model is needed, which is not considered in this work. Friswell and Mottershead [108] gave an excellent introduction to the area of model updating. The recorded responses and known loads are used to find these parameters by employing regression analysis.

- Nonparametric identification methods are more general in nature, as the system is regarded as a black box. Both type and location of the nonlinearities are unknown, thus creating admissible conditions for either an undetermined problem or an ill-posed one (which cannot be solved using FEM codes). An ideal nonparametric method has not been found but a number of techniques, such as Hilbert Transform or the Volterra Kernels, have been employed [36]. However, non-parametric methods, in most cases, do not yield a single model that would capture the entire dynamic behaviour, but rather result in different models for each value of the system parameter [109].

Masry and Caughey [110] laid the basis of one of the most used nonparametric identification methods: Restoring Force Surface (RFS). This time domain technique seeks to determine the nonlinear term of a SDOF system by measuring different state variables, including displacements and velocities and plotting them in a 3D diagram. This resulting diagram is then represented by Chebysev polynomials. Masry et al. [111] applied the RFS method to identify a MDOF system in a modal space and built a similar diagram. However, the localisation of nonlinearities in the original physical space becomes difficult because it is impossible to track back. It is a common problem that exists when employing a generalised space.

Al-Hadid and Wright [112] developed a force-state mapping technique to achieve the localisation of nonlinearities in a lumped model. They claimed that the use of Chebysev polynomials can be replaced with ordinary polynomials, with a faster and accurate identification for most nonlinearities. Therefore, in this thesis, general polynomials are used to represent nonlinearities in reduced models.

McEwan et al. [60] performed model reduction in a modal space formed by a set of modal modes when encountering geometric nonlinearity. In this work, a static nonlinear FEM code was used to prompt the generation of a reduced model. The idea of generating reduced models based upon FEM results has been studied extensively ([60]– [65]). All these methods construct the reduced model in modal spaces and take advantage of the power of commercial codes. Attar and Dowell [66] developed a reduced nonlinear structural model that expresses the strain energy functions as a polynomial in its modal space, and mentioned POMs can be used in place of the normal modes.

In this thesis, the technique used can be regarded as parametric. A reduced model is assumed in a POD feature space. The parameters of the reduced model appear explicitly and are constant, as opposed to the nonlinear case in which such parameters are amplitude dependent.

Commercial FEM codes are employed as a process external to the procedure of parametric identification and thus achieve the goal of leveraging the power of commercial codes to increase the range of problems that can be solved. With the assumed model,

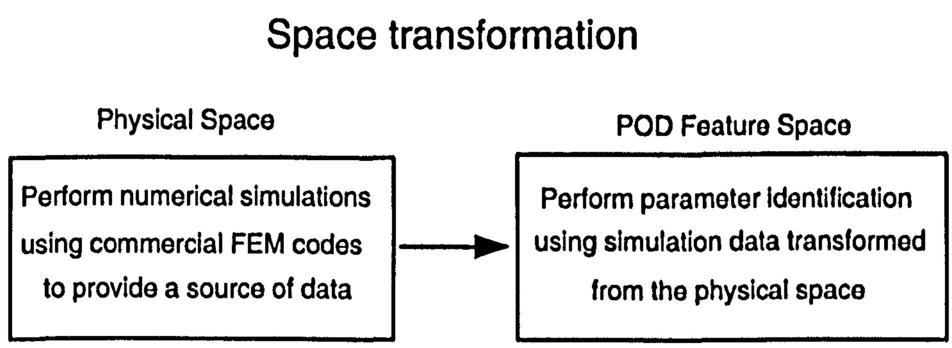

Figure 3.2: Space transformation

the simulation data obtained from the commercial FEM codes are used to modulate the model and provide a solution in the form of identified system parameters, shown in Figure 3.2. The space transformation between the physical space and the POD feature space can be determined by a transformation matrix $\mathbf{P}_r$ whose columns are the dominant POMs according to the reduction criterion (see Equation 3.38)

$$\mathbf{x} = \mathbf{P}_r\mathbf{z} + \bar{\mathbf{x}} \tag{3.43}$$

where $\mathbf{x}$ and $\mathbf{z}$ are the state variables in the Lagrangian space and in the POD feature space respectively, and $\bar{\mathbf{x}}$ is the mean vector with each element as the mean of the corresponding state variable time series.

In this thesis, the least square method is used to perform the parametric identification. The identified model in the POD feature space is capable of predicting the physical responses within a limited range, however, the physical nonlinear components in the physical space remain a black box. The use of POD-based generalised model reduction has at least three advantages over the other generalised space based model reduction approaches, thus making it more attractive from a computational point of view:

- The consideration of nonlinearities in terms of statistics improves the generality of this approach.
- The existence of the reduction criterion makes it relatively easy to construct a reduced model.
- The effectiveness of POMs results in a very low-dimensional model and therefore

allows for further improvement in computational performance of parameter studies.

3.7 Modelling global dynamics using a reduced model

A typical structure has many DOF but much of the qualitative dynamic behaviour may be derived from the study of a corresponding low-dimensional model. For such studies, it is necessary to vary parameters. In structures, the important parameters which may be varied are the forcing amplitude, forcing frequency and structural damping for a given nonlinearity. A control over initial conditions is also needed. For some set of parameters, a nonlinear structure may exhibit more than on type of dynamic regimes, depending on its initial state. Thus to obtain the global behaviour of a structure and the dependable regimes, simulations need to be carried out for a range of initial conditions as well as the control parameters. While it is desirable that response be explored for a large range of control parameters, some of them may lie far away from the normal state of a structure and may occur infrequently only. It is of interest also to examine the vulnerability of the structural response to different forms or levels of nonlinearity. For some structures, a periodic form of excitation gives the worst response. It helps to understand the long term dynamics of a structure with minimum of complexity. In practice, it could be a pulse force or some other forcing function varying with time.

A parameter study, explained in Chapter 2.2.1, becomes very tractable if the model can be constructed based on a few POMs. Once the POD feature space is obtained, a reduced model can be constructed in the POD feature space. This reduced model has the potential of effectively performing parameter studies for nonlinear structures and therefore may be one of the best tools for structural engineers to use to understand the global behaviour of the nonlinear structures.

Clearly, due to a loss of the information contained in the original model, the reduced model cannot provide identical results for the whole parameter space. However, the reduced model is able to approximate reality to some extent. For example, Sanchez and Nayfeh [113] used a SDOF model to characterise the global behavior of the system by bifurcation diagrams that identify the instabilities that appear when one of the excitations is slowly varied.

To enure the safety and robustness of a nonlinear structure, the understanding of global qualitative behaviour is perhaps more important than a rigorous quantitative evaluation based on an allowable safe value. Therefore, the main objective in this thesis is to understand global behaviour of nonlinear dynamic structures rather than specify an accurate but very small safe region. Pushover analysis uses a similar strategy and is based on the assumption that the response of the structure can be related to the response of an equivalent SDOF system [2]. Vamvatsikos and Cornell [21] developed incremental dynamic analyses to produce estimates of the dynamic capacity of the global structural system.

The proposed approach of conducting parameter studies can be divided into three stages. The first stage consists of generating structural responses for a set of system parameters using a FEM model. The second stage is to build a reduced model in a POD feature space using the above data and the dynamics contained in the data. Two different methods are proposed to build up a reduced model in this thesis. The first one subsequently explained in Chapter 5 and illustrated in Figure 5.1, uses nonlinear static FEM simulations. The second one proposed in Chapter 6 and illustrated in Figure 6.1, uses nonlinear dynamic FEM simulations. The former is limited to the case of geometric nonlinearity, while the latter is capable of handling different nonlinearities. During the third stage, simulations are carried out using the reduced model and if necessary the model is refined to extend the range of system parameters. Figure 3.3 illustrates this approach schematically. By performing a parameter study, dependable regions in the parameter space of the system can be identified. Dependable regions are those where the response of the system does not change significantly in comparison to the changes in loading and system parameters.

3.8 Conclusion

In this chapter, model reduction methods were reviewed to identify a proper method which takes advantage of FEM capabilities but does not require a lot of computational effort to study the vulnerability and integrity of nonlinear dynamic structures.

Typical model reduction methods in structural dynamics, based upon physical coordinate space, require the modification of mass and stiffness matrices of nonlinear FEM models and thus, cannot make use of codes of commercial FEM packages. Therefore, they are not suitable for implementing a parameter study of complex nonlinear structures.

Model reduction methods, based upon a generalised space, may provide an effective reduced model to investigate the global behaviour of a nonlinear dynamic structure, with reasonable computational cost. These methods, based on statistical feature extraction, have many potential advantages, in nonlinear structural dynamics, over those based upon physical insights, as the dynamic behaviour of the nonlinear structures can be approximated more effectively by a small number of space basis. These methods, based on statistical feature extraction, have been shown to be applicable in conjunction with commercial FEM codes, which opens a new frontier for their application to more complex nonlinear structural systems.

The use of a POD feature space, potentially, provides an excellent tool to study dynamic behaviour of nonlinear structures and therefore can be used to assess the vulnerability of nonlinear dynamic structures. A reduced model constructed in the POD feature space will make it practical to do parameter studies and to investigate the global behaviour of nonlinear structures.

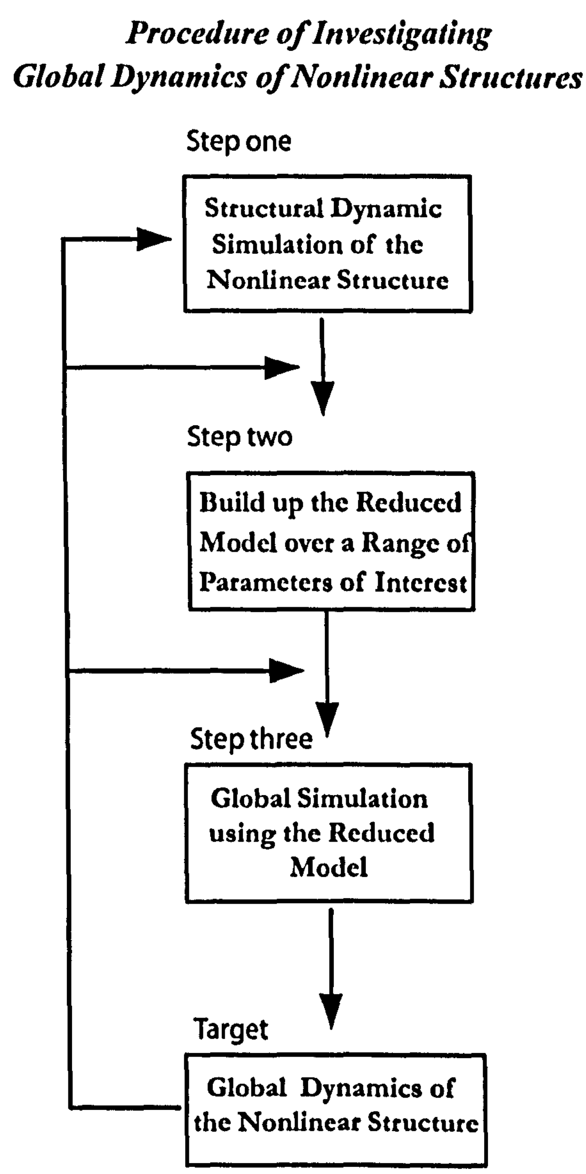

Figure 3.3: Procedure of global modelling

Chapter 4

POM-based Vulnerability Assessment

4.1 Objectives

- To introduce Vulnerability Theory of linear static structures
- To propose a new approach to assess vulnerability of nonlinear dynamic structures by means of POMs
- To illustrate the proposed approach on a planar truss with material nonlinearity and examine its effectiveness

4.2 Introduction

A lesson from many structural failures is that the risk of incredible scenarios is not zero - they do happen and when they do there are enormous consequences. In such situations, it is but natural for engineers to review their approach to design methods. In 1968, 'disproportionate' failure of a block of flats at Ronan Point due to a gas explosion led to the way the structures were designed. Building Regulations and the codes of practice were revised to include additional criteria in the form of 'key elements' and tie bars. Following the collapse of World Trade Centre towers in September 2001, there has been a renewed interest amongst designers, owners and governments in protecting buildings against terrorist attacks and to avoid progressive collapse. It is notable that SCOSS

(Standing Committee on Structural Safety in UK) [114] had emphasized the need to avoid possible progressive collapse mechanisms even prior to WTC collapse. A report by the Institution of Structural Engineers [115] called for research and development on 'vulnerability to progressive collapse' and many other interrelated topics. Revisions to Building Regulations in the UK now require a systematic risk assessment of hazards for Class 3 structures [116].

Although robustness is defined in many different ways by different groups, a structure may be called robust if it can withstand arbitrary damage. Conversely a structure is vulnerable if a small damage produces disproportionately large consequences. One insight into the lack of robustness is gained by identifying how a system is vulnerable since this indicates how it is weakest. A structure which is not properly configured or formed is a potential hazard. A theory of structural vulnerability, reported previously (e.g. [117], [118]) has been developed to identify vulnerable scenarios for a linear static structure. The failure scenarios can then be analysed for different external actions. In this chapter, a new approach that builds upon and complement the structural vulnerability theory by including nonlinearities and dynamics, is proposed.

4.3 A new vulnerability assessment method

A new method for performing a vulnerability assessment of a nonlinear dynamic structure using POMs, is proposed. The POM features of a nonlinear structure reflect the statistical features that are very useful for representing and characterising structural dynamics, described in Section 3.3.3. Hence, the use of POMs has the potential to efficiently assess vulnerability of complex nonlinear structures. An investigation into vulnerability studies is closely related to damage detection in structural dynamics. When the modes of structural failures are finite and known, the vulnerability of a structure can be defined in terms of a comparison between two different statistical features of the structure viz. the original initial state and the damaged state. Hence, feature extraction is a key step for vulnerability assessments. Most of the damage identification methods rely on linear structural models, and cannot account for the nonlinear effects of such a damage scenario [119]. POMs have the increased amount of information from loads and better sensitivity to structural parameter changes than linear features (e.g. modal basis). Thus, POMs have the potential to enhance this damage identification significantly. There have been some developments on the application of POD in relation to damage identification. Lanata and Grosso [120] detected damage initiation using the product of POMs and corresponding POVs. Location of damage was identified by studying the changes of POMs. Galvanetto and Violaris [121] selected the change of the first POM as an indicator of damage to study a linear cantilever and used the discontinuity on the slope of the difference of the first POMs between damaged structures and undamaged structures to locate damage.

With the support of the structural vulnerability theory, a new approach is developed for the vulnerability assessment of structures where dynamics effects and non-linear effects become important. The proposed approach uses POMs to investigate the effects of the external actions, as well as member failures. The motivation behind this work is to take advantage of the spatial POD information to improve the understanding of robustness of nonlinear structures.

4.4 Structural vulnerability analysis

4.4.1 Structural vulnerability theory

Structural vulnerability theory ([117], [118], [33]) is an innovative systems theory of the form of a structure. The purpose of the theory is to help provide structural integrity by addressing the way in which a structure is connected together. The theory enables the form of a structure to be described so that the quality of its connectivity can be measured. This quality is called the 'well-formedness' of the structure. For static conditions well-formedness is a function of, amongst other things, stiffness of the members and it is obtained as:

$$q = \|\mathbf{K}_{ii}\| \tag{4.1}$$

where $\mathbf{K}_{ii}$ is the sub-matrix associated with the joint i. This measure is used to create a hierarchical model of the structure. The hierarchical model starts with the identification of primitive structural 'rings' (or rounds in a 3D structure) made of joints and members at the first and familiar definition of a structure. Clusters of these rings are then formed according to their well-formedness and the degree of connectivity. New sets of rings of clusters are formed to provide a second level of definition of the structure. The process of clustering is repeated to form even higher levels of definitions until one single cluster, the whole structure, remains. The most well-formed parts of the structure appear early at the bottom of hierarchy and those with weaker links join later.

A failure scenario is a sequence of deteriorating events that damage a structure. This may result in the structure becoming a mechanism. Structural vulnerability theory is concerned with identifying failure scenarios that result in disproportionate consequences. These are found by searching for the most vulnerable parts of a structure. In other words, these clusters are then 'unzipped' by a series of deteriorating events (e.g. by introducing a pin into a member) to form a failure scenario. The systematic search of the hierarchical model of the structure results in a set of failure scenarios which are then evaluated with respect to their vulnerability. The analysis leads to different types of failure scenarios and which include the minimum demand scenario and the most vulnerable scenario. In recent work [122], failure scenarios have been subsequently examined for the chance of failure under specific actions and loads thus producing a measure of structural risk.

The vulnerability of a structure is evaluated in terms of the effort required for a damage and the structural consequences produced by that damage. Damage effort is determined using member properties and is used in a relative sense. Relative damage demand measure is defined as the ratio of the damage demand of a failure scenario to the maximum possible damage demand (i.e. failure of all members in the structure). The consequences of a failure scenario in terms of the damage in structural form have been defined as the separateness of the structure. The separateness for a failure scenario is the ratio of the loss of structural well-formedness caused by the failure scenario to the well-formedness of the undamaged structure. The ratio of the separateness caused by a failure scenario to the relative damage demand of that failure scenario determines the vulnerability measure, which is a measure of the vulnerability of a structure. It indicates the efficiency of the sequence of deteriorating events in causing damage to the structure, where, the higher the vulnerability measure, the higher the disproportionateness of the failure scenario. More details are available in([123], [124], [33] and [125]). However, most of this work is for linear static structures.

4.4.2 Well-formedness of dynamic systems

It is well established that sudden failure of a member can lead to vibrations. A member failure due to buckling has a potential to cause a dynamic jump depending upon the rate of change of load decrease as compared to the stiffness of the remaining structure. In a sudden failure of a member, energy stored in a member is released causing a state of vibrations. Although the duration of such vibrations may be short but the structure is likely to see transient loads and displacements greater than the values given by a static analysis. Hence, for dynamic systems the well-formedness measure should also be a function of the mass and damping properties.

A preliminary study [33] resulted in a new measure for linear dynamic systems based on an equivalent stiffness which is analogous to impedance in electrical circuits. For steady-state vibrations, well-formedness has been obtained as:

$$q = \|\mathbf{K}_{jj} - \omega_n^2 \mathbf{M}_{jj}\| \tag{4.2}$$

where $\mathbf{K}_{jj}$ and $\mathbf{M}_{jj}$ are the stiffness and mass sub-matrices at joint j and ω is a natural frequency of the system. It is evident that for no vibrations this measure reduces to Equation 4.1, the one used for static cases. Also for higher modes of vibrations, well-formedness measure will go on reducing. For linear systems where multiple modes get excited, well-formedness can be obtained by considering the relative contributions of different modes. Clustering sequences corresponding to Equation 4.1 (static case) and Equation 4.2 were found to be different for some cases.

4.4.3 An example

A truss structure [125], as shown in Figure 4.1, is modelled as a pin-jointed frame and vulnerability analysis is performed using the computer program SAVE [126]. This uses the measure given by Equation 4.1.

A common sense study of this structure suggests that damage to one of the main members (viz. member 1, 2 or 3) will lead to total collapse unless bracings are able to provide alternate load paths. However, it is not easy to predict the quality of these load

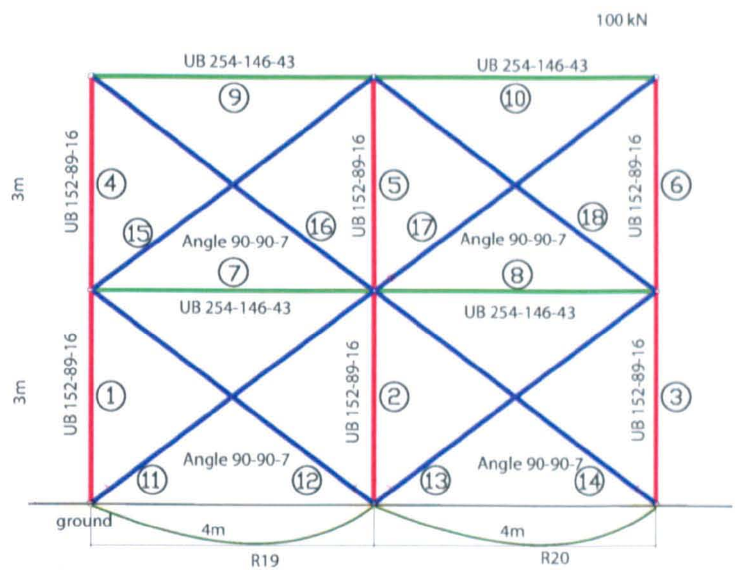

Figure 4.1: An example truss for vulnerability analysis

paths for different external loads.

Figure 4.2 shows the clustering hierarchy for the truss structure. The results of the search for failure scenarios are summarized in Table 4.1. It is evident that the minimum demand scenario (the one that requires least effort to cause damage) and the minimum failure scenario (the one that causes the least consequences) are different. The maximum failure scenario (the one with the highest vulnerability measure) for static case results when members 14, 11, 1, and 3 are damaged. Total collapse of the structure can occur in many different ways but the one with the highest vulnerability measure is the same as the maximum failure scenario in this example structure. The detailed calculation procedure can be found in [124] and [126].

Figure 4.3 to 4.5 illustrate a set of failure scenarios obtained using vulnerability theory which result in total collapse. The critical damage events are the removal of all four diagonals in the ground floor (failure scenario FS 1) and were identified as the maximum failure scenario as they produce the highest vulnerability measure in Table 4.2. Although, structural vulnerability theory does not consider any applied loads, it does represent, the scenario that requires the least amount of effort to cause maximum consequences.

It is worth noting that the numerical values obtained here help in ranking different

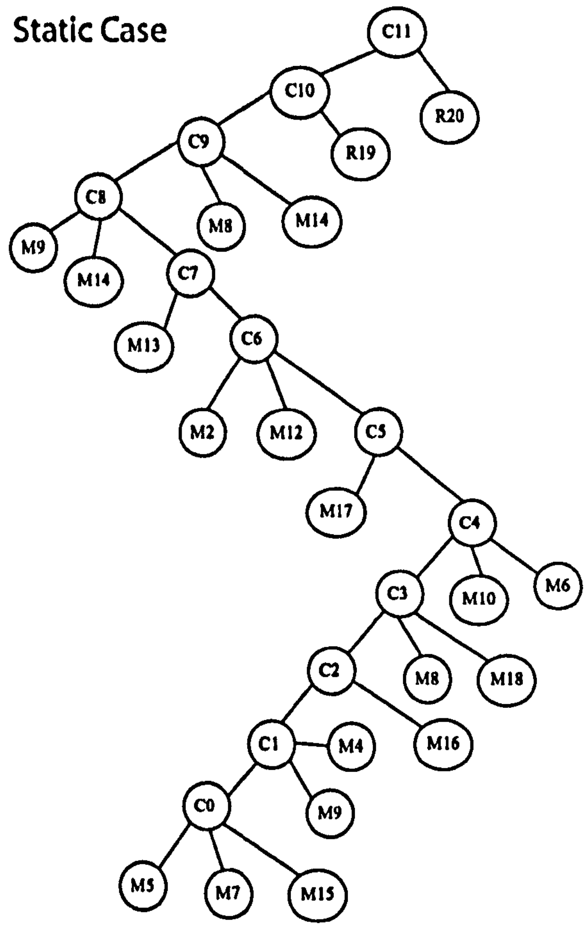

Figure 4.2: Clustering hierarchy for the example structure using wellformedness defined by Equation 4.1

Type of failure scenario	Minimum demand scenario	Minimum failure scenario	Maximum failure scenario	Total failure scenario (max)	Specific failure scenario
Deterioration events	Member 12 (pin)	Member 11,1 (pin)	Member 14,11,1,3 (pin)	Member 11,14,13,12 (pin)	Member 15 (pin)
Damage demand	0.011	0.05	0.099	0.044	0.011
Structural consequence	0.051	0.015	1.0	1.0	0.071
Vulnerability measure	4.611	0.303	10.077	22.534	6.401

Table 4.1: Failure scenarios for the example

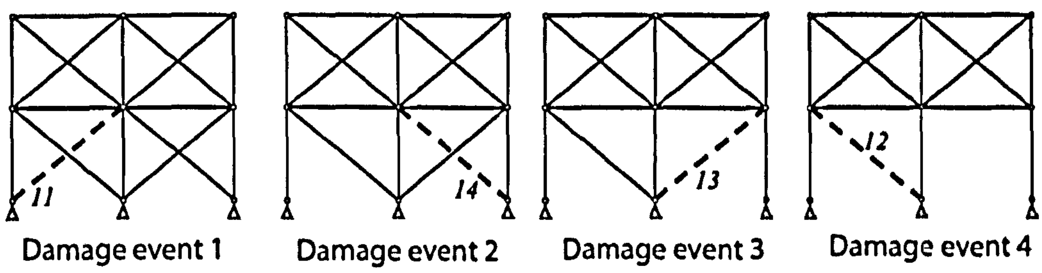

Figure 4.3: Total failure scenario FS1

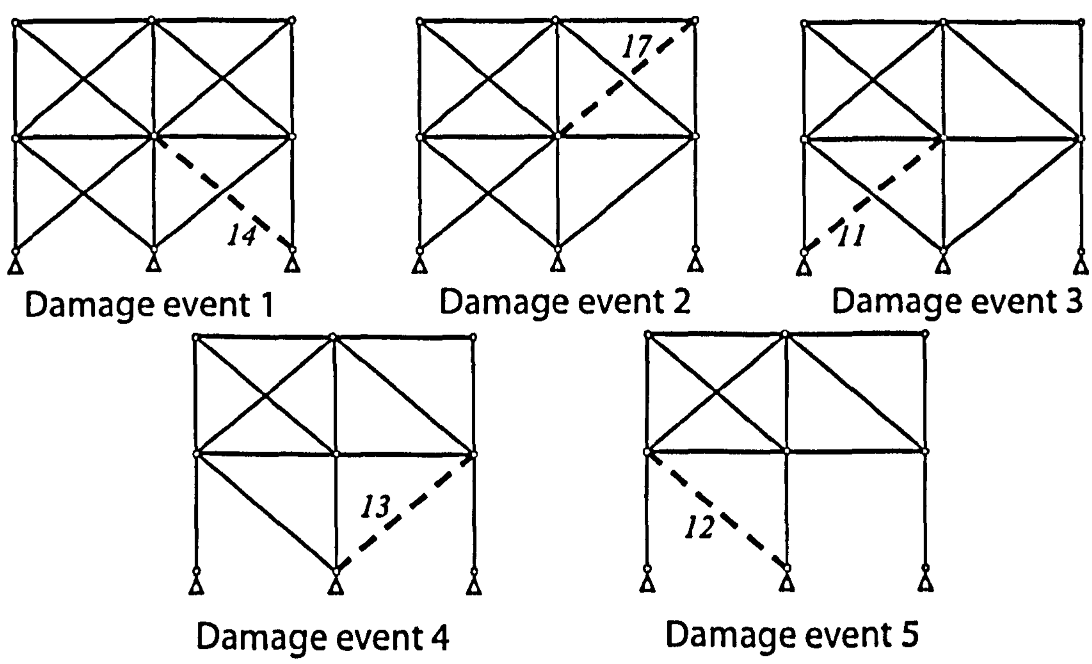

Figure 4.4: Total failure scenario FS2

failure scenarios for a given structure. The results in [127] show that such ranking can differ when properties governing dynamic behaviour are included. Clearly it is not easy to identify the set of loads which would result in the identified maximum failure scenario. To overcome these limitations, a new approach is presented in the next section. It includes the dynamic loads and nonlinearities in a structure.

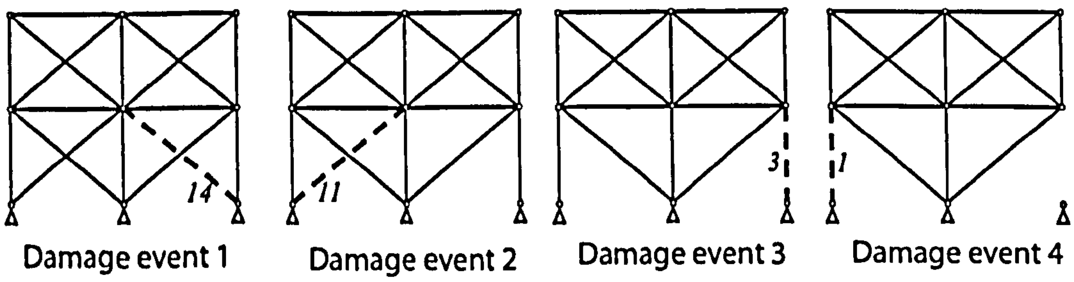

Figure 4.5: Total failure scenario FS3

Failure scenario	Damage demand	Structural consequence	Vulnerability measure
FS1 (see Figure 4.3)	0.044	1.0	22.534
FS2 (see Figure 4.4)	0.055	1.0	18.027
FS3 (see Figure 4.5)	0.099	1.0	10.077

Table 4.2: Vulnerability results of static analysis

4.5 Vulnerability assessment using POMs

In a structure, displacements at different nodes are highly correlated. This correlation stems from basic engineering principles such as energy balance and deformation compatibility that exist among nodal displacements. As described in Chapter 3.5, POD is a good tool to exploit the correlation among states variables and effectively represent the information hidden in structural responses. More importantly, as a global feature, POMs extracted by using POD are sensitive to the changes in the corresponding nonlinear structural system and could be used for vulnerability studies.

4.5.1 The proposed method

The study of variations of vibration properties is one effective method that identifies the changes of the whole structural behaviour [119]. Natural frequency and mode shape are common global characteristics of a structure. The study of their changes can detect and locate the presence of damage ([128], [129] and [130]). However, they only represent the linear properties of the structure and corresponding boundary conditions and lack enough sensitivity of identifying damages. Sohn and Law [68] proved the superior performance of Ritz basis over modal basis in the area of damage diagnoses and states that the

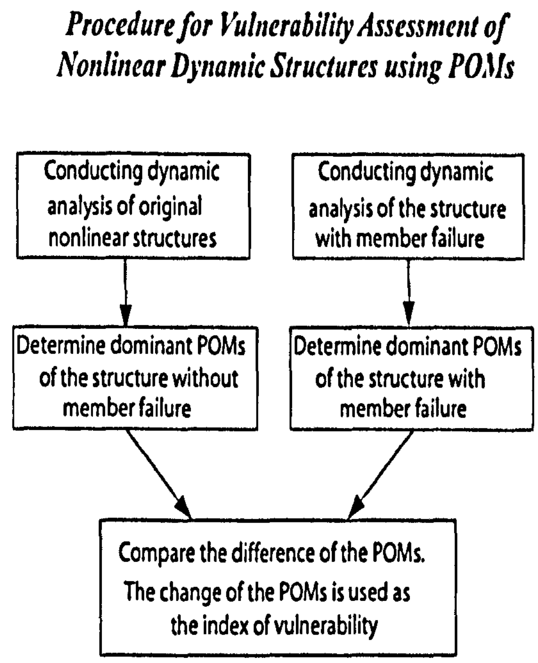

Figure 4.6: The procedure of generating a measure of vulnerability using POMs

increased amount of information and better sensitivity to structural parameter changes, could improve the results of damage detection, test-analysis correlation, model refinement and system identification. However, Ritz basis require the physical-insight knowledge e.g. mass and stiffness matrices, which is not available for practical structures, explained in Section 3.3.2.

In contrast, POD is based upon statistical feature extraction and thus does not require the physical-insight knowledge. Resulting POMs can represent characteristics of nonlinear structures and can be effectively used to assess their vulnerability. Hence, the change of a POD feature space, represented by a set of POMs, is selected as a measure of vulnerability of nonlinear dynamic structures. The proposed approach is outlined in Figure 4.6. The primary goal is to quantitatively identify some characteristics of the nonlinear dynamic structure which change as a result of the structural failure. A comparison of the POMs before and after failure leads to a simple but effective way to assess vulnerability of nonlinear dynamic structures. During this comparison procedure, all nodal displacements of nonlinear structures are used to determine the basis of a POD feature space. Failure scenarios determined by using static vulnerability analysis (Section 4.4.1) are used.

The influence of a member failure can be examined by comparing the POMs for the original structure and for the damaged structure. The vulnerability of a structure in such cases will depend on the identification of vulnerable members in the member topology of the structure. Based on this, a new measure of vulnerability of structure to damage propagation has been developed as

$$q_{POD} = \Sigma_{i=1}^{n} \lambda_i (\phi_i^{orig} - \phi_i^{damage})^2 \tag{4.3}$$

where λ_i is ith POV, and ϕ_i^{orig} and ϕ_i^{damage} are ith POMs of the original and damaged structure respectively. The magnitude of the measure gives relative vulnerability of the damaged member. The measure includes the effects of loads unlike the previous work in [33]. When comparing different structures, a robust structure is the one where resulting changes in the above measure are the least.

In the next section, POMs will be applied to assess the structural vulnerability of a truss with material nonlinearities. The purpose of this analysis is to complement the results obtained with the static vulnerability analysis in Section 4.4.1. The static vulnerability analysis identifies potential weakness in a structure by examining the way a structure is connected together and limits its application to linear structures as this approach does not consider loads. The new vulnerability analysis proposed, provides a general procedure of quantitatively and qualitatively assessing the vulnerability of nonlinear dynamic structures. The computation of POMs is closely associated with the loads and different loads might lead to different POMs. However, an ideal structure would be the one which shows the least changes in POMs as the loads changes.

4.5.2 A numerical example

A plane truss as shown in Figure 4.7 is considered. Figure 4.8 depicts the DOF information of the truss. This truss has previously been analysed with linear material model has previously been analysed utilising structural vulnerability theory (Section 4.4.3) using the measure given by Equation 4.1 and the most vulnerable failure scenario is found to be the successive failure of member 11, member 14, member 13 and member 12.

For the present analysis, a nonlinear material model was chosen. For the bars under

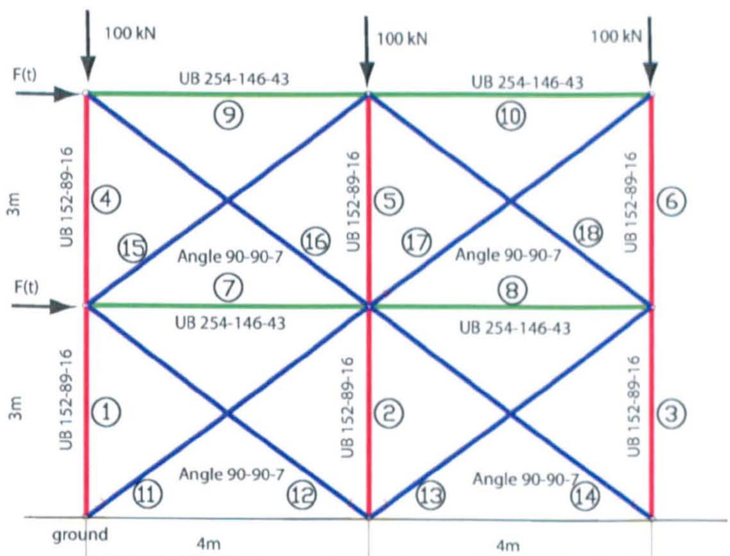

Figure 4.7: Truss configuration and loads

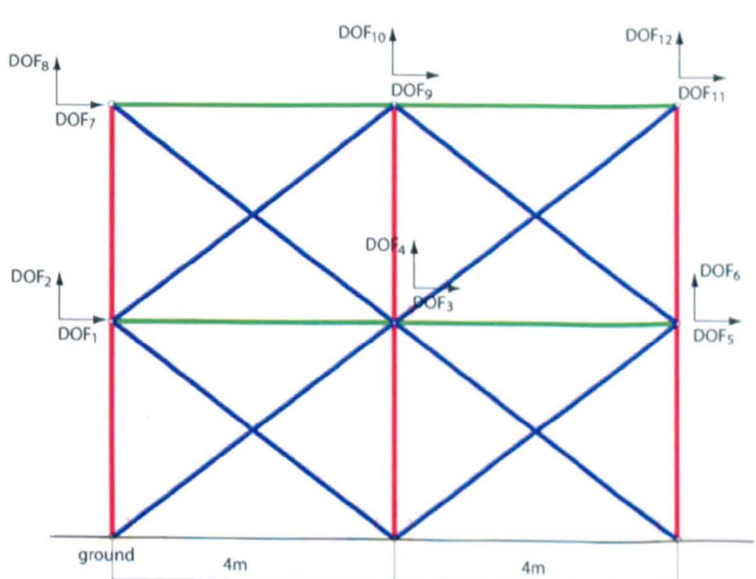

Figure 4.8: Truss DOF

tension, a piecewise-linear stress-strain material relationship was used

$$E = \begin{cases} 210e9\,MPa & \text{for } \epsilon \leq 0.0013 \\ 35e9\,MPa & \text{for } 0.0013 < \epsilon \leq 0.0039 \\ 5e9\,MPa & \text{for } \epsilon > 0.0039 \end{cases} \tag{4.4}$$

where E is the Young's modulus and ϵ the axial strain of bars. Similarly, for the bars under compression, the material relationship, to take into account the influence of buckling, was modified as

$$E = \begin{cases} 210e9\,MPa & \text{for } \epsilon \leq 0.001 \\ 2e9\,MPa & \text{for } \epsilon > 0.001 \end{cases} \tag{4.5}$$

Two horizontal harmonic loads of the form $F(t) = Fsin(\omega t)$, and three constant vertical loads were applied on the truss. The amplitude of the loads were selected such that the truss behaved nonlinearly. Viscous damping of 2% was also included. Numerical simulations for different cases, described subsequently, were carried out to obtain the displacement time histories of the truss using Dynamic Solver [17]. The behaviour under steady state conditions was recorded by disregarding the first $10s$ data. These response time series were calculated using a time step of $0.001s$ and a time window of $20s$. The horizontal displacement time series at all nodes had been used, while the number of the samples in time were 15000. The time series were arranged to form the response ensemble X, as in Equation 3.33, following the procedure described in Chapter 3. Each column represents a displacement time series at a particular node, while each row represents the spatial distribution of the structural response at a sampling time. The resulting response ensembles were employed to deduce the corresponding POMs. The orthogonal POMs are time invariant and therefore form a POD feature space.

4.5.3 Numerical results and interpretation

From a design point of view, there are three important cases that must be investigated to enable an understanding of the vulnerability and integrity of nonlinear dynamic structures.

- the consequences resulting from a member failure

- the change of the structural behaviour due to a change in the system parameters
- the failure scenarios using vulnerability theory

A. Member failures In order to investigate the vulnerability of the truss, POMs were obtained for different damaged states and compared against the POM of the undamaged structure. A nonlinear material model was used. A lateral harmonic force with an amplitude of $20kN$ and a frequency of 5Hz was applied. Here the magnitudes are not that important because the purpose here is to analyse the effectiveness of POMs in capturing the damage to the system.

Figure 4.9 and 4.10 show the first three POMs and their changes, respectively, corresponding to the damage to member 1 (an exterior column), member 2 (an interior column), member 11 (a bracing) and member 12 (another bracing). The failure of member 1 causes a bigger change in POM-based vulnerability measure as compared to the failure of the other members. This result matches with the findings of a detailed study undertaken separately [125], using structural vulnerability analysis in Section 4.4.3. This suggests that POMs have the potential to identify damage to a system.

The first POM shows identical changes resulting from the loss of either bracing 11 or bracing 12. This seems reasonable considering the positions of the bracings and their contribution in this highly redundant structure. However, the third POM, depicted in Figure 4.10, is able to capture visually the differences between the two. As a quantitative measure, Table 4.3 shows the vulnerability indices of these member failures, using Equation 4.3.

Event	Vulnerability measure
Remove Column 1	0.613
Remove Column 2	0.0986
Remove Brace 11	0.0273
Remove Brace 12	0.0269

Table 4.3: Vulnerability measures of member failures in terms of the change of POMs using Equation 4.3

Interestingly, the third POMs corresponding to the loss of interior and exterior columns

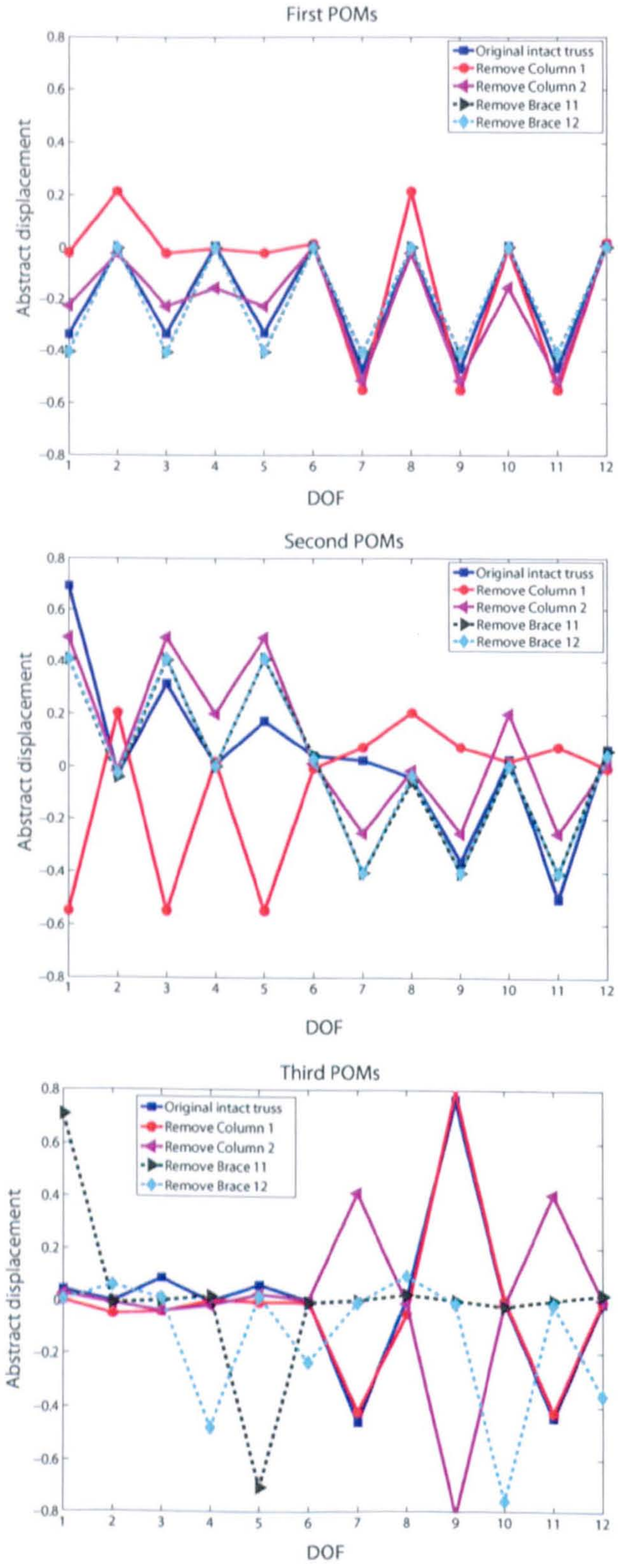

Figure 4.9: POMs corresponding to the failure of different members (frequency 5Hz)

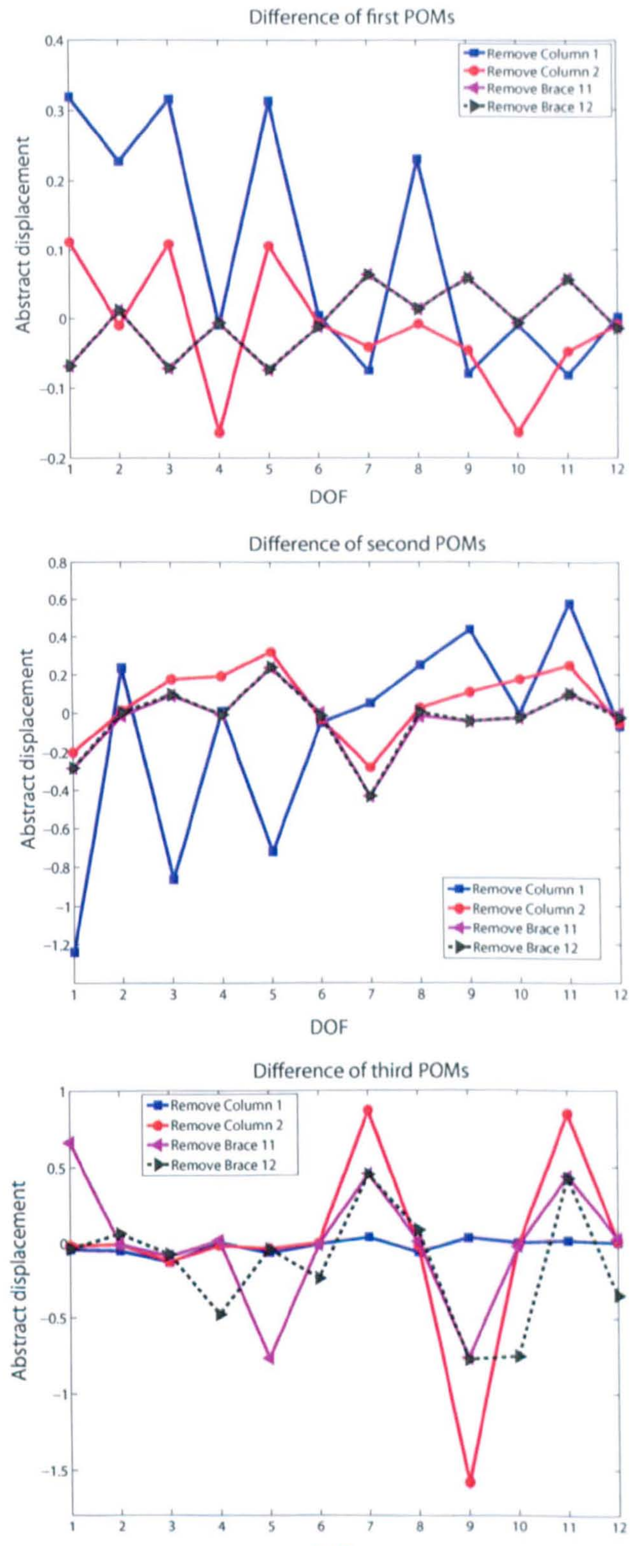

Figure 4.10: The change of POMs corresponding to the failure of different members, compared with the undamage structure(frequency 5Hz)

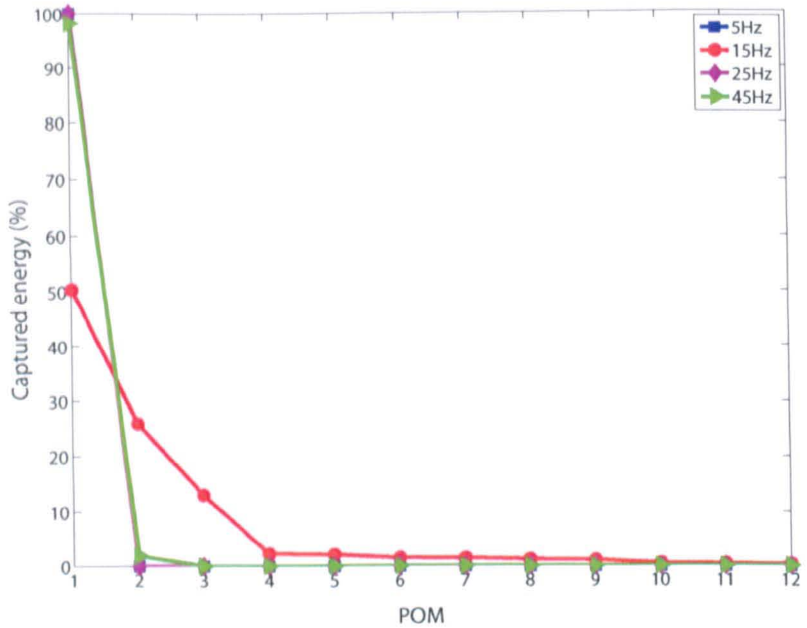

Figure 4.11: Energy captured by the POMs for excitation with 5Hz, 15Hz, 25Hz and 45Hz

are quite similar. The application of Equation 4.3 can help distinguish the different influence of their failures on the structural behaviour.

B. External loads First, the effect of excitation frequency, ω, was studied using the original structure. Lateral harmonic force with a range of frequencies from 5Hz to 200Hz was applied. Note that with a linear material model, the first few natural frequencies of the structure under consideration are about 16Hz, 45Hz, 90Hz and 125Hz.

Figure 4.11 shows that the eigenspectrum of selected response time series for different excitation frequencies to capture 99% of the response energy. The horizontal axis shows the numbers of POMs required to attain 99.99% of the average energy; the vertical axis shows the energy, depicted in Equation 3.35, captured by each POM. For most cases, the analysis identifies, essentially, the first two POMs with more than 99.99% of the total energy. This result shows that the response time series of the structure can be represented by the first two modes. When the excitation frequency is 15Hz, close to the first natural frequency of the structure, the first POM captures nearly 50% of the total energy whilst the second POM captures around 25.8% of the energy. This result suggests that the energy distribution in POMs can illustrate the complexity of structural response to some extent.

The first POMs corresponding to different values of excitation frequencies are shown in Figure 4.12. The horizontal axis corresponds to the size of the POM. It is evident that the first POMs follow a similar pattern under low-frequency excitations. Another similar pattern is observed under high-frequency excitations. The vibration pattern, dominated by the first POM, visually resembles the first linear model shape of the truss. The second POM reveals a relatively local vibration pattern and the third POM shows a more complex pattern in Figure 4.12. According to the un-presented work of the author of the thesis, it is found that the third POMs are sensitive to the sampling rate of the snapshot because of possible numerical errors. This result implies the inclusion of the third POMs might be prejudicial to the assessment of vulnerability.

However, around the excitation frequency of 15Hz the behaviour is quite different as this frequency is close to the first linear natural frequency of the truss. The motion of the structure cannot be captured fully with one or a few POMs, illustrated in Figure 4.11. This case indicates that the distribution of energy in the POMs might be able to illustrate the complexity of nonlinearity. This characteristic can be used to identify different parameter subspaces in which POMs must be separately determined to capture behaviour of nonlinear structures.

C. Failure scenarios POMs were also obtained for the most vulnerable failure scenario obtained using the approach given in Section 4.4.1. This failure scenario 1 consists of four damage events consisting of the failures of member 11, 14, 13 and 12 in succession, shown in Figure 4.3.

The POMs were obtained after each damage event and plotted in Figure 4.13. It is observed that the first POM changes after the loss of member 11 but there is no further change to this POM after the successive damage. However, the influence of successive damage events is observed in the second and third POMs.

It is observed that all of these damage events correspond to the loss of diagonal bracings. In contrast, results from failure scenario 3, plotted in Figure 4.5, show that the failure

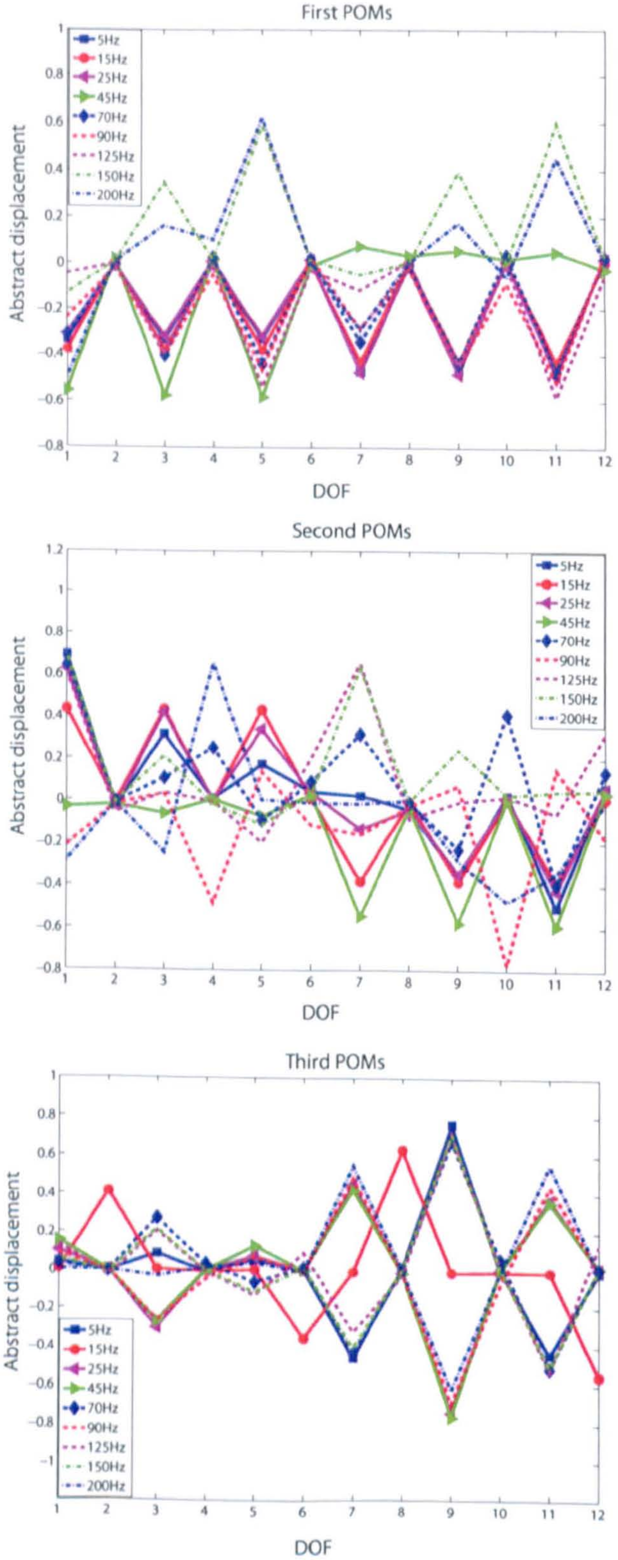

Figure 4.12: The first three POMs for the example truss over a range of frequencies (force amplitude $20kN$)

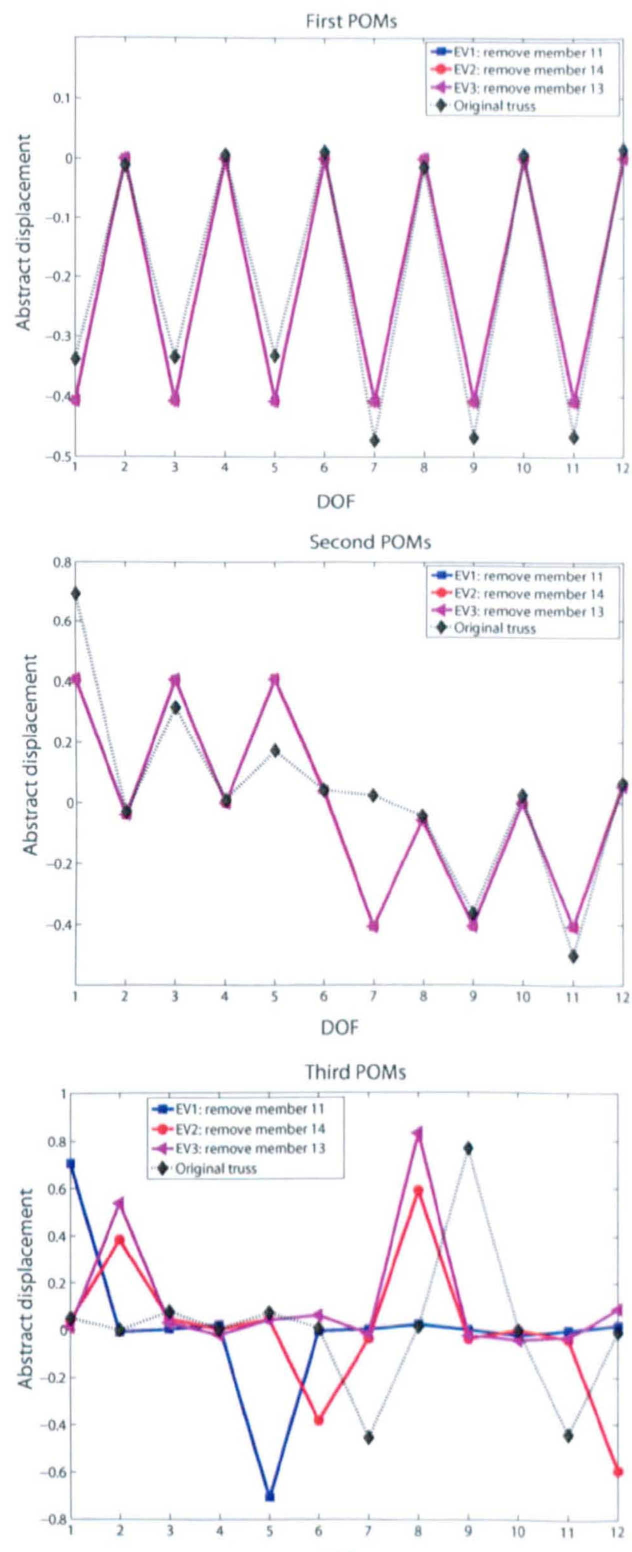

Figure 4.13: POMs after successive damage events in failure scenario 1 (frequency 5Hz)

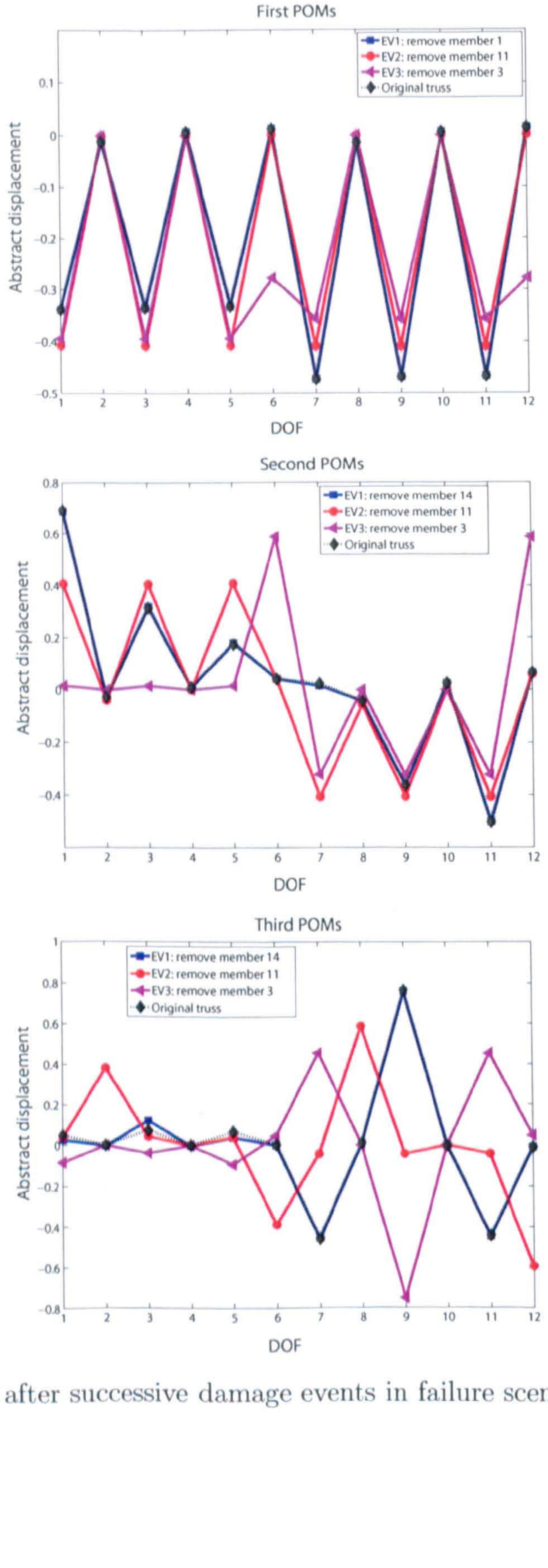

Figure 4.14: POMs after successive damage events in failure scenario 3 (frequency 5Hz)

of member 3 generates a change to the first and second POMs as shown in Figure 4.14. These results suggest that in terms of the influence of damage events, this approach can clearly distinguish the difference between the failure of columns and of bracings.

4.6 Conclusion

The two approaches discussed in this chapter are complementary in the sense that the first (Section 4.4) does not require a model of the loads while the second (Section 4.5) includes the effects of the dynamic loads and nonlinearities.

A measure of the quality of form of a structure is fundamental to the structural vulnerability analysis (Section 4.4). For the example structure, different failure scenarios were obtained by means of vulnerability analysis. The output from such analysis can help examine potential weakness in a structure although not all of them could be exploited by normal loads on the structure. However, the failure scenarios obtained could be further analysed for different external actions thus providing efficient means of counteracting them.

The second approach using POMs has the potential to examine the vulnerability of a structure where response can become nonlinear and where dynamic forces must be included. The properties of the POMs that capture domain features of dynamic systems are used to quantitatively assess the effects of member failures on the global behaviour of the structure. The change of this POD feature space, in terms of the change of its basis i.e. POMs, for some external actions gives a measure of the behaviour changes in the system and thus is an effective measure of vulnerability of members.

This new vulnerability measure has been studied for the cases of member failure, different external excitation and different failure seneccios. The results show that the vulnerability measure in terms of the change of the first and second POMs, is capable of indicating the influence of different member failures. However, the presence of numerical errors can reduce the capability of the approach, if the third or more higher level POMs are used, according to the un-presented work of the author. The use of higher level of POMs requires further studies.

The effectiveness of the proposed method using POMs showed a good potential for practical development because it is easy to implement and it can be integrated with any commercial code. It also provides a practical way to prevent bad structural design and assess existing structures.

Chapter 5

A New Model Reduction Method Based on Nonlinear Static Analysis

5.1 Objectives

- To propose a method of constructing reduced models in a POD feature space for geometrically nonlinear structure using nonlinear static FEM analysis and a parameter identification technique in combination.
- To examine the effectiveness of the proposed method using a fully clamped beam.
- To apply the method to generate reduced models of a planar frame.

5.2 Introduction

As described in Chapter 2, in order to understand global behaviour of complex nonlinear structures, it is necessary to perform a parameter study. However, there are no tractable computational tools available for the study. Mathematical tools in nonlinear dynamics primarily focus on explicit means of approaching this problem and do not have the ability to tackle realistic structures.

In such situations, numerical approaches, such as FEM, must be used. FEM simulations generate accurate results for complex nonlinear structures. For example, Sansour et al. [131] developed efficient FEM discretisation to successfully capture the exact nature of geometric nonlinearity, including chaotic motions. Fotouhi [132] used Ansys [133] to prove that FEM is a reliable approach and can produce acceptable results for large amplitude vibration analysis of very flexible beams. The application of FEM makes the dynamics of structures available in a numerical form. This contains valuable information on the temporal and spatial characteristics of structures, which can be extracted by applying model decomposition approaches described in Section 3.4. As concluded in Section 3.3, a solution would be to seek a more efficient generalised space than a physical space.

5.3 A new model reduction method

Following the idea of building up a reduced model in a generalised spaces, described in Section 3.6, a new POD-based reduction approach is proposed. The objective of this model reduction method is to seek an approximation of the solution in a generalised space spanned by a POD basis, defined by the space transformation matrix, P_r, associated with generalised DOF in the POD feature space. The following assumptions are made in this approach:

- Nonlinearities remain the same constant in static or dynamic analysis,
- Nonlinearities are indeed excited,
- Nonlinearities can be captured by commercial FEM codes.

In the proposed method, a reduced nonlinear model is constructed in a POD feature space, utilising information that can be extracted from any commercial FEM code. The POD feature space is more efficient than the modal space due to both the statistical characteristics of POD and the presence of the reduction criterion using POD. The reduced model constructed using only one or two POMs can capture dynamics of the original system over a parameter range.

Once a POD feature space has been determined according to the snapshot method described in Section 3.5.3, the proposed method transforms structural responses and known loadings in the original Lagrangian space into the POD feature space. A reduced model is constructed in the POD feature space by applying a least-squares technique to the transformed counterpart of those structural responses and loadings. Fig. 5.1 illustrates

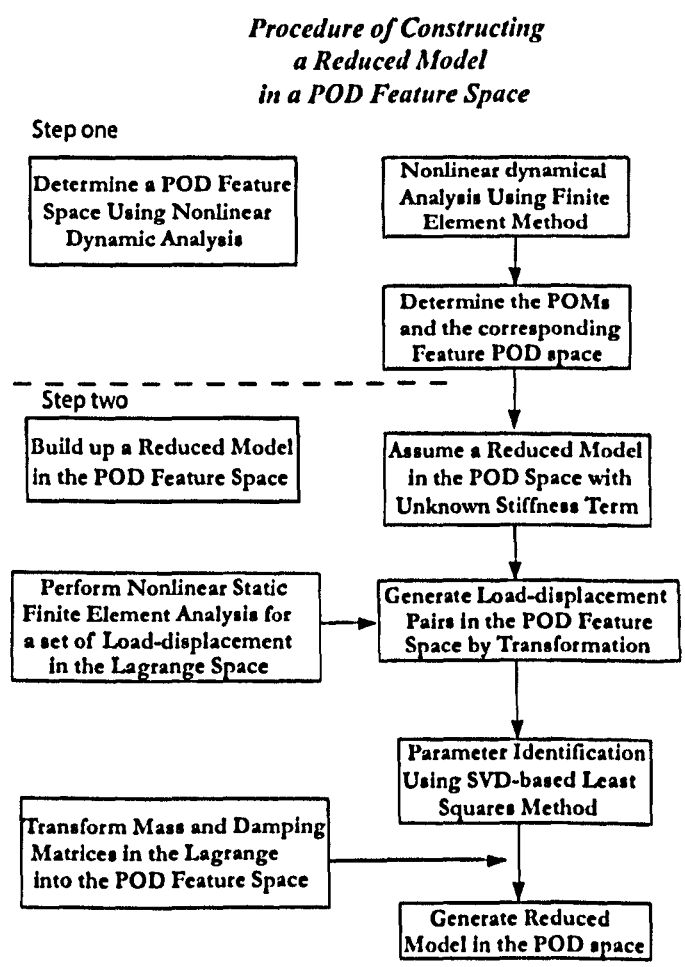

Figure 5.1: Procedure of generating a reduced model

this proposed method schematically. As explained in Section 3.6.3, this approach is a parametric method and well suited for the identification of nonlinear models which are required to perform parameter study. To begin with, the selection of a generalised space and the formulation of reduced models are briefly outlined. Subsequently, the estimation of nonlinear stiffness coefficients of the reduced model is described.

5.4 Selection of a generalised space

The use of a generalised space makes it possible to isolate the use of a commercial FEM code from the rest of the model reduction procedure. A variety of generalised spaces are possible, each with its advantages and limitations (See Section 3.3.2). For example, McEwan et al. [60] selected a modal space as a generalised space to deduce a reduced model of a nonlinear beam. The modal space is formed by a set of linear modal modes. Although modal modes of the underlying linear system are relatively easy to find for a planar structure, the number of modes that has to be kept is not a trivial matter. Additionally, modal basis obtained from the linearised system will, in general, not apply across the full loading range when nonlinearities are present. This is because loads applied on a structure will have a significant effect on the dynamic characteristics of the structure.

POD, as a multivariate statistical method, can be used to investigate the features of highly nonlinear systems, even with complicated geometries. POD approach results in POMs, feature decomposition vectors of the structural response that capture most of the energy within the first few modes. Therefore, the generalization and effectiveness of POD suggests that a POD feature space is better than a modal space as a generalised space to reconstruct a reduced model. The ramification is that the generation of POD basis requires more computational time than that of modal basis.

Nonlinear behaviour of structures such as planar frames with slender members, is due to geometric nonlinearity resulting from a combination of bending and axial stretching effects. Typically for beams, low-order modes involving bending are dominant. However, when structures undergo large deformations, stretching modes gain importance. The geometric nonlinearity couples bending deformation with axial stretching deformation through quadratic stiffness terms. Therefore, the modal modes used to capture the geometric nonlinearity, have to include stretching modes [61]. However in the absence of *a priori* knowledge, the selection of the number of the stretching modes is difficult [60]. The use of POMs overcomes this difficulty because they implicitly include bending modes and stretching modes.

Hence, a POD feature space was selected as the generalised space in which reduced models are reconstructed. The POMs are determined following the procedure described in Section 3.6.2. The selection of POD basis which forms the POD feature space, is achieved using POV criterion, explained in Section 3.5.4.

5.5 Formulation of reduced models

5.5.1 Formulation in a POD feature space

Suppose a nonlinear dynamical structural system can be discretisated by FEM with n spatial DOF $x_i, 1 \leq i \leq n$, which leads to n equations of motion in Lagrangian co-ordinates for forced vibration as follows:

$$\mathbf{M}\ddot{\mathbf{x}}(t) + \mathbf{C}\dot{\mathbf{x}}(t) + \mathbf{K}(x) = \mathbf{f}(t) \tag{5.1}$$

where $\mathbf{M}$ is the mass matrix, $\mathbf{C}$ is the mass proportional damping matrix, $\mathbf{K}(x)$ the stiffness matrix of the system, $\mathbf{f}(t)$ is the external load vector, $\mathbf{x}$ is a displacement vector and $\dot{\mathbf{x}}$ is a velocity vector, in the Lagrangian space. The displacement vector, $\mathbf{x}$, is transformed into a POD feature space, if $\mathbf{P}_r^T\mathbf{M}\mathbf{P}_r = \mathbf{I}$, by the relationship

$$\begin{aligned} \mathbf{z} &= \mathbf{P}_r^T\mathbf{M}(\mathbf{x} - \bar{\mathbf{x}}) \\ \textit{or} \qquad \mathbf{x} &= \mathbf{P}_r\mathbf{z} + \bar{\mathbf{x}} \end{aligned} \tag{5.2}$$

where $\mathbf{z}$ is a displacement vector in the POD feature space, $\bar{\mathbf{x}}$ is the the average displacement of each displacement time series and

$$\mathbf{P}_r = [\mathbf{p}_1\ \mathbf{p}_2\ \ldots \mathbf{p}_r] \tag{5.3}$$

is the transformation matrix containing the first r dominant POMs. In a typical case, the POD feature space contains only a few POMs which correspond to the highest POD values. This results in a much smaller number of displacements in the POD feature space than those in the original Lagrangian space. Substituting Equation 5.2 into Equation 5.1, the equation of motion of a reduced system becomes

$$\mathbf{M}_r\ddot{\mathbf{z}}(t) + \mathbf{C}_r\dot{\mathbf{z}}(t) + \mathbf{K}_r(\mathbf{z}) = \mathbf{f}_{re}(t) \tag{5.4}$$

where

$$\begin{aligned} \mathbf{M}_r &= \mathbf{P}_r^T\mathbf{M}\mathbf{P}_r \in R^{r \times r} \\ \mathbf{C}_r &= \mathbf{P}_r^T\mathbf{C}\mathbf{P}_r \in R^{r \times r} \\ \mathbf{f}_{re}(t) &= \mathbf{P}_r^T\mathbf{f}(t) \end{aligned}$$

where $\mathbf{M}_r$, $\mathbf{C}_r$, $\mathbf{K}_r(z)$ and $\mathbf{f}_{re}(t)$ are the mass, damping stiffness terms and the loads in the POD feature space, respectively. $\mathbf{K}_r(z)$ is the stiffness function of displacements $\mathbf{z}$ in the POD feature space. Matrices $\mathbf{M}_r$ and $\mathbf{C}_r$ are diagonal because of the orthogonality of the POMs. During the coordinate transformation, the number of DOF of the FEM model in the Lagrangian space is reduced by only considering r POMs that have a significant effect on the response within the parameter range of interest. Model reduction methods here seek solutions in the POD feature space generated by a transformation principle defined by Equation 5.2. It should be noted that the equations are coupled only through the stiffness term, $\mathbf{K}_r(z)$, which is an unknown function of transformed displacements, $\mathbf{z}$, in the POD feature space. $\mathbf{K}_r(z)$ cannot be determined because of the existing model coupling. However, by taking advantage of the relationships between the load, $\mathbf{f}(t)$, and the displacement, $\mathbf{x}$, in the Lagrangian space in Equation 5.1, the stiffness term, $\mathbf{K}_r(\mathbf{z})$, in the POD feature space in Equation 5.4 can be determined. For this purpose, system identification methods, briefed in Section 3.3.3 are used. In this thesis, a SVD-based least-squares technique is employed to determine this stiffness term, $\mathbf{K}_r(\mathbf{z})$, in the POD feature space. It uses transformed excitation and response data from commercial FEM codes.

5.5.2 Form of nonlinearities

The choice of mathematical form of nonlinearities has a significant effect on the behaviour and accuracy of the reduced model. Richards and Singh [134] tried various polynomial trial functions to account for the nonlinear behaviour. They concluded that a unique model is still not guaranteed. Masri and Caughey [110] used orthogonal polynomials to represent a non-linear restoring force surface. The introduction of orthogonal polynomials can minimise the likelihood of introducing rounding errors during the identification procedure, as every polynomial is linearly independent. Additionally, the orthogonality of the polynomials means that additional higher order terms may be added without having to re-compute the coefficients of the entire polynomial. However, Al-Hadid and Wright [112] argued that ordinary polynomials are better than orthogonal polynomials in terms of the representation of nonlinearities.

An ordinary polynomial approach has an advantage in that no normalization of the data is required, and no particular arrangement of the load-response pairs is required. It also has an advantage in a multi-mode identification context in that there is no increase in complexity with an increase in the number of basis functions. An increase in the number of basis merely requires the addition of more terms to the initial ordinary polynomial. The use of ordinary polynomials does however have some disadvantages:

- The lack of linear independence between the terms means that the least-squares computation must be repeated every time a term is added to, or removed from, the trial solution.

- The lack of linear independence between the terms also introduces the possibility of numerical ill-conditioning. Numerical ill-conditioning may occur particularly in instances where there are large numbers of basis functions in the approximating series, and where there are large numbers of data points. In these instances, two or more basis functions may be collinear or nearly collinear over the data points, leading to least-squares equations that are singular or near to singular. However, the use of the Singular Value Decomposition (SVD) can overcome this disadvantage.

Thus in this chapter and the next chapter, the stiffness terms of the assumed reduced models, represented by Equation 5.4, are approximated as ordinary polynomials (See

Equation 5.5) of the displacement in a POD feature space. The principle of using a polynomial is to model the relationship between the excitation and response of the reduced model. The number of possible terms increases rapidly with the increasing order of the polynomial. When only considering geometric nonlinearity, Muravyov and Rizzi [65] indicated that nonlinear stiffness term can be in polynomial form as the product of second and third modal displacements multiplied by unknown nonlinear stiffness coefficients. Hollkamp et al. [61] assumed that a cubic form of nonlinearities. Assume the nonlinearity of the state equations is static, and a general form of the stiffness (including linear and nonlinear terms) for the hth static case is assumed as

$$\mathrm{K}_r(\mathrm{z}) = \Sigma_{i=1}^{r} con_i + \Sigma_{i=1}^{r} a_h(i)\mathrm{z}_i + \Sigma_{i=1}^{r}\Sigma_{j=1}^{r} b_h(i,j)\mathrm{z}_i\mathrm{z}_j + \Sigma_{i=1}^{r}\Sigma_{j=1}^{r}\Sigma_{k=1}^{r} c_h(i,j,k)\mathrm{z}_i\mathrm{z}_j\mathrm{z}_k \tag{5.5}$$

where con_i, $a_h(i)$, $b_h(i,j)$ and $c_h(i,j,k)$ are the coefficients of constant, linear, quadratic and cubic terms of the stiffness in the POD feature space, respectively, and $\mathrm{z}_i, \mathrm{z}_j, \mathrm{z}_k$ are the displacements in the selected POD feature space corresponding to arbitrary applied loads. For the majority of instances of geometric nonlinearity, polynomials of up to order 3 have been found to adequately model $\mathrm{K}_r(\mathrm{z})$ in Equation 5.5 [60]. Also the resulting reduced model using a least-squares analysis can be sensitive to the particular static solutions, and in some cases may omit important terms due to the physical insights [61]. Thus, in this research, all of linear, quadratic and cubic terms are retained.

5.6 Estimation of nonlinear stiffness coefficients

When only considering geometrically nonlinear response, Przekop and Rizzi ([62], [64]) classified FEM-based model reduction methods into two categories: a) those in which the nonlinear model stiffness is directly evaluated from the nonlinear finite element stiffness matrix, and b) those in which the nonlinear model stiffness is indirectly evaluated. For example Shi and Mei [135] deduced reduced models directly through the manipulation of the FEM stiffness matrix. However, two problems preclude widespread use of the former, firstly, coupling of the bending and stretching models makes it impossible to perform condensation, as seen in Chapter 3 and secondly, commercial FEM codes cannot be modified. In contrast, the indirect stiffness evaluation methods can be implemented for use with commercial FEM codes in which the nonlinear stiffness is not available explicitly [63]. Hence, in this thesis, indirect stiffness evaluation methods are employed.

It is well known that static deformation of a nonlinear structure within the elastic range, depends only on the currently applied load, and not on the load path. Hence, it is reasonable to use the same stiffness function for static and dynamic simulations. Based on this assumption, removing inertial and damping terms in Equation 5.4, static relationship is defined as

$$\mathbf{K}_r(\mathbf{z}) = \mathbf{P}_r^T \mathbf{f} \tag{5.6}$$

If a set of statically applied loads and the corresponding displacements are given, then the unknown stiffness term, $\mathbf{K}_r(\mathbf{z})$ in Equation 5.6 that relates the static load-response pairs, may be identified using least-squares techniques. The load-response pairs can be determined from nonlinear static analysis using FEM codes, but these must be transformed into a POD feature space. This technique provides a means of efficiently simulating the response of geometrically nonlinear structures. A similar technique but using a modal space was proposed by McEwan et al. [60]. A commercial FEM code was used to construct static nonlinear test cases subjected to prescribed modal forces; the resultant modal displacements were used to construct a multidimensional surface, thus accounting for inter-modal coupling. Load and displacement pairs provided by the application of the static nonlinear FEM were used to identify a reduced model in a modal space.

Usually, the linear portion of stiffness in a reduced model is determined using modal analysis of linearised form of a nonlinear structure. As for the determination of its nonlinear portion, Hollkamp, Gordon and Spottswood [61] compared three approaches:

- Direct evaluation–This involves a direct manipulation of nonlinear stiffness matrix through modal transformation. The procedure requires access to the assembly of nonlinear stiffness matrices, which is not available in most commercial finite element codes. Galerkin projection is a typical case.

- Enforced displacements–A set of enforced displacement vectors which are a linear combination of the modal basis vectors, are applied in nonlinear static FEM analyses [65]. The displacements are obtained and then transformed into the modal space with the applied loads. Coefficients of the nonlinear stiffness are estimated by means of their relationship on a mode-by-mode basis.

- Applied loads–In this a set of applied load vectors which are a scaled linear combination of the modal basis vectors are employed as loads [60]. At first glance, the applied loads procedure appears to be similar to the enforced displacement procedure. There is a difference, however. The nonlinear static displacements computed from applied loads contain both bending and stretching components due to the nonlinear stiffness of the finite element formulation. Membrane displacements occur naturally without explicitly including applied loads based upon membrane modes. In the enforced displacement procedure, membrane displacements must be included explicitly by including membrane modes in the set of enforced displacements.

In the proposed method, nonlinear stiffness coefficients of the reduced model are determined indirectly by means of nonlinear static finite element codes. This uses a set of load vectors in the POD space. The procedure to find nonlinear stiffness coefficients of the reduced model is divided into two steps:

1. Load-displacement data in POD feature space–This step creates a set of load-response pairs in the Lagrangian space by employing FEM codes, and forms the corresponding counterparts in the POD feature space by employing the transformation matrix, P_r. This step will be explained further in Section 5.6.1.

2. Coefficients identification–This step identifies the coefficients of the stiffness term of the reduced model by employing a SVD-based least-squares technique. The least-squares technique involves the determination of the coefficients of the stiffness term such that the sum of the squares of the distances from the data points to the function is a minimum. This step will be illustrated further in Section 5.6.2.

5.6.1 Nonlinear static analysis

To generate load-response pairs in the Lagrangian space, consider a set of applied loads as a sum of arbitrarily weighted POMs

$$\mathbf{f}_k = a_{k1}\mathbf{p}_1 + a_{k2}\mathbf{p}_2 + a_{k3}\mathbf{p}_3 \dots a_{kr}\mathbf{p}_r \tag{5.7}$$

where $\mathbf{f}_k$ is the applied load vector in the Lagrangian space, corresponding to the kth load-response pair. $\mathbf{p}_i(i = 1, 2 \dots r)$ are the POMs considered in Equation 5.4, $a_{ki}(i = 1, 2 \dots r)$ are arbitrarily selected weights to activate geometric nonlinearity in structural responses and are determined as

$$a_{ki} = \tau_{ki}\lambda_i\eta \tag{5.8}$$

where λ_i is the corresponding POV. η is a load scaler which helps to ensure that nonlinearities are excited properly. τ_{ki} is the weight factor of the ith POM and and represents the contribution of ith POM to $\mathbf{f}_k$. τ_{ki} can be artificially assigned in terms of integers and therefore combined variation of τ_i would define a new load case. A series of load cases are conducted to excite the nonlinearities of the structure. The number of load-response pairs, np, depends on the number of the coefficients, nc, to be identified in Equation 5.5.

Each pair can be obtained easily in any commercial FEM code as these pairs only require nonlinear static analysis rather than nonlinear dynamic analysis. This characteristic significantly reduces computational costs.

The resulting displacements from a set of test cases, $\mathbf{x}$, along with a set of corresponding applied loads, $\mathbf{f}$, formulate the load-response pairs in the Lagrangian space. These load-response pairs are transformed into a POD feature space using the transformation matrix, $\mathbf{P}_r$, in Equation 5.3.

$$\begin{aligned} \mathbf{f}_{re,k} &= \mathbf{P}_r^T\mathbf{f}_k \\ \mathbf{z}_k &= \mathbf{P}_r^T\mathbf{M}(\mathbf{x}_k - \bar{\mathbf{x}}_k) \end{aligned} \tag{5.9}$$

where $\mathbf{f}_k$ and $\mathbf{x}_k$ are the load-response pair in the Lagrangian space and $\mathbf{f}_{re,k}$ and $\mathbf{z}_k$ are the load-response pairs in the POD feature space. The latter pair $\mathbf{f}_{re,k}$ and $\mathbf{z}_k$ are used to determine all unknown coefficients of the stiffness term in the reduced model.

5.6.2 Coefficients identification

The provision of load-response pairs through the solution of a set of static nonlinear finite element cases allows the stiffness term, $\mathbf{K}_r(\mathbf{z}_1, \mathbf{z}_2, \mathbf{z}_3)$ in Equation 5.4 to be identified using a SVD-based least-squares technique. The parametric identification problem involves the determination of the coefficients of the stiffness term such that the sum of the squares of the distances from the known data points to the function is a minimum.

Assume that there are np sets of load-response vector pairs given by nonlinear static finite element solutions. The value of $\mathbf{f}$ is known as it is the input into FEM codes and the value of $\mathbf{x}$ is known from simulation results using the finite element codes. Each pair of the load or displacement vectors in the POD feature space, are treated separately. Substituting Equation 5.9 into Equation 5.6, leads to a parametric identification equation for each load-response pair as

$$\mathbf{A}_k\mathbf{S} = \mathbf{f}_{re,k} \tag{5.10}$$

where S is a $nc \times m$ unknown matrix that consists of all unknown coefficients of the stiffness term in the POD feature space. $\mathbf{f}_{re,k}$ is a $(np \times m) \times m$ load matrix in the POD feature space and $\mathbf{A}_k$ is a $(np \times m) \times nc$ coefficient matrix. As explained in Chapter 4, the complexity of the dynamics of nonlinear systems determines the number of required POMs. Reduced models built from fewer POMs appear to be more robust in term of resistance to disturbance. Thus in this work, only two POMs ($m = 2$) are considered, and A_k and S are determined by

$$\mathbf{A}_k = \begin{bmatrix} 1 & z_1 & z_2 & z_1^2 & z_2^2 & z_1z_2 & z_1^2z_2 & z_1z_2^2 & z_1^3 & z_2^3 \\ 1 & z_2 & z_1 & z_2^2 & z_1^2 & z_2z_1 & z_2^2z_1 & z_2z_1^2 & z_1^3 & z_1^3 \end{bmatrix} \tag{5.11}$$

$$\begin{aligned} \mathbf{S} = [& \begin{matrix} con_1 & a_1(1) & a_1(2) & b_1(1,1) & b_1(2,2) & b_1(1,2) \\ con_2 & a_2(1) & a_2(2) & b_2(1,1) & b_2(2,2) & b_2(1,2) \end{matrix} \\ & \begin{matrix} c_1(1,1,2) & c_1(1,2,2) & c_1(1,1,1) & c_1(2,2,2) \\ c_2(1,1,2) & c_2(1,2,2) & c_2(1,1,1) & c_2(2,2,2) \end{matrix}]^T \end{aligned} \tag{5.12}$$

where each column in the coefficient matrix, $\mathbf{A}_k$, indicates coefficients of the stiffness term and each row in the coefficient matrix, $\mathbf{A}_k$, represents one identification calculation of one mode, using one of the np load-response pairs. The first column in $\mathbf{A}_k$ stands for one constant item in the stiffness term, $\mathbf{K}_r$. It is noted that to obtain an accurate stiffness term, the number of load-response pairs used should be greater than the number of POM modes used to form one set of overdetermined (the number of equations is larger than the number of unknown coefficients) algebraic equations, which results in

$$\mathbf{AS} = \mathbf{f}_{re} \tag{5.13}$$

where

$$\mathbf{A} = (\mathbf{A}_1^T, \cdots, \mathbf{A}_k^T)^T \tag{5.14a}$$

$$\mathbf{f}_{re} = (\mathbf{f}_{re,1}^T, \cdots, \mathbf{f}_{re,k}^T)^T \tag{5.14b}$$

Singular value decomposition (SVD) is a technique for finding the pseudo-inverse of a rectangular matrix, and hence solving systems of linear equations that are suspected to be ill-conditioned (the conditional number of the matrix is large). As such, SVD is a method to solve least-squares problems. This technique allows the $np \times m$ matrix to be represented as

$$\mathbf{A} = \mathbf{UWV}^T \tag{5.15}$$

where $\mathbf{U}$ is a $(np \times m) \times nc$ matrix standing for a column orthogonal filtered version of the components in $\mathbf{A}_k$, $\mathbf{V}$ is a $nc \times nc$ orthogonal matrix and $\mathbf{W}$ is a $nc \times nc$ diagonal matrix. All of the positive diagonal elements of $\mathbf{W}$ stand for the singular values of the components in $\mathbf{U}$. Some of the diagonal elements in $\mathbf{W}$ may be zero in the case of a near singular matrix. This situation indicates that these components in $\mathbf{U}$ do not contribute significantly to the characterisation of $\mathbf{A}_k$. The decomposition can be used to remove the non-significant components by setting $1/\mathbf{W}_j$ to zero in $\mathbf{W}^{-1}$ when equation (5.15) is solved

$$\mathbf{S} = \mathbf{VW}^{-1}\mathbf{U}^T\mathbf{f}_{re} \tag{5.16}$$

5.7 Assembly of the nonlinear reduced equations of motion

When the polynomial part related to linear and nonlinear stiffness of the reduced model is identified, the nonlinear dynamic model of the structure may be formed by including the inertial and damping terms, which are obtained by transforming original mass and damping matrix into the POD feature space using the orthogonality features of POMs as follows

$$\begin{aligned} \mathbf{M}_r &= \mathbf{P}_r^T \mathbf{M} \mathbf{P}_r \\ \mathbf{C}_r &= \mathbf{P}_r^T \mathbf{C} \mathbf{P}_r \end{aligned} \tag{5.17}$$

Clearly this approach requires an explicit knowledge of the mass and damping matrices, $\mathbf{M}$ and $\mathbf{C}$, in Equation 5.1. Non-mass-proportional damping is not considered here because it would lead to the presence of damping coupling terms in the reduced model. In order to simplify computation, $\mathbf{P}_r$ is normalised with respect to the mass matrix, $\mathbf{M}$, using

$$\mathbf{p}_i^{norm} = \frac{\mathbf{p}_i}{\sqrt{\mathbf{p}_i^T \mathbf{M} \mathbf{p}_i}} \tag{5.18}$$

where $\mathbf{p}_i^{norm}$ and $\mathbf{p}_i$ are the ith POM in Equation 5.3 after and before the normalisation, respectively. This simplifies Equation 5.17 into

$$\begin{aligned} \mathbf{M}_r^{norm} &= (\mathbf{P}_r^{norm})^T \mathbf{M} \mathbf{P}_r^{norm} = \mathbf{I} \\ \mathbf{C}_r^{norm} &= (\mathbf{P}_r^{norm})^T \mathbf{C} \mathbf{P}_r^{norm} = \alpha \mathbf{I} \end{aligned} \tag{5.19}$$

where α is the mass damping ratio. $\mathbf{M}_r^{norm}$ and $\mathbf{C}_r^{norm}$ are a diagonal unit matrix and a scaled diagonal unit matrix, respectively due to the orthogonormality of the normalised POMs.

5.8 Algorithm of the proposed method

A step-by-step procedure for the method, illustrated in Figure 5.1, is as follows:

1. Following the procedure of determining a POD space, given in Section 3.6.2, obtain the POMs and corresponding POVs for an external excitation with a specified amplitude and frequency.

2. Repeat Step 1, for other excitations with different amplitudes and frequencies.

3. Calculate averaged POMs, over a range of parameters of interest and select the dominant POMs, $\mathbf{P}_r$, to construct the POD feature space (r: the number of selected POMs).

4. Normalise the selected POMs, $\mathbf{P}_r$, with respect to the known mass matrix, using Equation 5.18 to obtain $\mathbf{P}_r^{norm}$.

5. Generate a load case, $\mathbf{f}_l$, using Equation 5.7 ($l : 1, 2, \cdots k$) (k: the number of load cases).

6. Perform nonlinear static analysis in a commercial FEM code and record the corresponding displacement, $\mathbf{x}_k$, form a load-response pair, $\mathbf{f}_k$ and $\mathbf{x}_k$ in the physical space.

7. Repeat Steps 5 and 6 after selecting different τ_{ki} in Equation 5.8. This results in k sets of load-response pairs, $\mathbf{f}_k$ and $\mathbf{x}_k$, in the physical space.

8. Transform the load-response pairs, $\mathbf{f}$ and $\mathbf{x}$, in the physical space into those, $\mathbf{f}_{re,k}$ and $\mathbf{z}$, in the POD feature using Equation 5.9.

9. Use the transformed response, $\mathbf{z}$, to form the coefficient matrix, A, using Equations 5.11 and 5.14.

10. Perform an SVD-based least-squares analysis using Equation 5.16 to determine S and hence form $\mathbf{K}_r(\mathbf{z})$ using Equation 5.5.

11. Transform the mass and damping terms M and C using Equation 5.19, into $\mathbf{M}_r^{norm}$ and $\mathbf{C}_r^{norm}$.

12. Assemble a reduced model as in Equation 5.4 using the above $\mathbf{K}_r(\mathbf{z})$, $\mathbf{M}_r^{norm}$ and $\mathbf{C}_r^{norm}$.

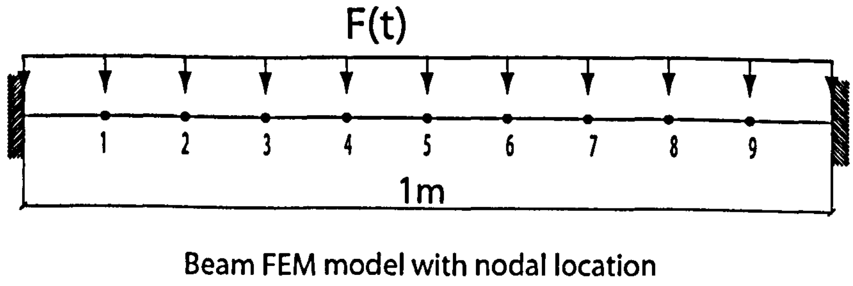

Figure 5.2: Model of the clamped beam with nodal location

Span	$1m$
Thickness	$0.01m$
Width	$0.03m$
Mass density	$7800kg/m^2$
Elastic modulus	$200e9Nm^2$
The Poisson ratio	0.3
Mass proportional damping factor	10

Table 5.1: Material and geometric properties of the beam

5.9 Numerical examples

Two different structures are studied in this chapter. The main purpose of the first example is give the details of the proposed method and also to examine its effectiveness. The second example is an application of the method to an engineering structure.

5.9.1 A clamped beam

In this section, to validate the approach proposed, a fully clamped beam example problem studied by McEwan et al. [60], shown in Figure 5.2, is considered. Table 5.9.1 shows the material and geometric properties of the beam.

The finite element model was formulated in Ansys [133] using 10 Beam189, which is a quadratic Timoshenko beam element. The the first six natural frequencies of the finite element model are 52.02Hz, 143.36Hz, 155.21Hz, 281.31Hz,424.73Hz, 466.54Hz, and match with those reported in [60]. A uniformly distributed, sinusoidally varying load was employed as in [60], i.e.

$$f(t) = f sin(2\pi f_{re} t) \tag{5.20}$$

	$0.5f_{re,1}$	$1.0f_{re,1}$	$1.5f_{re,1}$	$2.0f_{re,1}$
POM1	99.9981512	99.9973167	99.968506	99.9997329
POM2	0.0018485	0.0026832	0.031490	0.0002663
POM3	0.0000002	0.0000001	0.000003	0.0000008

Table 5.2: Energy distribution (%) of POMs over different excitation frequencies ($f_{re,1}$ is the first natural frequency of the beam)

τ_1	4	3	2	1	-1	-2	-3	-4

Table 5.3: Selection of the contribution factor τ_i for the beam case

where f is the amplitude of this uniformly distributed load along the beam, and f_{re} is the frequency of this load. A set of simulations were performed in which the amplitude f was selected as 1000 and the frequency was varied from 0 to 2 times the first natural frequency, 52.25Hz, of the beam (See Step 2 in Section 5.8).

The POMs obtained by following Step 3 described in Section 5.8, shown in Figure 5.3, have the property $\mathbf{P}_r^T\mathbf{P}_r = \mathbf{I}$ rather than $\mathbf{P}_r^T\mathbf{M}\mathbf{P}_r = \mathbf{I}$ since POMs are directly extracted from data. This implies that in order to describe mode shapes in the physical space using the POMs, the mass matrix must ne known [94]. The nodal location in Figure 5.3 are illustrated in Figure 5.2. Following Step 4, the POMs are normalised with the known mass matrix, **M**. The first two normalised POMs are, shown in Figure 5.4.

SDOF model

Assuming that only the first normalised POM, shown in Figure 5.4, is used to construct a SDOF reduced model, Equation 5.5 becomes

$$K_r(z) = con_1 + a_1 z + b_1 z^2 + c_1 z^3 \tag{5.21}$$

where z is the displacement in the POD feature space, $con1$ is the unknown constant term, a_1 is the unknown linear term, b_1 is the unknown quadratic term and c_1 is the unknown cubic term.

As only the first normalised POM, illustrated in Figure 5.4, is used to construct the

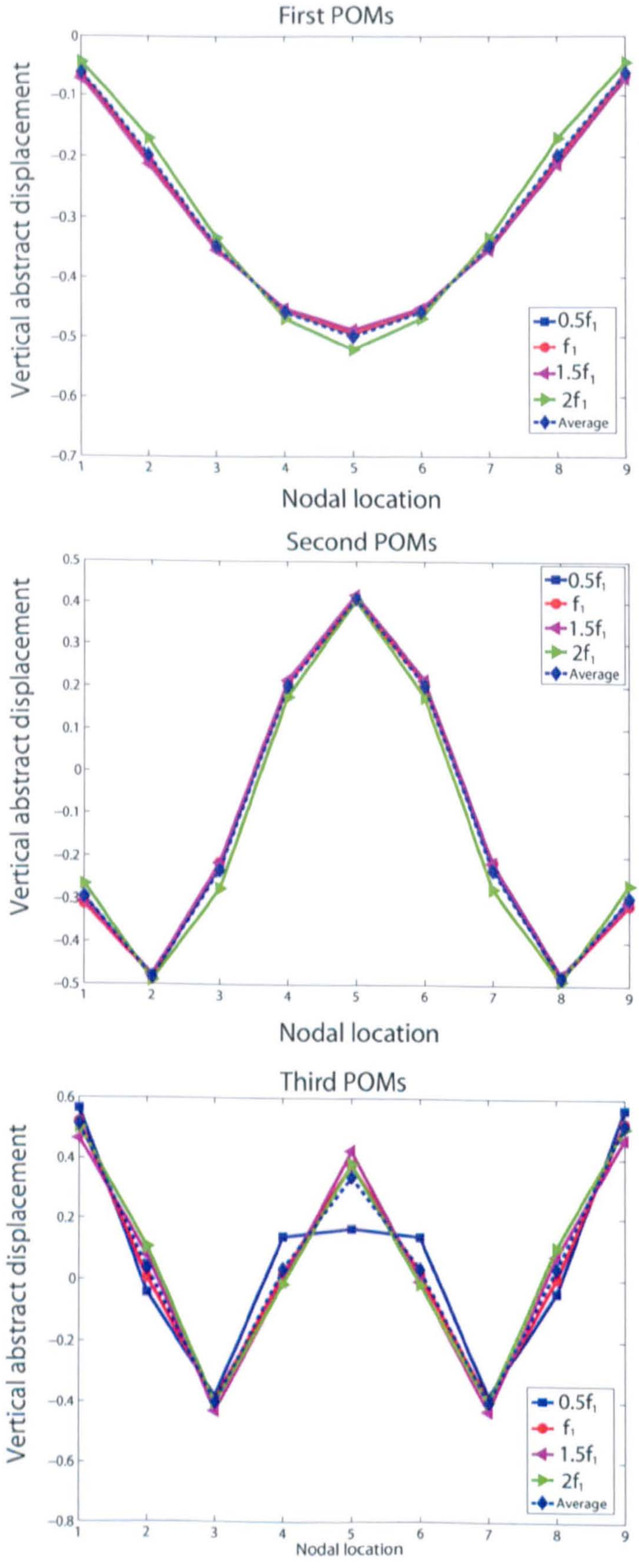

Figure 5.3: POMs of a fully clamped beam

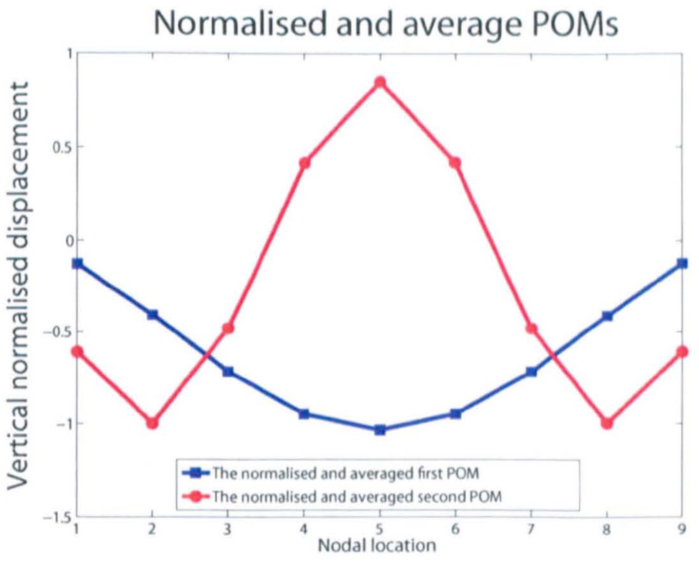

Figure 5.4: Normalised POMs of constructing the reduced model

SDOF model, Equation 5.7 and 5.8 become

$$\begin{aligned} \mathbf{f}_k &= a_{k1}\mathbf{p}_1 \\ a_{k1} &= \tau_{k1}\lambda_i\eta \end{aligned}$$

Where λ_i and η are 0.9999 from Table 5.2 and 1400, respectively. Changes of a_{k1}, described in Table 5.3, produce a set of loads.

Following Steps 8–10 in Section 5.8, the stiffness term, $K_r(z)$, of the SDOF model was identified as

$$K_r(z) = 0.074 + 1.37 \times 10^5 z + 8.39 \times 10^2 z^2 + 6.37 \times 10^8 z^3$$

and the inclusion of the mass and damping terms (see Step 11) leads to the SDOF model as

$$\ddot{z} + 10\dot{z} + 0.074 + 1.37 \times 10^5 z + 8.39 \times 10^2 z^2 + 6.37 \times 10^8 z^3 = -544.65 sin(2\pi f_{re} t) \quad (5.22)$$

where z and f_{re} are the displacement and the excitation frequency of the reduced SDOF model in the POD feature space, respectively. The damping coefficients, 10, and the excitation amplitude, −544.65, are obtained using Equation 5.17 and Equation 5.3, respectively.

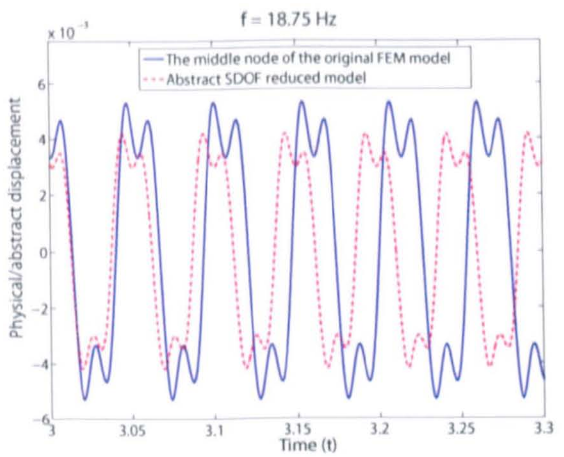

(a) f=18.75 Hz

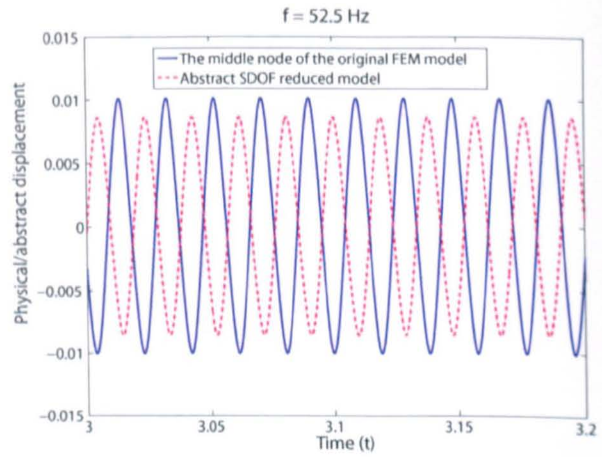

(b) f=52.5 Hz

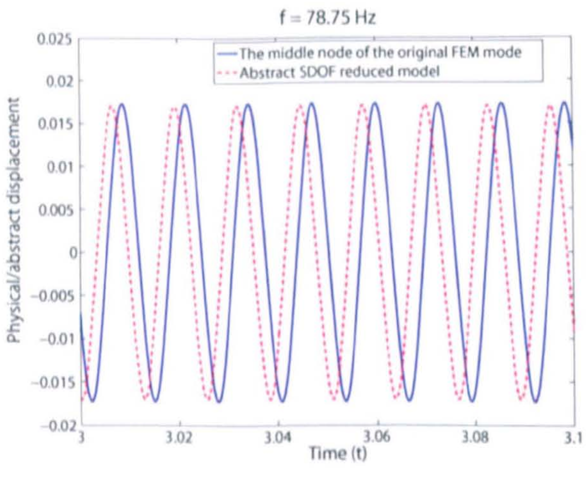

(c) f=78.75 Hz

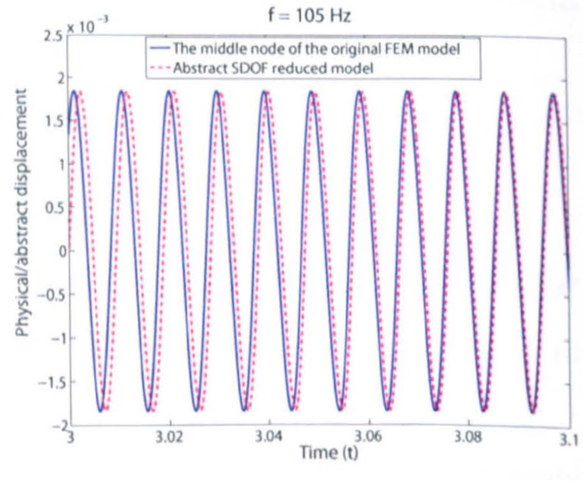

(d) f=105 Hz

Figure 5.5: Comparison of displacement time series between the SDOF reduced model and the middle node of the original FEM mode. Excitation frequency f(Hz): (a) 18.75 (b) 52.5 (c) 78.75 (d) 105

Comparison of results Figure 5.5 shows the comparison of displacement time series corresponding to different excitation frequencies at the middle node of the original FEM model and the resulting SDOF model, defined by Equation 5.22. In general, the reduced SDOF model shows excellent correlation with the original FEM model and qualitatively captures the dynamics of the beam within the selected parameter space, using only one

POM. Thus, the use of the POD space enables the more efficient generation of a reduced model, compared to typical generalised spaces such as Modal or Ritz spaces. Nevertheless, amplitudes are slightly reduced and there is some phase shift in low frequency range, as the original FEM model behaves nonlinearly in the low frequency range and behaves linearly in the high frequency range. These errors may be caused by the difference in damping between the original FEM model and the reduced SDOF model as when the excitation frequency increases the structural response moves from the velocity-sensitive region to the acceleration-sensitive region [46]. Additionally, information lost through the model reduction process, is another potential cause.

Figure 5.6 shows the comparison of phase spaces corresponding to different excitation frequencies at the middle node of the original FEM model and the resulting SDOF model. These pictures also show that the SDOF reduced model qualitatively captures the characteristics of the original FEM model, although the SDOF model has better agreement with the original FEM model when the excitations frequencies increase.

Figures 5.7 – 5.10 show the comparison of Fourier frequency spectrum, corresponding to different excitation frequencies at the middle node, of the original FEM model and the resulting SDOF model. At the lowest frequency, 18.75Hz, the response is dominated by the fundamental frequency and superharmonics of order 3 and 5 are observed, shown in Figure 5.7.

Integrity study The investigation of global dynamics of a nonlinear structure requires a computationally more efficient model but it may be less-accurate. This SDOF model satisfies this requirement. Using the SDOF model, a global behaviour of the beam was investigated. Based on such investigations a judgement can be made about the integrity of the structure for a range of parameters which is currently limited to a set of values.

The resulting integrity diagram, shown in Figure 5.11, gives results in the POD space and it is difficult to map these back to the physical space due to the fact one-against-one mapping between the physical space and the POD space does not exist, when non-uniform excitation is considered. However, this limitation can be overcome to a large extent by mapping the safety bounds from the physical space to the POD space.

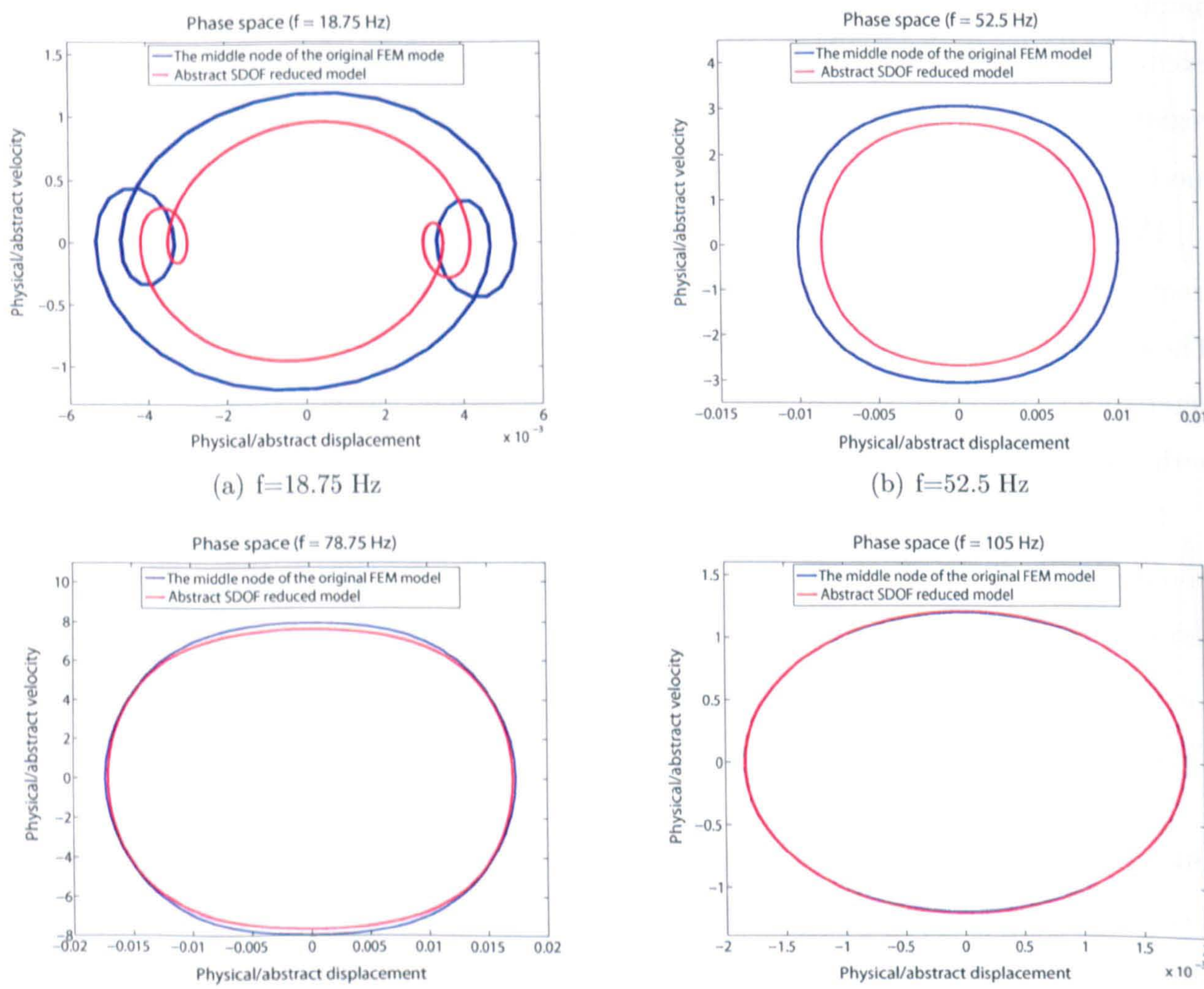

(a) f=18.75 Hz

(b) f=52.5 Hz

(c) f=78.75 Hz

(d) f=105 Hz

Figure 5.6: Comparison of phase spaces between the SDOF reduced model and the original FEM model at the middle node. Excitation frequency f(Hz): (a) 18.75 (b) 52.5 (c) 78.75 (d) 105

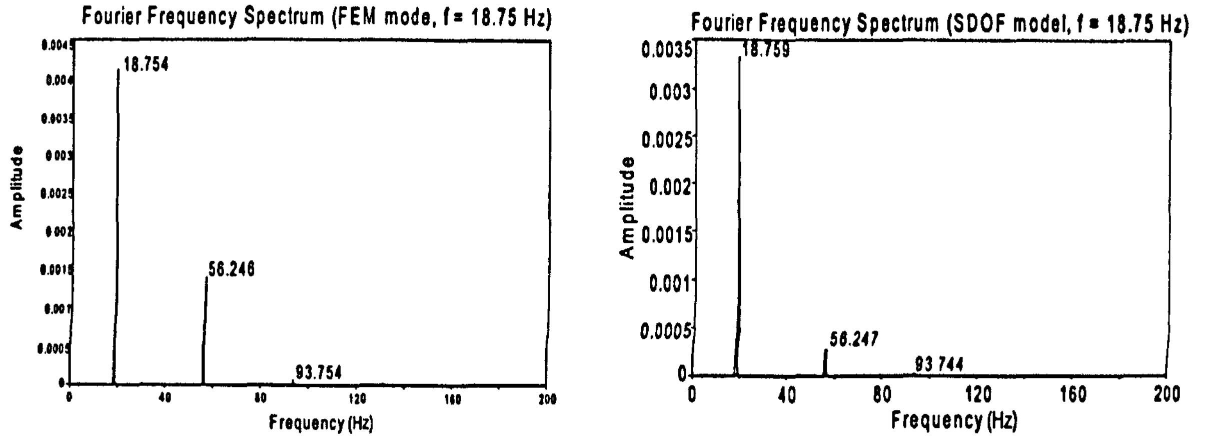

Figure 5.7: Comparison of the Fourier frequency spectrum corresponding to excitation frequency of 18.75 Hz (a) The FEM model (b)The SDOF reduced model

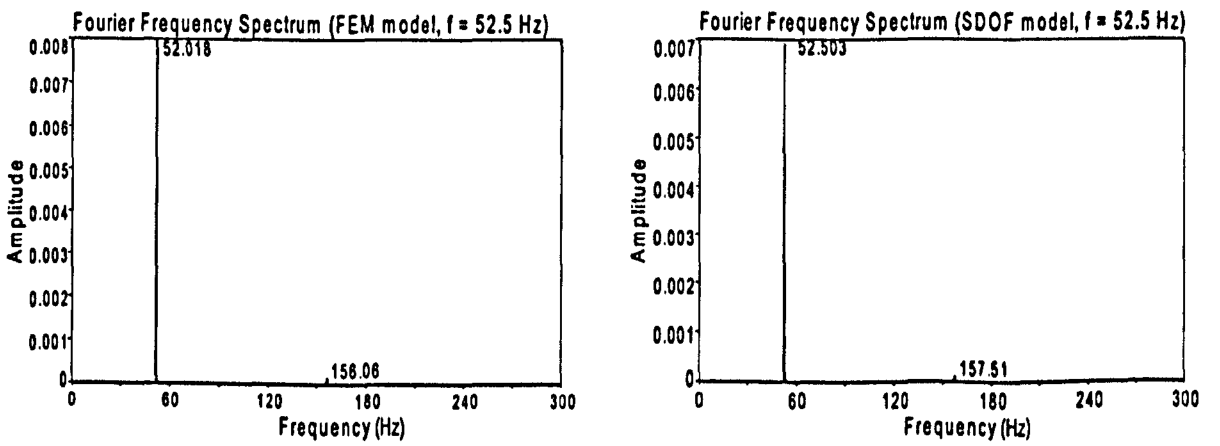

Figure 5.8: Comparison of the Fourier frequency spectrum corresponding to excitation frequency of 52.5 Hz (a) The FEM model (b)The SDOF reduced model

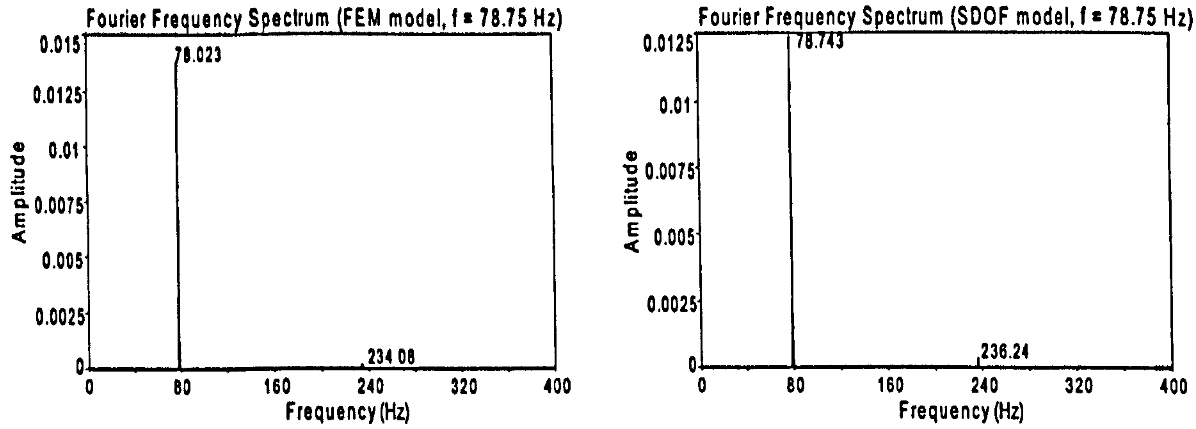

Figure 5.9: Comparison of the Fourier frequency spectrum corresponding to excitation frequency of 78.75 Hz (a) The FEM model (b)The SDOF reduced model

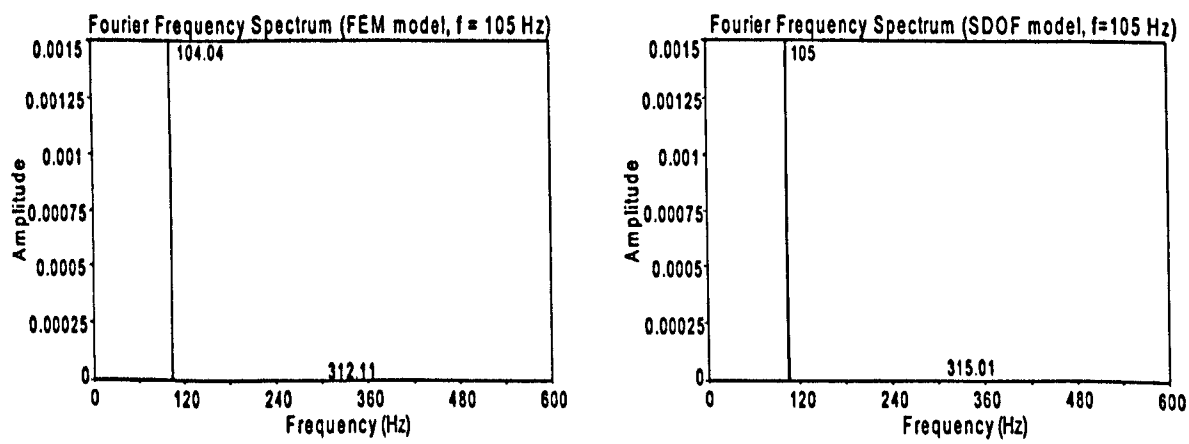

Figure 5.10: Comparison of the Fourier frequency spectrum corresponding to excitation frequency of 105 Hz (a) The FEM model (b)The SDOF reduced model

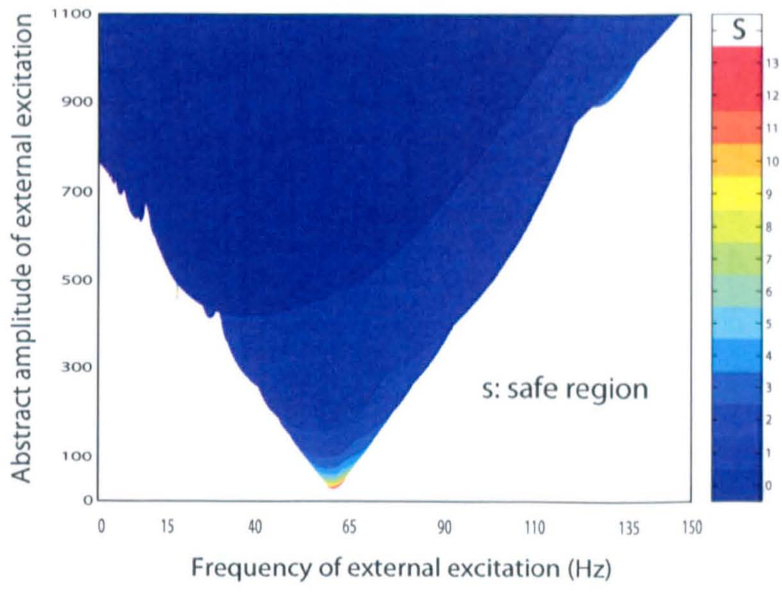

Figure 5.11: Integrity diagram using the SDOF model of the clamped beam(critical abstract displacement: 5)

5.9.2 A planar frame

A planar frame shown in Figure 5.12 is considered to apply the proposed method. Table 5.9.2 lists material and geometric properties of the frame.

Finite element model

A finite element model of the portal frame was constructed in Ansys [133] using two-dimensional elastic beam elements. A lumped mass formulation was utilised. The first

Column length	6m
Column cross-sectional area	$47.2e-4m^2$
Column second moment of area	$22.1e-6m^4$
Beam length	10m
Beam cross-sectional area	$47.2e-4m^2$
Beam second moment of area	$55.37e-6m^4$
Mass density	$5875\ kg/m^3$
Elastic modulus	$210e9Nm^2$
Poisson's ratio	0.29

Table 5.4: Material and geometric properties of the frame

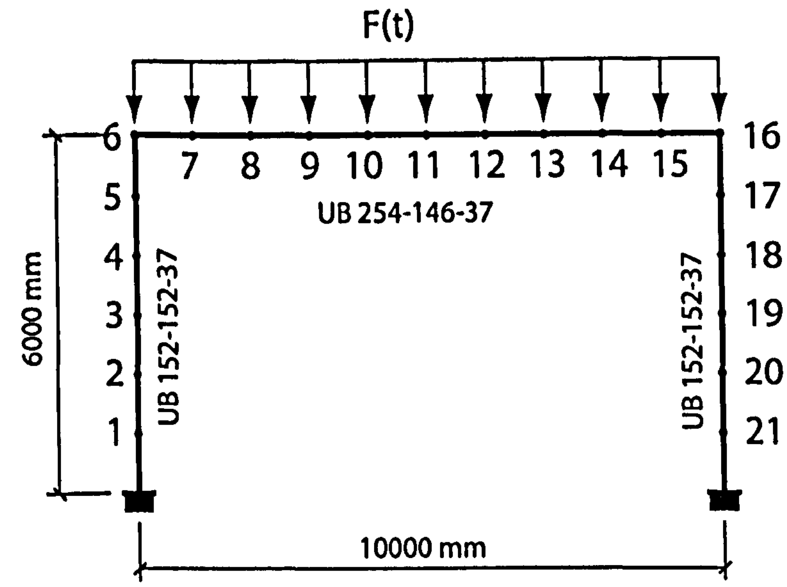

Figure 5.12: An example frame

few natural frequencies of the frame assuming linear behaviour, are 4.28Hz, 11.53Hz, 29.17Hz, 31.47Hz and 43.68Hz, respectively. Figure 5.13 depicts the first three modal shapes of the frame.

The transient analyses were performed with varying vertical harmonic excitation, $f(t)(= F sin(2\pi f_{re} t))$, shown in Figure 5.12. Frequencies of external sinusoidal excitation were chosen as 4Hz, 5Hz, 6Hz, 8Hz, 15Hz and 20Hz. Excitation amplitudes of 100kN was considered. The displacement responses were recorded at 21 spatially different locations, shown in Figure 5.12, from 10s to 20s.

Here only vertical translation DOF are considered. Time history for initial 10 seconds is discarded to eliminate the transient effects from the structural response. 50 records of displacement and velocity were taken during each cycle. Figures 5.14 and 5.15 show the dynamic information of the middle node (node 11 in Figure 5.12) at the excitation frequencies 5Hz and 8Hz, respectively. There are large amplitude motions, which is not for practical design but to demonstrate the method. It is also noted that the results in Figure 5.14 are influenced by the first modal shape, shown in Figure 5.13a, as the excitation frequency, 5Hz, is close to the first natural frequency, 4.28Hz. Figure 5.15 shows that as the excitation frequency is increased to 8Hz, the influence of the first modal shape decreases. Figure 5.15b shows non-elliptical shape that is typical of a nonlinear

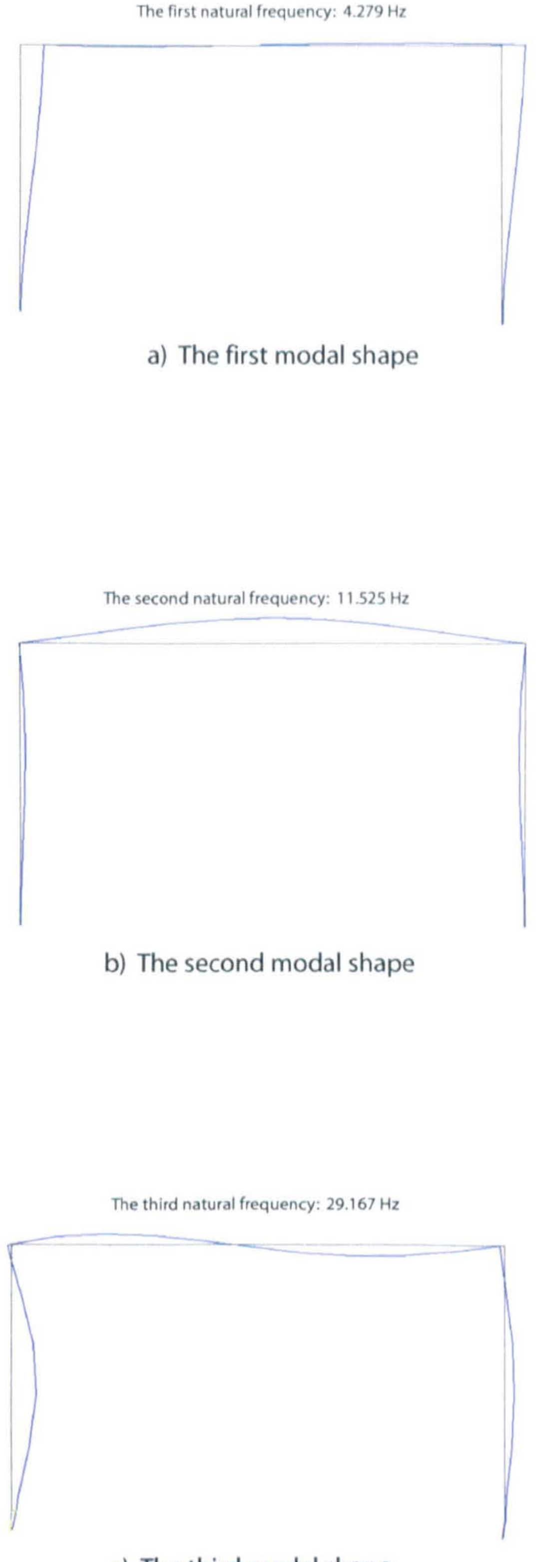

Figure 5.13: Modal shapes of the example portal frame

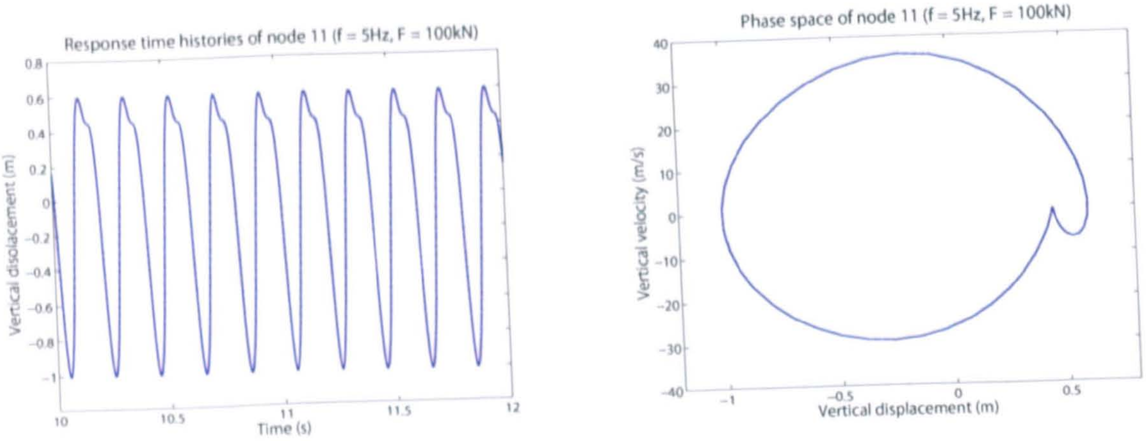

Figure 5.14: Responses of the middle node of the frame to excitation frequency of 5Hz and amplitude 100kN (a) The displacement time histories (b) The phase space

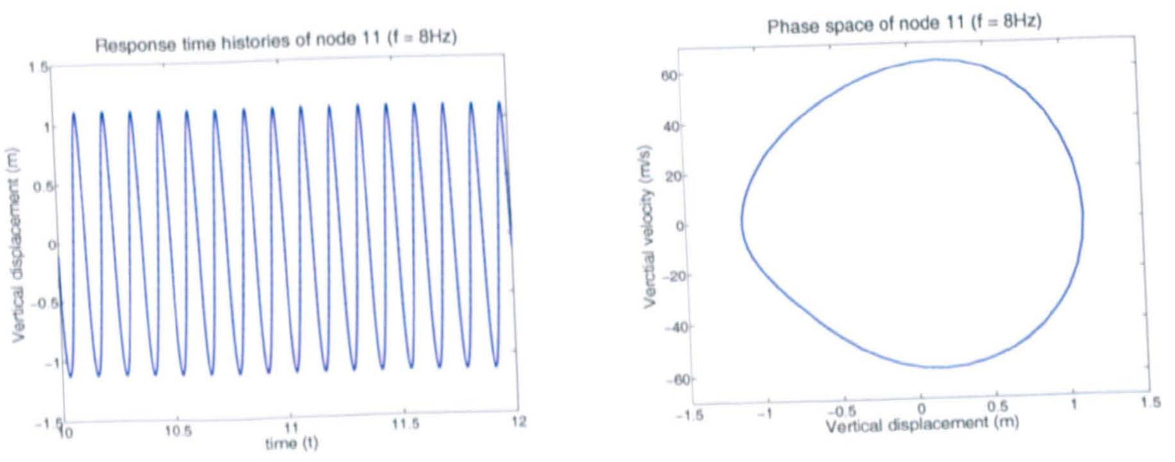

Figure 5.15: Responses of the middle node of the frame to excitation frequency of 8Hz and amplitude 100kN (a) The displacement time histories (b) The phase space

periodic orbit.

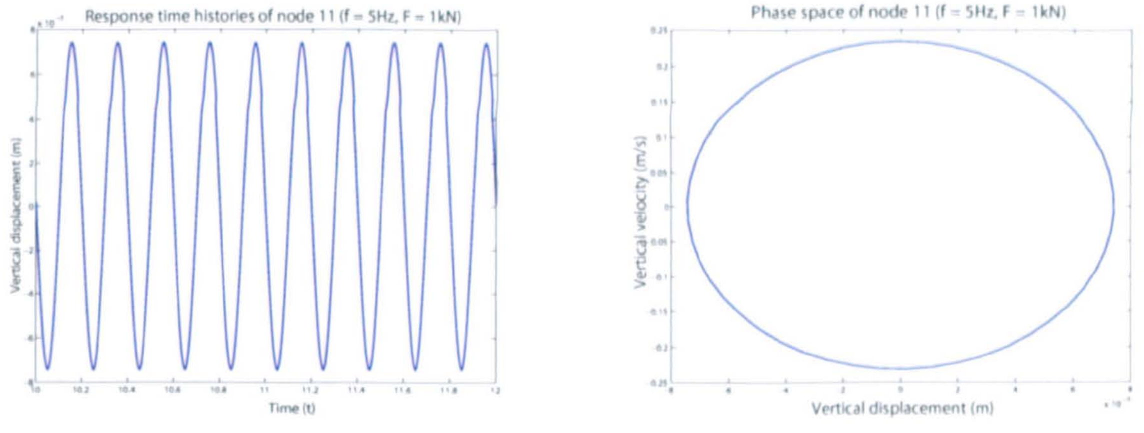

Figure 5.16: Responses of the middle node of the frame to excitation frequency of 5Hz and amplitude 1kN (a) The displacement time histories (b) The phase space

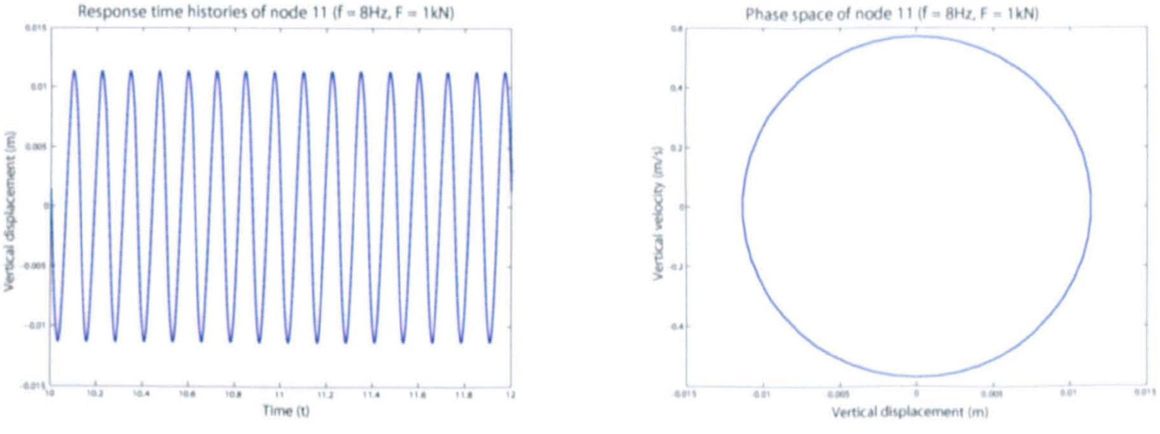

Figure 5.17: Responses of the middle node of the frame to excitation frequency of 8Hz and amplitude 1kN (a) The displacement time histories (b) The phase space

It is also noted that FEA simulations at the low excitation amplitude, $1kN$ (only 1% of the amplitude used before), shown in Figures 5.16 and 5.17 prove that the feature shown in Figures 5.14 is due to nonlinearity rather than higher modes.

Formulation of a reduced model

Having defined the finite element model in Ansys, the procedure described in Section 5.8 was applied for the generation of a reduced model in a POD space.

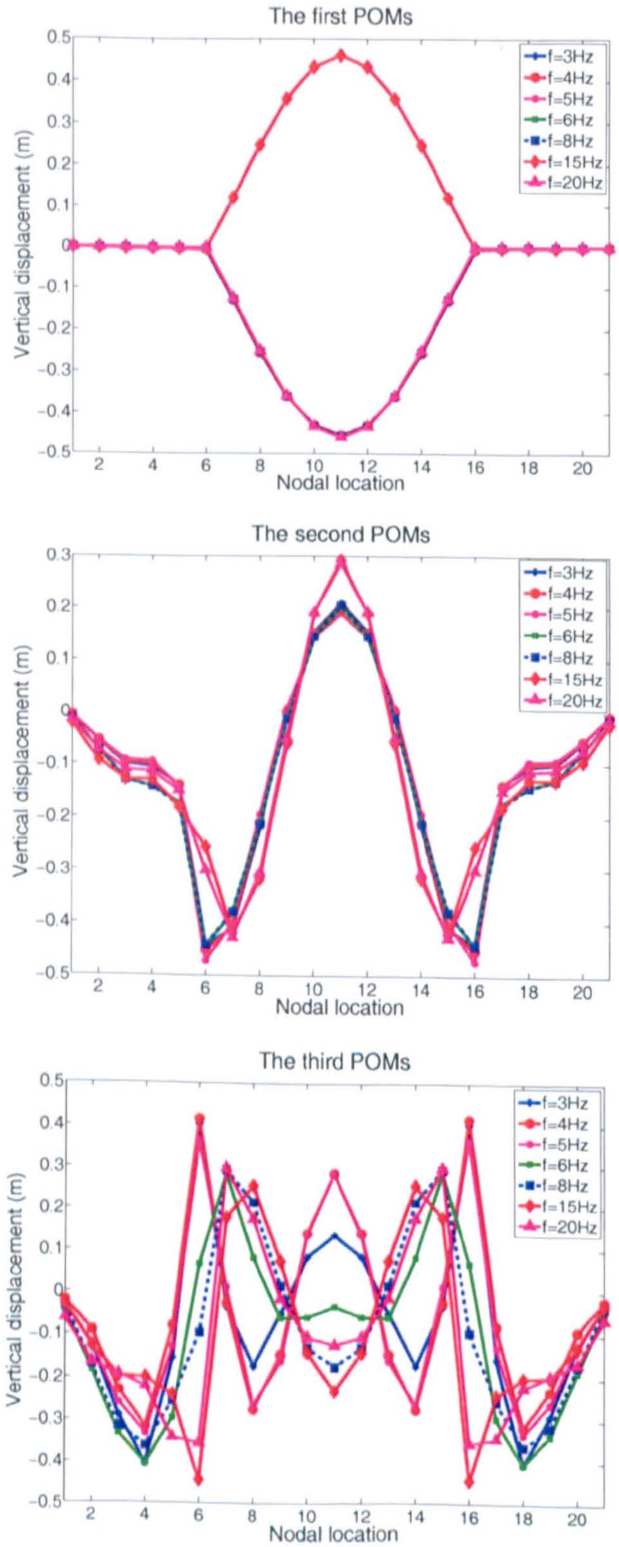

Figure 5.18: POMs over a range of excitation frequencies

Excitation frequency	3Hz	4Hz	5Hz	6Hz	8Hz	15Hz	20Hz
POM1	99.9932	99.9937	99.9919	99.9696	99.9745	99.9184	99.9886
POM2	0.0068	0.0063	0.0081	0.03	0.0251	0.0462	0.0113

Table 5.5: Energy distributions (%) of POMs over different excitation frequencies

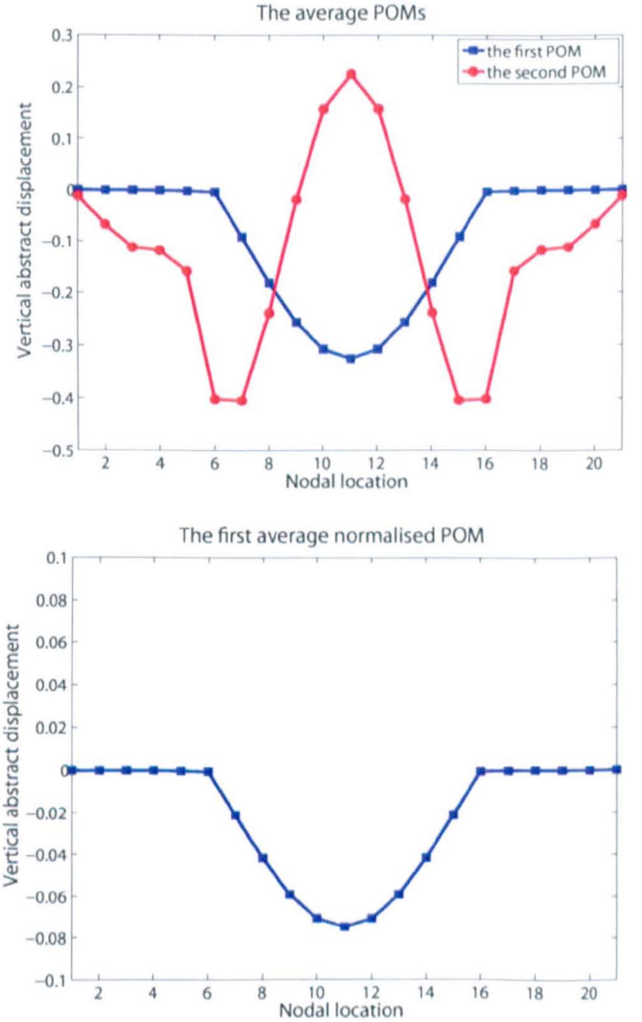

Figure 5.19: The average, normalised POMs over a range of excitation frequencies

τ_1	6	5	4	3	2	1	-1	-2	-3	-4	-5	-6

Table 5.6: Selection of the contribution factor τ_i for the portal case

Figure 5.18 shows the first three POMs. The first POMs overlap at the excitation frequencies from 3Hz to 20Hz, except at 15Hz, shown in Figure 5.18a. Hence, the first POM derived from one frequency condition can be used as an approximation for POMs of other frequencies. Table 5.5 illustrates their energy distributions. Due to the fact that all the first POMs contain at least 99.9% of the energy. This suggests that the first POM can fully capture the structural behaviour of the cantilever. Only the first normalised POM was utilised in the model, shown in Figure 5.19 (See Steps 4 and 5). A reduced nonlinear model of the frame was constructed using a combination of the POD feature space and a set of nonlinear static solutions, using the values of τ_i, given in Table 5.6 (see Steps 5–7).

Following Steps 8–10 in Section 5.8, the stiffness term, $K_r(z)$, of the SDOF model was identified (see Step 10) as

$$K_r(z) = 4.62\times10^3+5.38\times10^3z-77.7z^2+1.8z^3-4.73\times10^{-2}z^4+1.15\times10^{-3}z^5-1.91\times10^{-5}z^6$$

The SDOF reduced model is dominated by quadratic stiffness and higher order polynomial terms can be ignored. The inclusion of the mass and damping terms (see Step 11) leads to the SDOF model as

$$\ddot{z} + 10\dot{z} + 4.62\times10^3 + 5.38\times10^3z - 77.7z^2 + 1.8z^3 = -46.5sin(2\pi f_{re}t) \tag{5.23}$$

where z and f_{re} are the displacement and the excitation frequency of the reduced SDOF model in the POD feature space, respectively. The damping coefficients, 10, and the excitation amplitude, −46.5kN, are obtained using Equation 5.17 and Equation 5.3, respectively.

Evaluation of the reduced model

The frame was analysed using the original FEM model and the corresponding reduced model in Equation 5.23. Figure 5.20 shows that the phase space of the original system is similar with that of the reduced model at the excitation frequencies, 5Hz and 8Hz, although the phase space of the SDOF reduced model is scaled. Figure 5.21 and 5.22

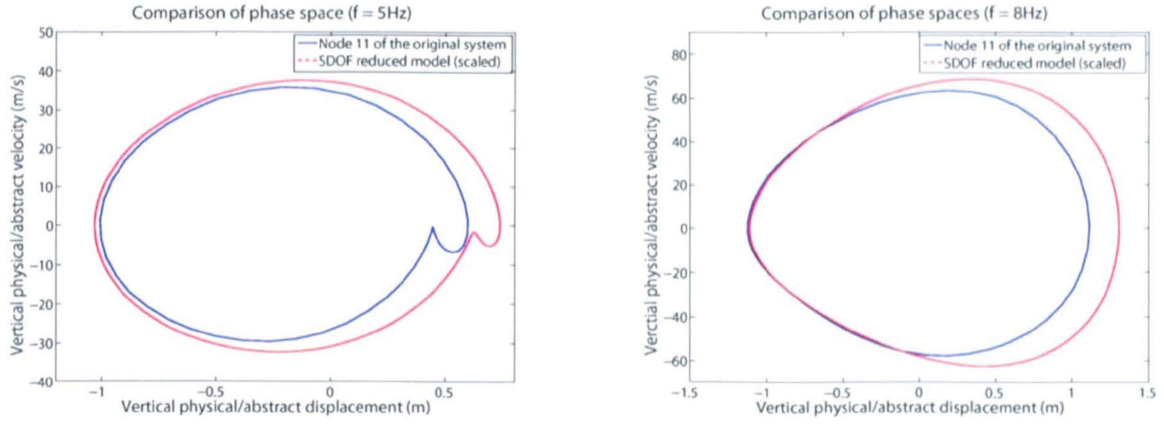

Figure 5.20: Comparison of the phase space corresponding between the node 11 of the original system and the SDOF reduced model *to excitation frequency of (a) 5Hz (b) 8Hz*

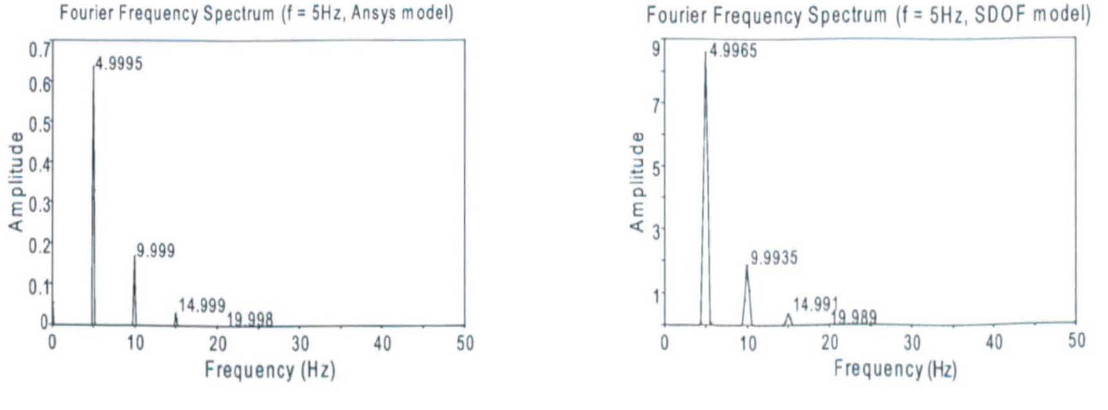

Figure 5.21: Comparison of the Fourier frequency spectrum corresponding to excitation frequency of 5Hz (a) The FEM model (b) The reduced model

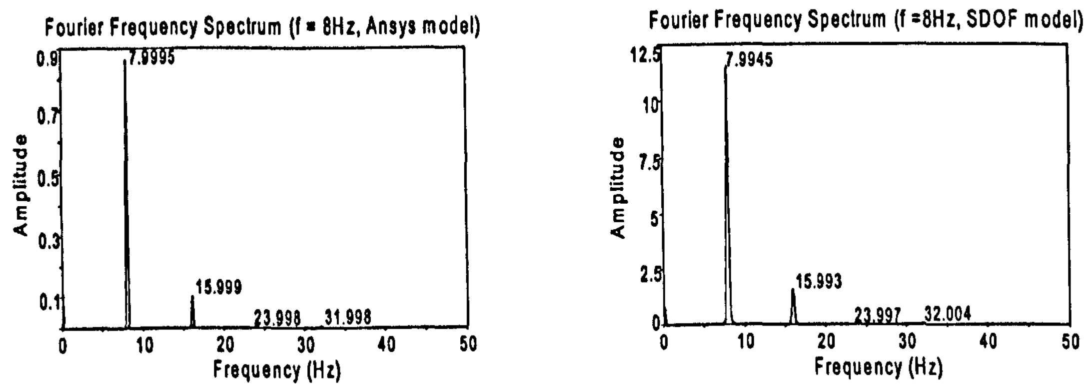

Figure 5.22: Comparison of the Fourier frequency spectrum corresponding to excitation frequency of 8Hz (a) The FEM model (b) The reduced model

show that there is an excellent agreement between the Fourier frequency spectrum generated with Node 11 of the original FEM model and the reduced model, corresponding to the excitation frequencies, $5Hz$ and $8Hz$. Similar results were obtained for different excitation frequencies. Therefore, the SDOF reduced model captures the characteristics of the original system.

5.10 Discussion

1. The proposed method relies on POD to determine a POD feature space, which efficiently represents the characteristics of response time histories obtained from numerical simulations. This feature space is appealing by its generality and efficiency for representing global dynamics of nonlinear structures using its best orthogonal basis, POMs.

2. The proposed method is novel in that it both uses the efficiency of the POD feature space and utilises commercial packages as much as possible without modifications to the codes themselves. This approach minimises development time and costs, and allows the proposed method to be easily integrated with any software already in use within an structural design environment.

3. There are several limitations to the proposed POD-based approach that should be

addressed. In this method, POD spaces are constructed using dynamics of all nodes of the FEM modes and the explicit knowledge of the mass, damping matrices of the structure, a situation not possible with analysis of real structures. The other limitation is inherent in using nonlinear static solutions, that is, it can only model the nonlinearity captured by nonlinear static FEM codes, e.g., geometric nonlinearity. To overcome these limitations, a more general approach which can handle all kinds of nonlinearities in elastic structures, is proposed in the next chapter.

4. Limited load-displacement vector pairs are selected in an arbitrary way, which might result in an unstable reduced model as this proposed method does not enforce the stability of the reduced model. It is necessary to choose a set of loads to the original model so the responses reflect all the dynamics needed. However, even though the identified reduced model may fit the simulation or experimental data, there is not guarantee that the reduced model is stable over the parameter range of interest.

5. The resulting reduced model is capable of studying global dynamics of the nonlinear structure because of its low dimensionality and good approximation to structural behaviour. However, results should be interpreted carefully. In some case the truncation of POMs might have a significant effect on the results due to nonlinear coupling. This is a trade-off between accuracy and efficiency of reduced models. In this research, efficiency is more important than accuracy due to the requirement of performing parameter studies.

5.11 Conclusion

In this chapter, an approach to construct a reduced model using commercial FEM static codes has been presented. This approach initially postulates an explicit motion of equation with a polynomial stiffness function in a POD feature space. A set of nonlinear static finite element simulations are performed to capture the relationships between loads and deflections. The high-dimensional relationships are transformed into the low-dimensional ones in the POD space. Based on the low-dimensional relationships, a SVD-based least-squares analysis is then used to identify unknown coefficients of the stiffness term. The inclusion of mass and damping matrices completes the construction of the reduced model.

To validate the proposed method, a fully clamped beam was studied. A comparison of dynamic information between the reduced model and the original FEM model over a range of the excitation frequencies shows that there is an excellent correlation between the responses, although some information is lost due to the model reduction.

A SDOF reduced model has demonstrated that keeping a single POM qualitatively capture the dynamics of the original FEM model of a nonlinear beam and a portal frame.

Chapter 6

A New Model Reduction Method Based on Nonlinear Dynamic Analysis

6.1 Objectives

- To propose a new method for extracting a reduced model in a POD space for nonlinear elastic structures by using Harmonic Balance Method and a parameter identification method in combination.
- To examine the method using a highly nonlinear cantilever
- To use the method proposed to investigate the global behaviour of a cantilever with one side stop

6.2 Introduction

In the previous chapter, a POD-based model reduction method was proposed for nonlinear systems. This method was devised to determine stiffness term of a reduced model in a POD feature space by retrieving relationships between loads and responses through nonlinear static FEM analyses. This method can be used to treat geometrical nonlinear systems. The resulting reduced model is reasonably accurate and computationally efficient. However, an explicit knowledge of the mass and damping matrices must be available *a priori* for its implementation. In this chapter, a more general POD-based model reduction method is proposed to consider more types of nonlinearities described in Section 2.4, including boundary nonlinearity.

6.3 A new model reduction method

Following the strategy presented in Section 3.6 to construct a reduced model in a generalised space, a novel POD-based method is proposed to handle more types of nonlinearities than the method proposed in Chapter 5. Three basic assumption are made in this proposed method as follows:

- Response time histories of nonlinear systems can be approximated by a set of periodic orbits
- Nonlinearities are indeed excited
- Nonlinearities can be captured by commercial FEM codes

In this approach, dynamic relationships between loads and responses are used to construct a reduced model, rather than static ones employed in Chapter 5. The dynamic relationships are represented by abstract response time series that are obtained by transforming response time histories in the original Lagrangian space into a POD feature space. Nonlinear dynamic finite solutions are used to produce the response time histories corresponding to different amplitudes and frequencies of external excitations.

With the use of harmonic balanced method and least-squares technique in combination, all model coefficients of the reduced model are determined using the abstract response time histories in the POD feature space. The advantage of this proposed method is its ability to handle complex dynamic structures with any kind of elastic nonlinearity. However, this method may introduce more computational effort as well as difficulty in estimating parameters of the reduced model due to the strong nonlinearity of nonlinear systems.

Firstly, a POD feature space is constructed using a commercial FEM code. Secondly, a form of an expected reduced model is postulated in the POD feature space, similar to

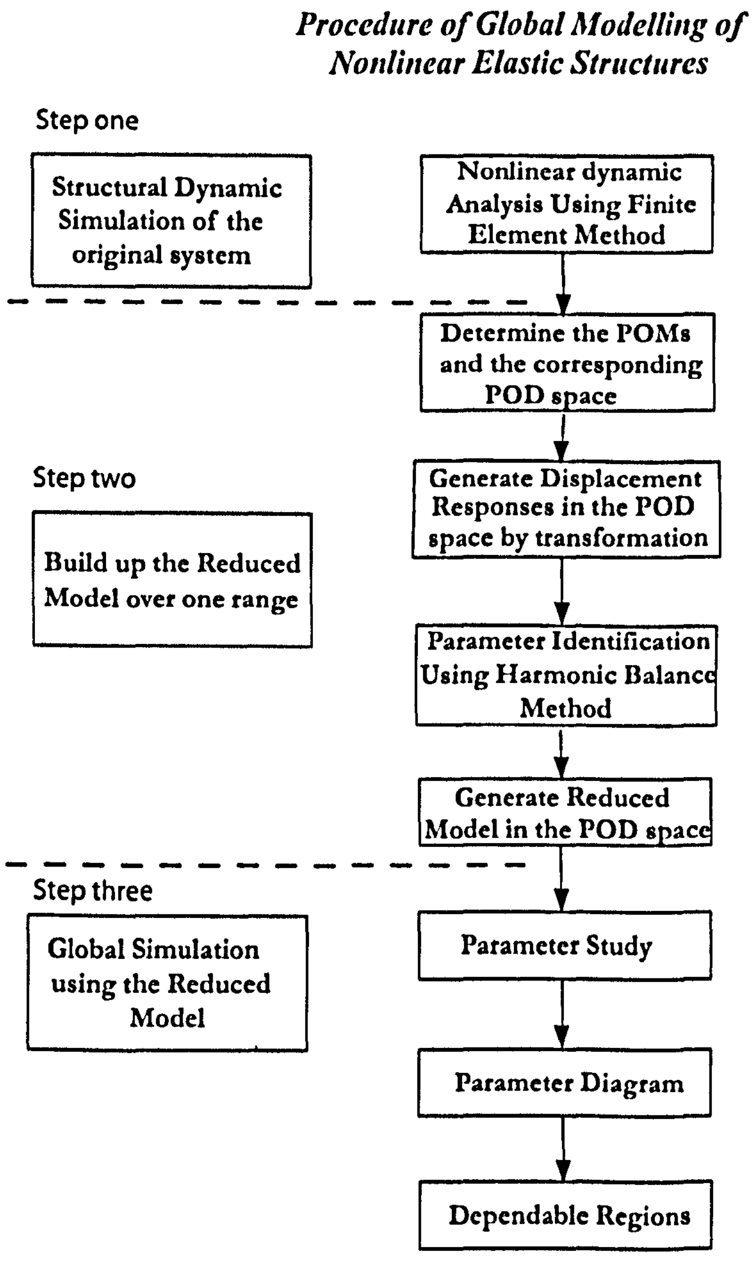

Figure 6.1: Procedure of the investigation of global behaviour of nonlinear dynamic structures

that presented in Chapter 5. However, in order to consider nonlinear inertia, nonlinear damping and other nonlinearities presented in elastic structures, a more general form is assumed and the coefficients of mass, damping and stiffness terms are to be identified. This overcomes the limitation of Chapter 5 approach in that mass matrix is not required. Finally, the assumed reduced model is identified using the generalised displacement time series rather than the load-response pairs used in Chapter 5. Figure 6.1 illustrates the proposed method schematically.

6.4 Formulation of reduced models

The interaction of the nonlinear structures with the loads is complicated and it is difficult to model the nonlinearities. Hence, modelling deterministic systems will still attempt to fit an assumed function to the data, like the approach in Chapter 5. The idea combines the model reduction capabilities of POD with standard system identification techniques to generate a reduced model. Its governing equation is assumed as

$$\mathbf{M}_r\ddot{\mathbf{z}} + \mathbf{C}_r\dot{\mathbf{z}} + \mathbf{K}_r(\mathbf{z}) = \mathbf{f}(t) \tag{6.1}$$

where $\mathbf{M}_r$, $\mathbf{C}_r$, $\mathbf{K}_r(\mathbf{z})$, and $\mathbf{f}(t)$ are the mass, damping, stiffness, and external excitation in a POD feature space, respectively.

For nonlinear structures with large DOF, it is extremely difficult to classify the sources of nonlinearities. Moreover, when reconstructing a reduced model, the form of nonlinearities might change. Hence, the type and form of nonlinearities are in general unknown and series functions are needed to approximate the nonlinearities from mathematical point of view. The most widespread approach is to assume stiffness terms in form of polynomial and to solve Equation 6.1 in the least-squares sense. In this work, it is assumed that no other knowledge of the reduced model is available except for external excitations. Hence, the stiffness term, $\mathbf{K}_r(z)$ in Equation 6.1 is approximated as

$$\mathbf{K}_r(\mathbf{z}) = con_i + \Sigma_{i=1}^{r} a_h(i)\mathbf{z}_i + \Sigma_{i=1}^{r}\Sigma_{j=1}^{r} b_h(i,j)\mathbf{z}_i\mathbf{z}_j + \Sigma_{i=1}^{r}\Sigma_{j=1}^{r}\Sigma_{k=1}^{r} c_h(i,j,k)\mathbf{z}_i\mathbf{z}_j\mathbf{z}_k + \cdots \tag{6.2}$$

where con_i, $a_h(i)$, $b_h(i,j)$ and $c_h(i,j,k)$ are the coefficients of constant, linear, quadratic and cubic terms of the stiffness in the POD feature space, respectively. This equation is similar with Equation 5.5 but with more higher level terms. Some disadvantages of using ordinary polynomial series are overfitting and poor numerical conditions [35].

6.4.1 Nonlinear dynamic analysis

The goal of this part, similar to Section 5.5, is to provide the knowledge of the applied load and of the response of the system in a POD feature space.

FEM simulations

A few nonlinear dynamic FEM simulations are performed to suitably capture dynamics in the form of numerical records. In these simulations, the frequencies and amplitudes of the external excitation are varied to satisfy two functions as follows:

- Characterise the parameter range of interest so that an optimum POD basis and the corresponding POD feature space can be identified,
- Provide enough data (the number of orbits) to generate an over-determined algebraic equation for performing parametric identification. This requirement will be explained later.

Alignment of displacement time series

In commercial FEM codes, to accelerate computational speed of nonlinear dynamic analysis, a technique, called Automatic or Adaptive Time Stepping, is commonly used. Its purpose is to decide whether or not to reduce the present time step size, and redo the substep with a smaller step size when achieving convergence is difficult. However, the use of this technique results in non-uniformly sampled records. For Fast Fourier Transformation (FFT) calculations, it becomes necessary to perform the data alignment. A one-dimensional data interpolation Matlab [136] function *interp1*, is used. This function adjusts the displacement time series of FEM simulation results, from the recorded sampling rate to a constant one.

Space transformation

The aligned displacement records or time series in the Lagrangian space are transformed into the POD feature space by using Equation 3.43

$$\mathbf{z} = \mathbf{P}_r^T(\mathbf{x} - \bar{\mathbf{x}}) \tag{6.3}$$

where $\mathbf{z}$ and $\mathbf{x}$ are the displacement time series in the POD feature space and the Lagrangian space, respectively. $\bar{\mathbf{x}}$ is the mean of nodal displacement time series in the the Lagrangian space and $\mathbf{P}_r$ is the POD transformation matrix with r dominant POMs. The same transformation matrix $\mathbf{P}_r$ can be used for the load time series

$$\mathbf{f}_{re}(t) = \mathbf{P}_r^T\mathbf{f}(t) \tag{6.4}$$

where $\mathbf{f}_{re}(t)$ and $\mathbf{f}(t)$ are the external excitation, in the POD feature space and in the Lagrangian space, respectively. This transformation is conducted on the assumption that the dominant POMs determined by the displacement time series can be used to perform a space transformation for the external excitation.

6.4.2 Coefficients identification using Harmonic Balance Method

Identification of nonlinear system ranges from methods which simply detect the presence or type of nonlinearity, to those which seek to quantify the dynamic behaviour through a mathematical model [35]. The method proposed in this chapter belongs to the latter. Masri et al. ([110], [111]) proposed the Restoring Force Surface method (RFS) to perform an efficient and reliable coefficients identification of nonlinear systems. Although in principle arbitrarily complex nonlinear system could be identified, in practice the computational burden makes it impractical. A simple solution is to use diagonal mass and damping matrices, as in Chapter 5. Alternatively, frequency based system identification methods can be used. These include the Volterra and Wiener series, higher-order spectra, Harmonic Balance Method, and the Reverse Path Method [35]. These methods help to select significant signal frequency data and reject the noise. In this work, the Harmonic Balance Method is selected to perform the coefficient identification because of its simplicity and generality.

Harmonic balance method

The Harmonic Balance Method (HBM) [40] functions by first substituting a temporal Fourier series expansion of the solution variables into the governing equation. For example, for a dynamic system, represented by Equation 6.1, the displacement $z(t)$, velocity $\dot{z}(t)$ and acceleration $\ddot{z}(t)$ signals can be approximated by the truncated Fourier series expansions as follows:

$$z(t) \approx \frac{a_0}{2} + \sum_{i=1}^{n}(a_i cos i\omega t + b_i sin i\omega t) \tag{6.5}$$

$$\dot{z}(t) \approx \sum_{i=1}^{n} i\omega(-a_i sin i\omega t + b_i cos i\omega t) \tag{6.6}$$

$$\ddot{z}(t) \approx \sum_{i=1}^{n} -i^2\omega^2(a_i cos i\omega t + b_i sin i\omega t) \tag{6.7}$$

where ω is the fundamental frequency of the system, $a_i, b_i (i = 0, 1, \ldots, n)$ are the HBM Fourier coefficient variables, and n is the number of overall harmonics used in the truncated Fourier series expansion.

The Fourier expansions of the quadratic and cubic terms are expressed as

$$z^2(t) \approx \frac{c_0}{2} + \sum_{i=1}^{n}(c_i cos i\omega t + d_i sin i\omega t) \tag{6.8}$$

$$z^3(t) \approx \frac{e_0}{2} + \sum_{i=1}^{n}(e_i cos i\omega t + f_i sin i\omega t) \tag{6.9}$$

Substituting the Equations (6.5 - 6.9) into Equation 6.1 and collecting the terms associated with each harmonic $cos(n\omega t)$ and $sin(n\omega t)$ yield a system of $2n + 1$ algebraic equations for Fourier coefficients a_i, b_i, c_i, e_i and $f_i (i = 0, 1, \ldots, n)$ as all the harmonic terms are equal to zero. In other words, the principle of harmonic balancing is to equalize all frequency components on both sides of the equation. Generally, it is a reasonable assumption that the overall system is dominated by low-frequency dynamics. Thus, only a finite number of harmonics are important, and all higher order harmonics are negligible. By doing so, high frequency noise is filtered out. The resulting solution of Equation 6.1 is approximate because of the truncation of higher order harmonics. This approach has been applied to solve nonlinear ODEs [40].

Coefficients identification

HBM can be used to identify parameters of a nonlinear system because of its simplicity and capacity for handling highly nonlinear systems. Yasuda et al. ([41], [42]) proposed a method of parametric identification for nonlinear systems using HBM in an inverse way in which HBM was implemented as a nonlinear identification tool. Yuan and Feeny [137] extended the method to chaotic systems, by making use of the unstable periodic orbits extracted from the response time series of the chaotic systems. Due to the randomness-similar characteristic of chaos, the POMs of a chaotic orbit are expected to better capture the system dynamics than any other set of POMs extracted from a non-chaotic response [96]. Further, Liang and Feeny [138] proved that extraction of periodic orbits is not necessary for the identification of chaotic systems under periodic excitation. Any long segment of a chaotic orbit can approximate a long period unstable periodic orbit and it can also be used in HBM.

When a base acceleration excitation is applied to a SDOF system, Equation 6.1 becomes

$$\mathbf{M}_r\ddot{\mathbf{z}} + \mathbf{C}_r\dot{\mathbf{z}} + \mathbf{K}_r(\mathbf{z}) = \mathbf{M}_r A_{base}^{POD} \cdot sin(\omega t) \tag{6.10}$$

where $\mathbf{z}$ is the state variable, ω is the frequency of base excitation and A_{base}^{POD} is the amplitude of base excitation in the POD feature space. When only one POMs are considered, $K_r(z)$ represents the stiffness term as

$$K_r(z) \approx \sum_{i=0}^{n} a_i z^i \tag{6.11}$$

where a_i are unknown polynomial coefficients. The coupling terms are not considered, although an extension is straightforward, following the idea shown in Equation 5.5.

Following the procedure, illustrated in the previous part, substituting Equations 6.5

- 6.9 into Equation 6.10, and balancing the Fourier coefficients of all sets of harmonics between the left hand side and right hand side of the equation, leads to the equations for parameter identification for each periodic orbit as

$$\mathbf{A}_k\mathbf{s} = \mathbf{f}_{re,k} \quad k = 1, 2, \ldots k \; (k : Number\ of\ orbits) \tag{6.12}$$

where $\mathbf{A}_k$ is the Fourier coefficient matrix

$$\mathbf{A}_k = \begin{pmatrix} 0 & \frac{a_0}{2} & \frac{c_0}{2} & \frac{e_0}{2} & \cdots \\ \omega b_1 & a_1 & c_1 & e_1 & \cdots \\ -\omega a_1 & b_1 & d_1 & f_1 & \cdots \\ 2\omega b_2 & a_2 & c_3 & e_2 & \cdots \\ -2\omega a_2 & b_2 & d_2 & f_2 & \cdots \\ \vdots & \vdots & \vdots & \vdots & \vdots \end{pmatrix} \tag{6.13}$$

and s is the unknown parameter vector

$$\mathbf{s} = \{\frac{c}{m} \frac{k_1}{m} \frac{k_2}{m} \frac{k_3}{m} \cdots\}^T$$

and $\mathbf{f}_{re,k}$ is the combination of Fourier vector of base excitation and acceleration time series

$$\mathbf{f}_{re,k} = \{0,\ \omega^2 a_1,\ A_{base} + \omega^2 b_1,\ 4\omega^2 a_2,\ 4\omega^2 b_2,\ \cdots\}^T \tag{6.14}$$

where $\mathbf{A}_k$ and $\mathbf{f}_{re,k}$ correspond to the kth orbit. $\mathbf{A}_k$ is a $(2m+1) \times (n+1)$ matrix and $\mathbf{f}_{re,k}$ is a $2m+1$ vector in which m is the number of harmonics, n is the number of terms in the polynomial.

Thus, all of the system parameters, including $\frac{c}{m}$, and polynomial coefficients, when $(2m+1) > (n+1)$, can be obtained by left-multiplying Equation 6.12 by $\mathbf{A}_k^T$ and performing a relevant inverse manipulation, i.e.

$$\mathbf{s} = (\mathbf{A}_k^T\mathbf{A}_k)^{-1}\mathbf{A}_k^T\mathbf{f}_{re,k} \tag{6.15}$$

A least-squares method is used to solve this equation. When considering k sets of periodic orbits, a new matrix equation is formulated as follows

$$\begin{aligned} \mathbf{A}\mathbf{s} &= \mathbf{f} \\ \mathbf{A} &= (\mathbf{A}_1^T, \cdots, \mathbf{A}_k^T)^T \\ \mathbf{f} &= (\mathbf{f}_{re,1}^T, \cdots, \mathbf{f}_{re,k}^T)^T \end{aligned} \tag{6.16}$$

where s contains the coefficients of the reduced model, A is the total FFT coefficient matrix, f the total FFT load matrix and k is the number of orbits used. Similarly, the vector s can be solved by using least square method in terms of

$$\mathbf{s} = (\mathbf{A}^T\mathbf{A})^{-1}\mathbf{A}^T\mathbf{f}_{re} \tag{6.17}$$

The basic assumption of using HBM here relies on the fact that a nonlinear system, when subjected to a harmonic excitation, still exhibits a periodic response that is sufficiently close to a pure sinusoidal. Although it is recognized that the response of a nonlinear system, will have several harmonics of a given natural frequency, the amplitude of the sub-harmonics or super-harmonics are relatively small as compared to the amplitude corresponding to the given frequency. Thus, by matching the relationships between the fundamental harmonics of the response and the excitation, the parameters of the reduced model can be identified. This is achieved using the SVD-based least-squares method as in Chapter 5. Due to the fact that any chaotic orbit, if long enough, is an approximation of some unstable periodic orbits. The longer the chaotic orbit, the better the approximation [138]. Then this HBM-based identification technique can be applied upon the unstable periodic orbits to identify the unknown parameters.

To measure the error between the response records z_i and the predicted values of the reduced model, $\hat{z}_i$, a mean-square error (MSE) indicator is defined as

$$MSE(z) = \frac{100}{n\sigma_z^2}\Sigma_i(z_i - \hat{z}_i)^2 \tag{6.18}$$

where n is the total number of samples and σ_z^2 is the variance of the measured input. A MSE value of less than 5% indicates good agreement while a value of less than 1% indicates an excellent match.

6.5 Advantages of the model reduction method

The approach proposed in this chapter has some similarity to the approach proposed in Chapter 5 in that both of these approaches reconstruct a reduced model in a POD feature space with the help of commercial FEM codes. However, there are a number of important differences. Firstly, in Chapter 5, coefficients of the unknown stiffness term are determined using the transformed load-response pairs generated from nonlinear static FEM solutions. In the approach presented here, coefficients of all the terms in the reduced model (not just stiffness term) are identified using the transformed displacement time series derived from nonlinear dynamic FEM solutions. The process is repeated over different external excitations with different amplitudes and frequencies until a predetermined algebraic equation has been formulated. Secondly, because the displacement time series are used to perform parametric identification in this chapter, a special technique is needed to select the most important information contained in the displacement time series to conduct a least-squares analysis. HBM is selected to achieve this requirement. Thirdly, the approach proposed in this chapter overcomes the limitations of the approach proposed in Chapter 5 viz.

- Identical stiffness term for static and dynamics cases
- Requirement to have explicit mass and damping matrices
- Inability to model concentrated nonlinearities

6.6 Algorithm of the proposed method

A step-by-step procedure for the method is as follows:

1. Following the procedure of determining a POD space, given in Section 3.6.2, obtain the POMs and corresponding POVs for an external excitation with a specified amplitude and frequency.
2. Repeat step 1, for other excitations with different amplitudes and frequencies, $\mathbf{f}$.
3. Calculate averaged POMs, over a range of parameters of interest and select the dominant POMs, $\mathbf{P}_r$, to construct a POD feature space.

4. Transform the response time histories, $\mathbf{x}$, in the physical space corresponding to an excitation case, into those, $\mathbf{z}$, in the POD feature using Equation 6.3.

5. Transform all the load time histories, $\mathbf{f}(t)$, in the physical space corresponding to the same excitation case, into those, $\mathbf{f}_{re}(t)$, in the POD feature space using Equation 6.4

6. Repeat steps 4 and 5 to obtain a set of response and excitation time histories, $\mathbf{f}_{re}$ and $\mathbf{z}$, in the POD feature space.

7. For the kth orbit, use Equation 6.5- 6.9 and Equation 6.13 to calculate the coefficient matrix, $\mathbf{A}_k$, using Equation 6.12.

8. Use Equation 6.14 to calculate the coefficient matrix, $\mathbf{f}_{re,k}$, using Equation 6.12.

9. Repeat step 5 and 6 for all k sets of orbits to form $\mathbf{A}$ and $\mathbf{f}$ using Equation 6.16.

10. Perform an SVD-based least-squares analysis using Equation 6.17 to determine $\mathbf{s}$ and hence $\mathbf{K}_r(\mathbf{z})$, $\mathbf{C}_r$.

11. Assemble a reduced model as in Equation 6.1 using the above $\mathbf{K}_r(\mathbf{z})$ and $\mathbf{C}_r$.

The algorithm described above has been implemented in a MATLAB [136] program and can be directly applied to experimental data as well, although in this work only numerical data are used. Once all of the coefficients of the reduced model are identified, the model may be used to perform parameter study.

6.7 Numerical example

6.7.1 A cantilever

Many engineering structures (e.g. multi-story buildings) can be modelled as beam-like continuous systems. A nonlinear elastic cantilever with a rigid stop on one side, studied by Moon and Shaw [30], can simply represent the event in which a building under seismic excitation collides with its neighbouring building. Therefore, the study of the nonlinear dynamics of the cantilever is an important problem and is used to examine the approach presented in the previous section. The cantilever is $188mm$ long, $9.5mm$

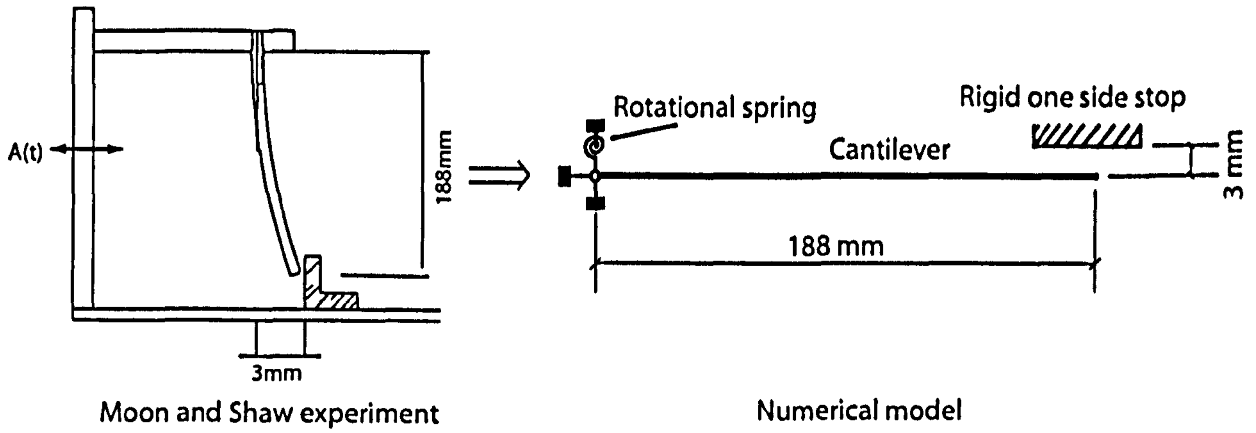

Figure 6.2: Model of the cantilever (Moon and Shaw's cantilever)

wide, and $0.23mm$ in depth. Its material has Young's modulus of $210 \times 10^9 MPa$, with mass density $7850kg/m^3$, Poisson's ratio 0.29 and material damping coefficient 0.05. The fixed end of the cantilever is subjected to a sinusoidal base excitation. The system has a Rayleigh damping with damping coefficient, β, 0.05. Its nonlinear characteristics include a nonlinear boundary condition caused by the stop with $3mm$ gap, as shown in Fig. 6.2, and geometric nonlinearity caused by large deformation. The motion of the free end is constrained by the stop, limiting the amplitude of the free end in one direction. These system parameters are held constant throughout the process of FEM simulations.

A rotational spring was set up to model experimental boundary conditions at the clamped end of the cantilever, and its stiffness value was determined by matching its natural frequencies with those measured by Moon and Shaw [30]. With the stiffness of the rotational spring equal to $7.3 \times 10^{-2} N/m^2$, the first three natural frequencies show a good match as shown in Table 6.1.

Sources	Natural frequency		
	first	second	third
Moon's values [30]	4.3	26	73
Moorthy's values [29]	4.4	28.6	81.6
Ansys results using the idealised model	4.3	29	84

Table 6.1: Comparison of the natural frequencies (unit:Hz)

The commercial FEM code Ansys [133], was used to perform a series of nonlinear dynamic analysis of the cantilever using at least 50 the Euler-Bernoulli beam element, Beam3 in Ansys. The selection of this beam element was based upon the assumption that the thickness of the beam is so small compared with the length that the effects of shearing deformation and rotatory inertia of the beam can be neglected [34]. Consistent mass modelling, adaptive time stepping and surface-to-surface contact algorithm were utilised. Frequencies of external sinusoidal excitation were swept from 3Hz to 12Hz in steps of 1Hz, with a constant excitation amplitude 0.6g (g is the acceleration of gravity). The excitation frequency induces a change in the duration of contact and therefore it has a large effect on the response. The transverse displacement responses were recorded at 10 spatially different locations from 10s to 40s. The axial displacement responses were not used because the approximation of the reduced model for the axial displacement is not as good if only a few POMs are used [139]. This limitation can be overcome by performing an independent POD analysis for these axial displacements or by selecting more POMs.

The response of the cantilever for a specified excitation frequency is characterised by time history, phase space and Fourier frequency spectrum of the free end. The dynamics of the free end of the cantilever from 10s to 40s at the excitation frequency of 3 Hz, are shown in Figure 6.3. The nearly vertical drop part of the phase space, depicted in Figure 6.3b, corresponds to the sudden velocity change that is expected at each contact. Figure 6.4 portrays the dynamics of the free end at the excitation frequency of 7Hz. Successive contacts between the free end and the stop typically occurred at different displacement values. The response of the free end remains irregular and apparently non-periodic for the duration of the simulation.

As the excitation frequency is increased over 12Hz, contacts disappear as the cantilever cannot contact the stop for high frequency excitations. No chaotic solutions were found in the simulations.

6.7.2 Identification of the reduced model

Although in this example contact boundary implies the existence of piecewise linear stiffness, it is assumed the polynomials can represent the reduced model as there is no *a priori* knowledge on the coupling between contact nonlinearity and geometric nonlinearity.

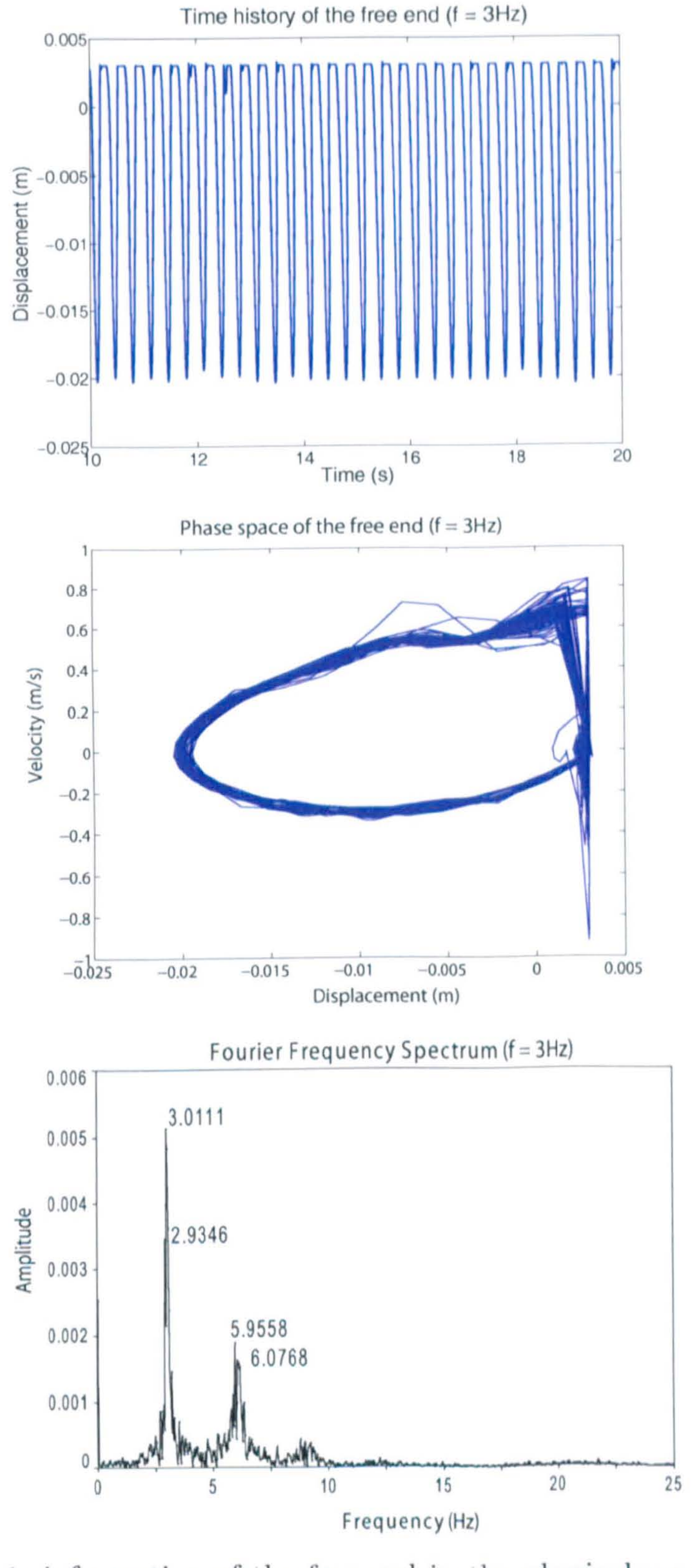

Figure 6.3: Dynamic information of the free end in the physical space corresponding to the excitation frequency of 3 Hz

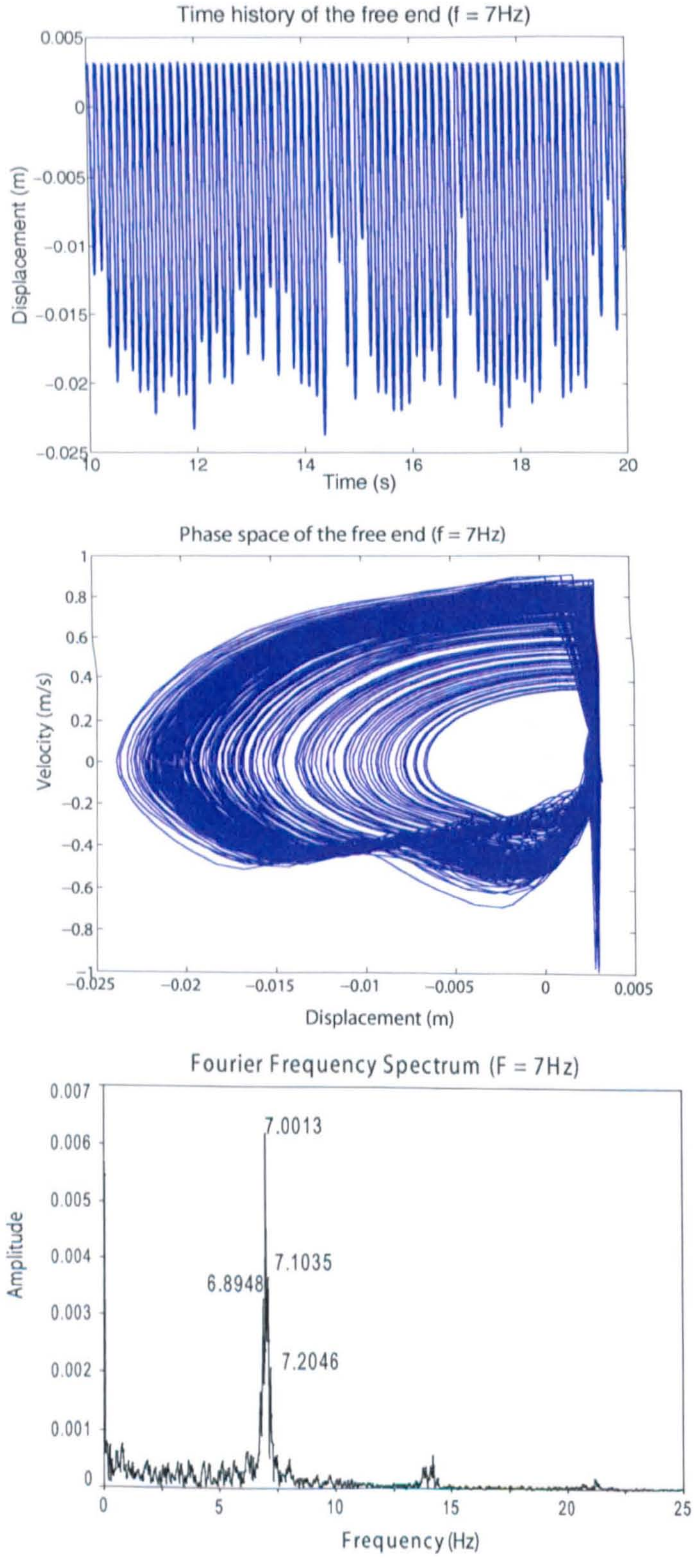

Figure 6.4: Dynamic information of the free end in the physical space corresponding to the excitation frequency of 7 Hz

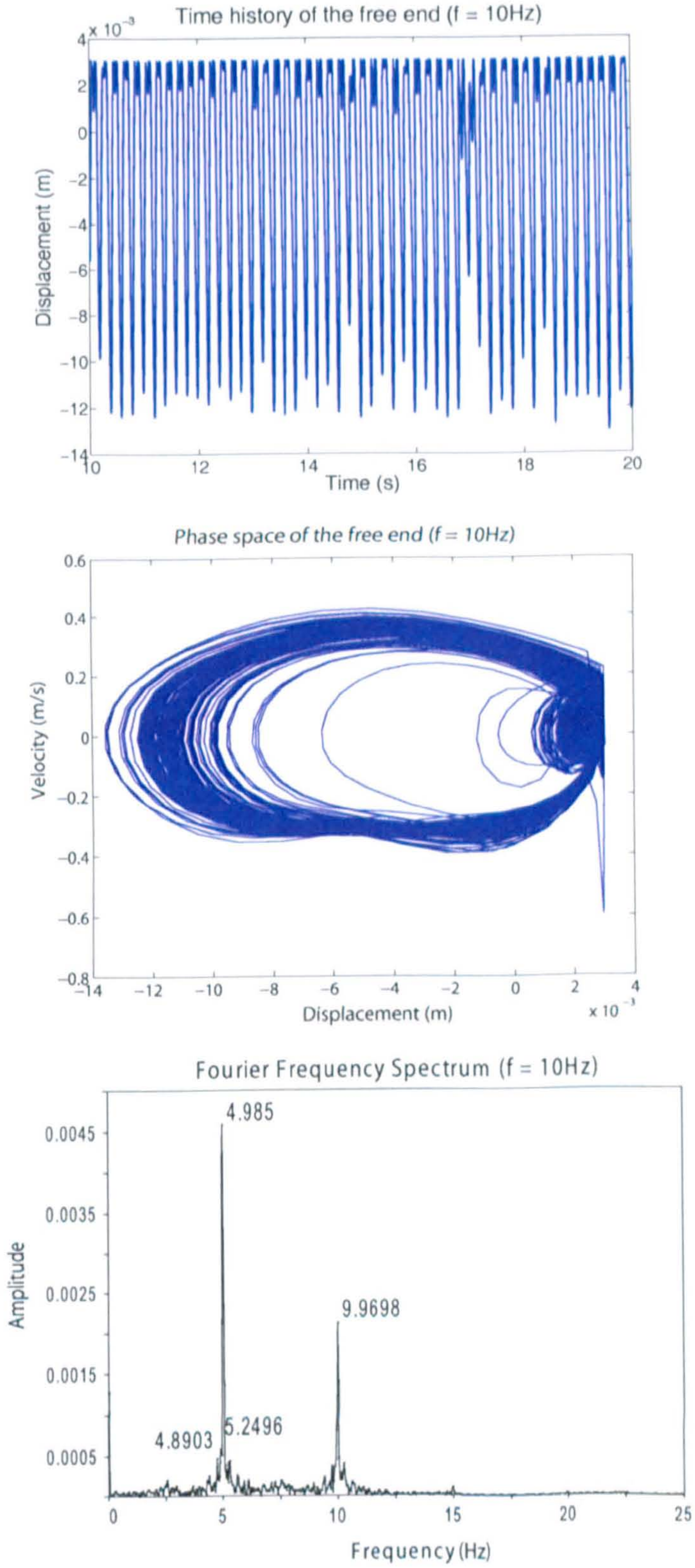

Figure 6.5: Dynamic information of the free end in the physical space corresponding to the excitation frequency of 10 Hz

Excitation frequency	3Hz	4Hz	5Hz	6Hz	7Hz	8Hz	9Hz	10Hz	11Hz	12Hz
POM1	99.90	99.81	99.71	99.66	99.63	99.58	99.54	99.81	99.63	99.98
POM2	0.10	0.19	0.28	0.34	0.37	0.41	0.45	0.18	0.37	0.02

Table 6.2: Energy captured by the first two POMs for different excitation frequencies

Following Steps 1 and 2 in Section 6.6, POMs were determined firstly. Table 6.2 shows the energy captured by the first two POMs for a range of excitation frequencies. The first POM is dominant and appears to govern the dynamics of this cantilever.

Figure 6.6 shows that as the excitation frequency is increased to 9Hz, energy transfers from the first POM to the second POM. This indicates increasing nonlinearity effects and the complexity of the structural behaviour. This also indicates that the dimensionality of the corresponding dynamics increases and reduced models should be constructed by taking into account the first and second POMs. However, due to the fact that all the first POMs contain at least 99.5% of the energy, it was assumed that the first POM can fully capture the structural behaviour of the cantilever.

Figures 6.6 and 6.7 show that the first two POMs are similar, both in terms of model shape and in terms of energy distribution for different frequency conditions. This suggests that the POMs derived from one frequency condition can be used as an approximation for the POMs of other frequencies. Therefore, POD feature space was identified using only the averaged first POM (See Step 4 in Section 6.6). This finding also paves the way towards using a SDOF reduced model over a range of frequency conditions.

Following the procedure in Section 6.4.1 (Step 4 of the algorithm) and using Equation 6.4, the transformation of the displacement time histories over a range of excitation frequencies, resulted in the corresponding displacement time histories in the POD feature space. Only the average first POM is used to form the transformation matrix, P_r. Comparison of two time histories of the free end displacements between the physical space and the POD space, corresponding to the excitation frequencies 3Hz and 7Hz, are shown in Figure 6.8 and Figure 6.9, respectively. The abstract displacement time histories in the POD space have similar dynamic characteristics except amplitude with those in the physical space. They are non-symmetric due to the one-side stop. The load time series in the physical space was also transformed into the corresponding POD feature space, using

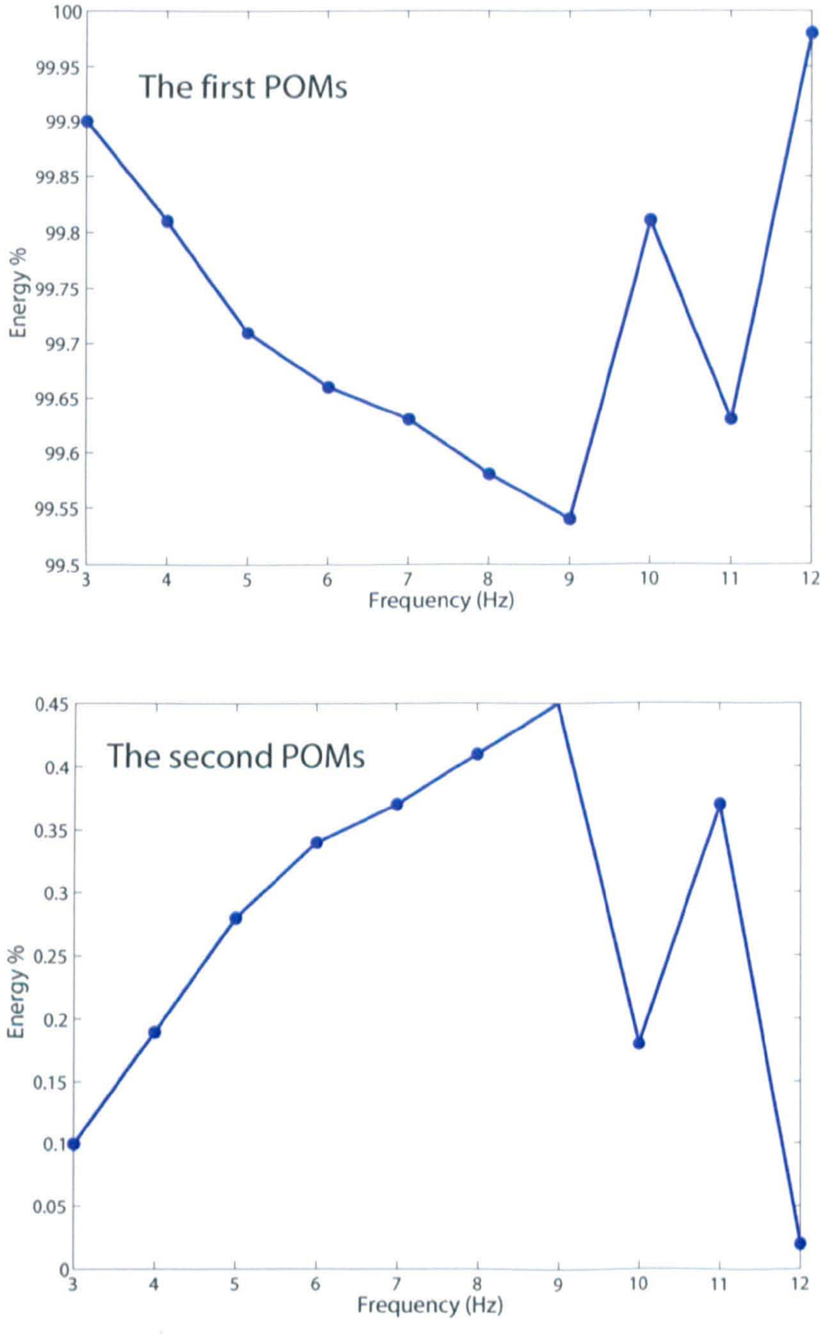

Figure 6.6: Energy distribution among POMs over a range of the excitation frequencies for the example cantilever

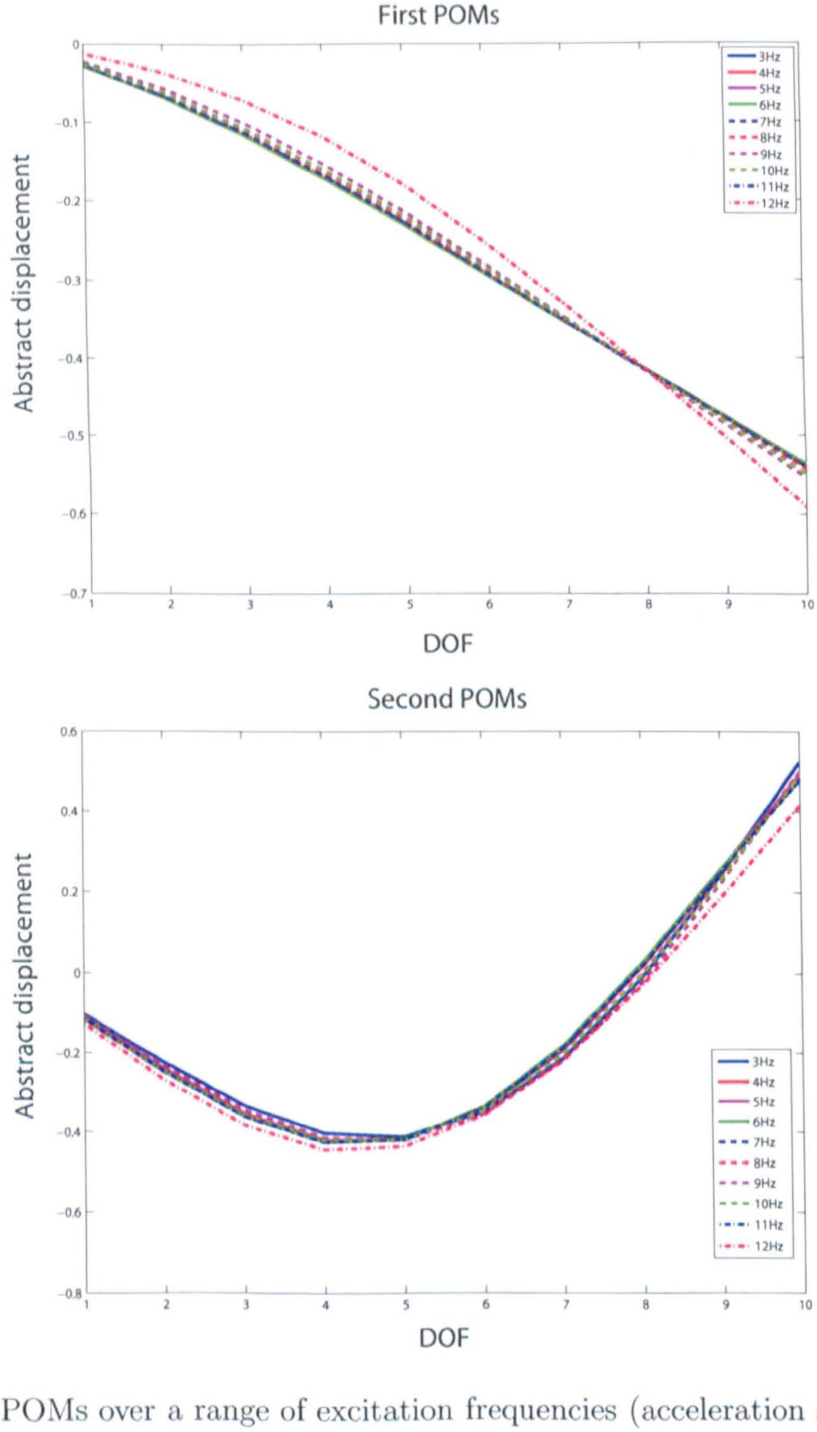

Figure 6.7: POMs over a range of excitation frequencies (acceleration amplitude: 0.6g)

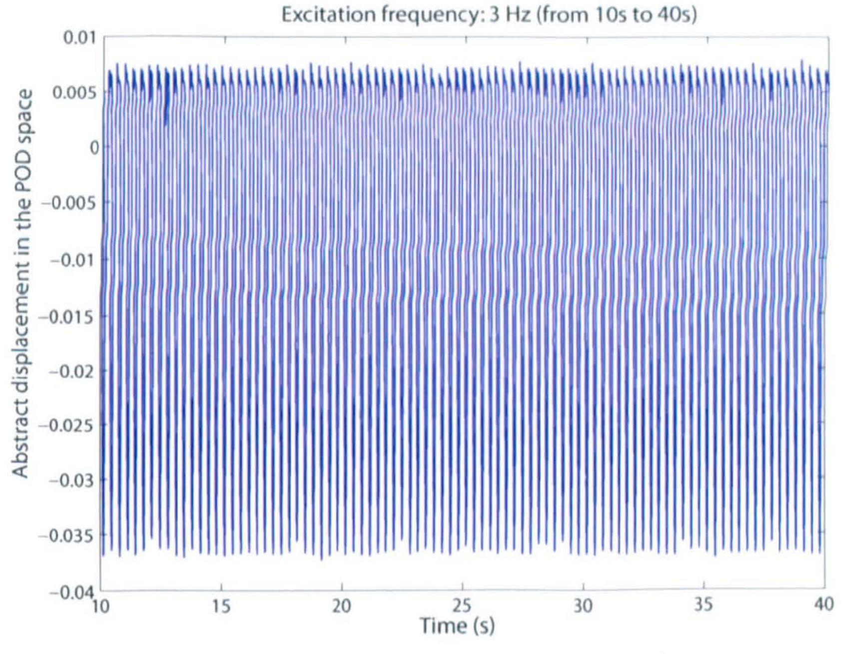

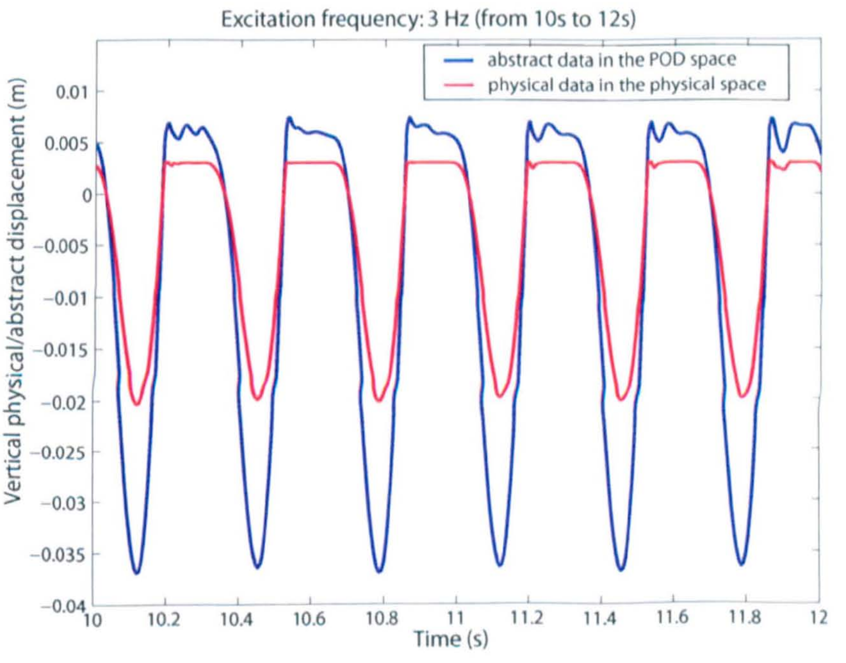

Figure 6.8: Displacement time series in the POD feature space corresponding to excitation frequency of 3Hz and its comparison with that in the physical space

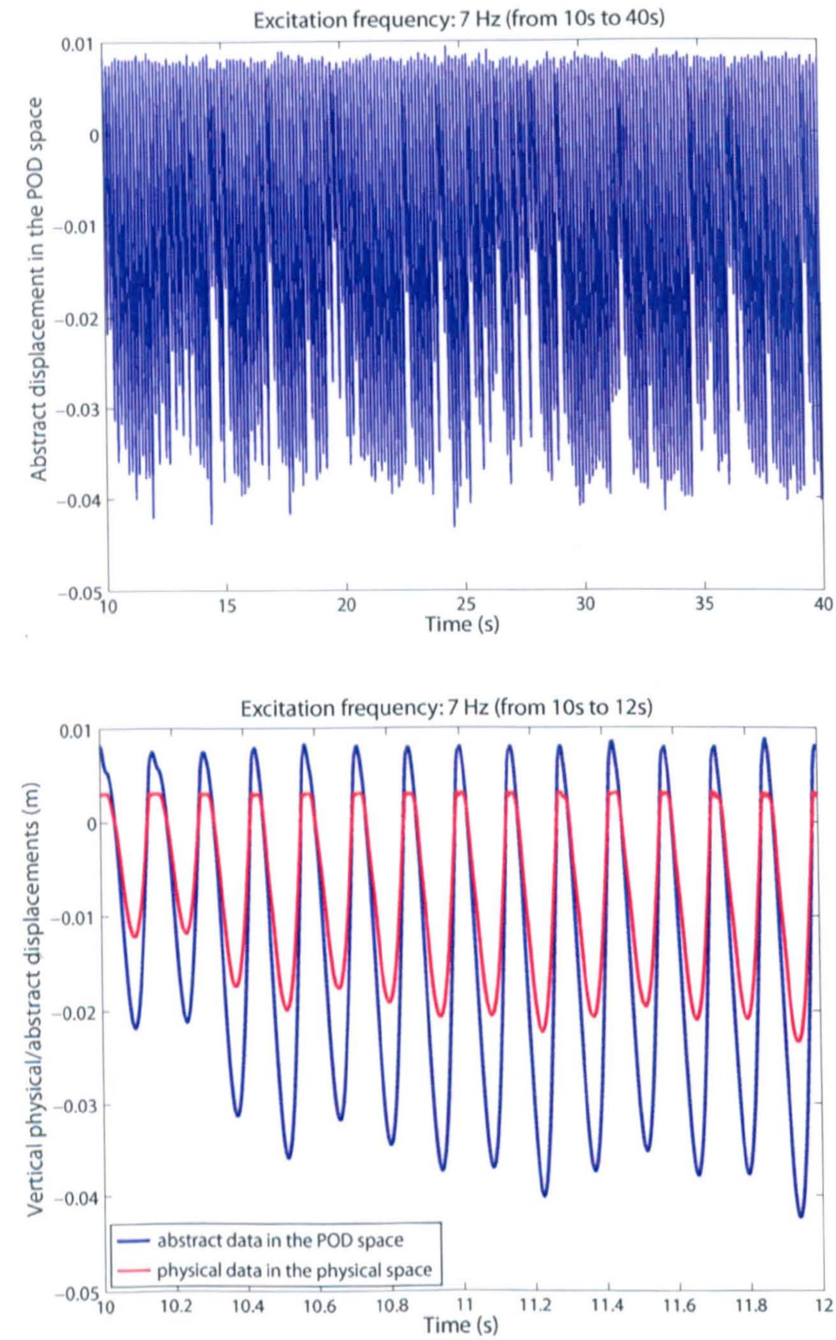

Figure 6.9: Displacement time series in the POD feature space corresponding to excitation frequency of 7Hz and its comparison with that in the physical space

the same transformation matrix, P_r (See Step 5).

Number of harmonics	c	k_1	k_2	k_3	k_4	k_5	k_6	MSE
4	6.99	-2.32e3	-1.28e5	8.65e7	-6.15e9	1.59e11	-1.40e12	4.2%
5	6.28	-1.58e3	-1.16e5	7.47e7	-5.43e9	1.44e11	-1.32e12	5.7%
6	5.96	-1.17e3	-9.97e4	6.87e7	-5.15e9	1.41e11	-1.32e12	7.2%

Table 6.3: Results of parameter identification using different number of harmonics, using 60T

Following [138], an orbit length of nT (T is the period of the external excitation and $n = 60, 80, 90$) was selected as the length of segment to divide recorded time series into periodic orbits for performing parametric identification using HBM (see Step 10). It is noted that from Equation 6.6 and 6.7, the computational errors in the obtained velocity and acceleration is amplified by $i\omega$ and $i^2\omega^2$. Thus, the velocity and acceleration time series are considered to be contaminated mainly by high frequency noise. In other words, the integration calculation of noisy signals introduces noise amplification effects, in particular low-frequency noise amplification, which distorts the velocity and displacement estimates. This effect causes parameter bias and errors in the associated coefficients in the model [140].

The final column of Table 6.3 shows the MSE value obtained using Equation 6.18, corresponding to different number of harmonics. The use of 4 harmonics produces the best result. Hence, the number of polynomial terms to represent the stiffness part of Equation 6.10, was chosen as 6, while the number of harmonics used was 4. The use of only the first 4 terms of harmonics filters out the possible high frequency computational noise and results in an identification process that is noise resistant to some extent.

Minimum length	c	k_1	k_2	k_3	k_4	k_5	k_6
60T	7.0	-2.31e3	-1.26e5	8.63e7	-6.15e9	1.59e11	-1.41e12
80T	7.01	-2.31e3	-1.22e5	8.65e7	-6.22e9	1.62e11	-1.45e12
90T	6.99	-2.32e3	-1.28e5	8.65e7	-6.15e9	1.59e11	-1.40e12
Mean values	7.0	-2.31046e3	-1.25e5	8.64e7	-6.169e9	1.60e11	-1.42e12

Table 6.4: Results of parameter identification using different segment lengths

The identified coefficients of the equation of motion of the reduced SDOF model represented by Equation 6.10, are given in Table 6.4.

Thus, a SDOF reduced model is identified and Equation 6.10 becomes

$$
\begin{aligned}
&\ddot{z} + 7\dot{z} - 2.31 \times 10^3 z - 1.25 \times 10^5 z^2 + \\
&8.64 \times 10^7 z^3 - 6.17 \times 10^9 z^4 + 1.6 \times 10^{11} z^5 - 1.42 \times 10^{12} z^6 \\
&= A_{base}^{POD}(2\pi f t)
\end{aligned}
\tag{6.19}
$$

6.7.3 Evaluation of the reduced model

The cantilever was analysed using the original FEM model and the corresponding reduced model in Equation 6.19. When contacts are involved it is not always possible to obtain pointwise time domain convergence between the simulated and reconstructed results due to sensitive dependence on initial conditions. Figure 6.10 and 6.11 show that there is a good agreement between the Fourier frequency spectrum generated with the original FEM model and the reduced model, corresponding to the excitation frequencies, 3Hz and 7Hz. Similar results were obtained for different excitation frequencies. It is noted that a FEM simulation using Ansys with a set of parameters took around 20 hours, whiles a simulation using the reduced model with the same set of parameters took 0.0009s on average.

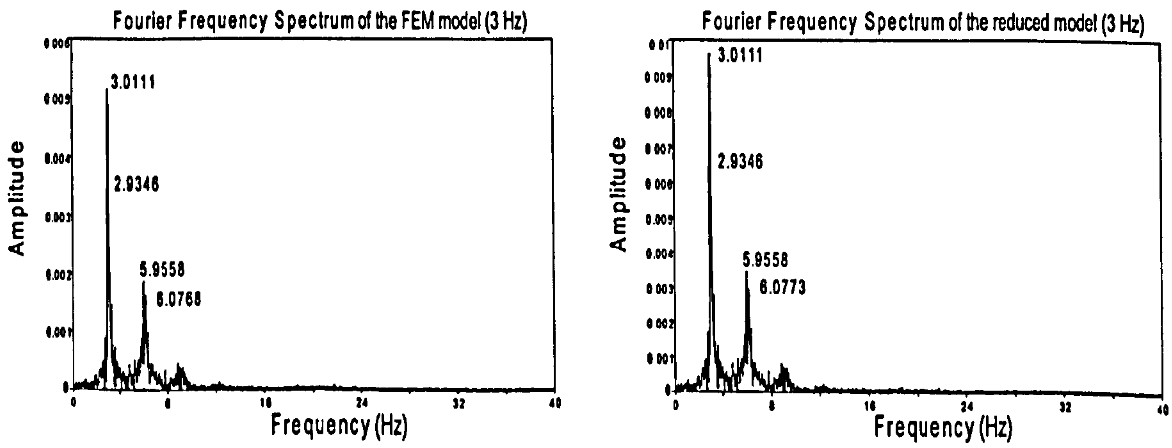

Figure 6.10: Comparison of the Fourier frequency spectrum corresponding to excitation frequency of 3Hz (a) The FEM model (b) The reduced model

Two differences exist between the reduced model and the original FEM model: a) Integration algorithm, and b) damping. In the reduced model, a 4/5th order Runge-Kutta algorithm was used rather than the Newmark method as employed in the FEM

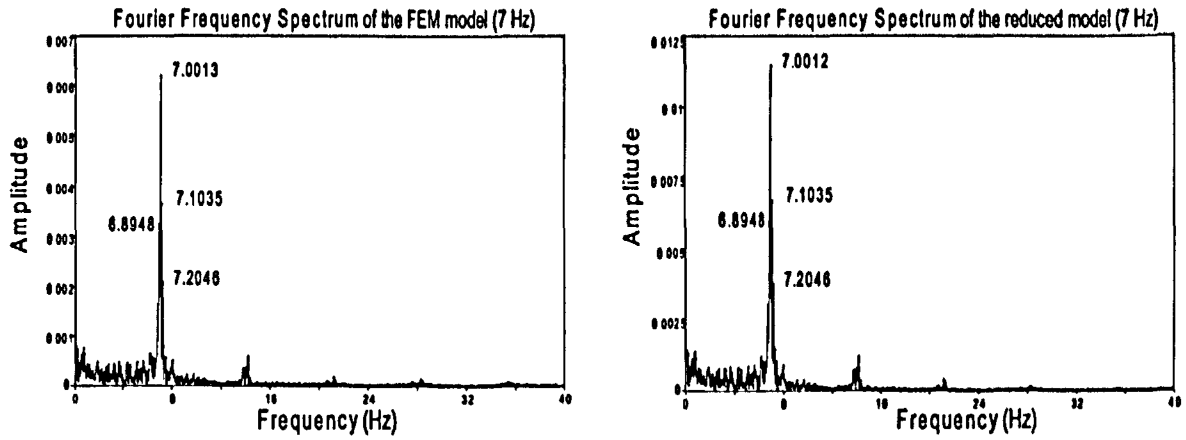

Figure 6.11: Comparison of the Fourier frequency spectrum corresponding to excitation frequency of 7Hz (a) The FEM model (b) The reduced model

model. With regard to damping, the FEM model used Rayleigh damping as its stiffness-proportional part supplies higher damping at higher frequencies. This feature, although attractive numerically, might not be accurately modelled by the assumed viscous damping. The proposed method can be easily extended to consider more complex damping terms. To further evaluate the differences, these issues need to be resolved.

For validation of unknown systems, comparison of fractal dimensions, bifurcation diagram and Lyapunov exponents can be employed [96]. However for this simulation case, where the parameters are known, direct comparison is the best tool.

6.8 Study for global dynamics

The reduced model was obtained using limited set of parameters and is expected to be only an approximation of the full FEM model, since the reduced models change when the excitation parameters or the system parameters are changed. However, the reduced models may be significantly different when the parameter variation is large. Therefore, a number of reduced models with its own range of parameters may need to be identified.

The global dynamics of the example structure was explored using the resulting reduced model, defined by Equation 6.19. Varying the amplitude and frequency of external excitation $A \cdot sin(\omega t)$, the parameter study for the reduced model was conducted using a tool [15] which uses a classical 4/5th order Runge-Kutta algorithm.

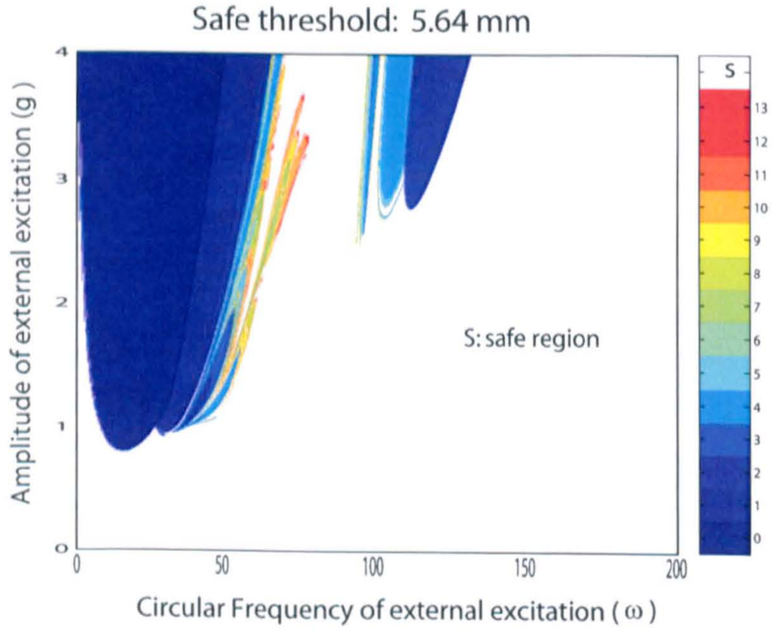

Figure 6.12: Integrity diagram using the reduced model of the cantilever (critical abstract displacement: 5.64)

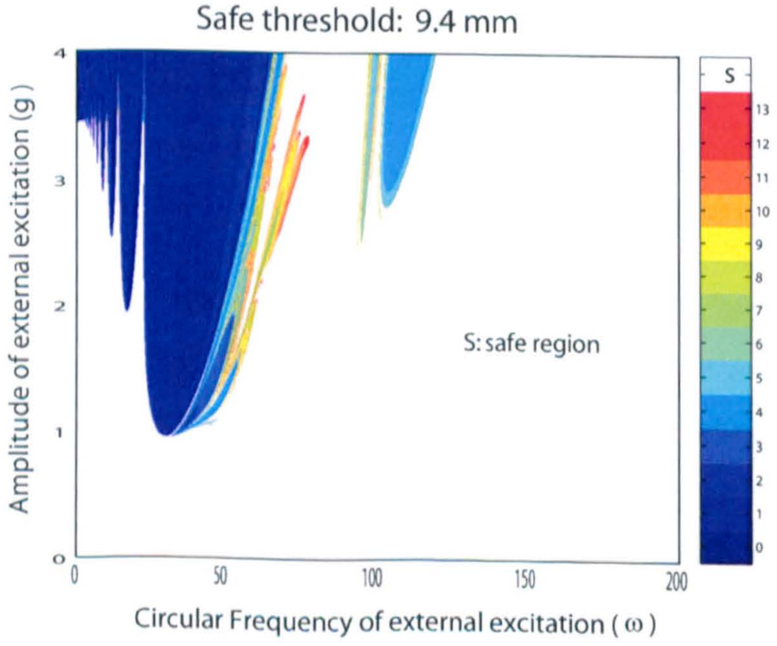

Figure 6.13: Integrity diagram using the reduced model of the cantilever (critical abstract displacement: 9.4)

The results are shown in Figure 6.12 and Figure 6.13. Different colours represent the number of forcing cycles till the displacement of the model exceeds a critical value and hence the model fails. White colour stands for the safe region in which the displacement is within an allowable threshold. In Figure 6.12, the critical value was chosen to be 5.64, while in Figure 6.13, it was chosen to be 9.4. As expected, the latter has a smaller safe region. A region over a frequency ω from 40 to 80, is found to be less dependable. This is broader than the range, from 60 to 66, over which chaotic vibrations were observed in [30]. It is also noted that the integrity diagram was obtained using the reduced model to perform more than one million simulations and only lasted 15 minutes using a desktop PC. In other words, a leverage factor at around 83 millions, in term of computation time is achieved using the reduced model.

6.9 Discussion

- The form of nonlinearities in a POD feature space is assumed to be unknown and a polynomial function of displacement is used to represent nonlinearities in this thesis. This offers the ability to handle various nonlinearities, including geometric, and boundary nonlinearities. However, the method cannot handle hysteresis effect or dissipative effect, due to the limitation of the assumed mathematical form. This can be overcome by selecting other mathematical forms, for example, both $\mathbf{z}$ and $\dot{\mathbf{z}}$ can be considered as state variables in the assumed reduced model. When there is some physical knowledge of the system, it might be useful to choose mathematical forms that closely approximate the known physical knowledge. For example, a discontinuous function might lead to a better result in the case of contact and a polynomial function cannot be applied in a situation where hysteretic behaviour is expected.

- An important benefit of the proposed method is that it can be integrated with any commercial numerical tools or experimental measuring techniques to explore global dynamics of nonlinear dynamic structures. This characteristic extends application of this method to structural systems with complicated geometry and complex non-linearity, without any understanding of the dynamics of the physical systems. While the example studied in this chapter does not have a large DOF, the method is applicable to large DOF systems. The more complex a nonlinear structure behaves, the more useful would the method become in constructing a reduced model that captures the dominant features of the global behaviour of the structure over a range of parameters of interest. In this chapter, the simulation was limited to a SDOF system without consideration of modal coupling. Although MDOFs models are required to improve the accuracy of the reduced model, this may lead to complex model couplings and introduce extra computational costs. This improvement is not necessary for understanding the global behaviour of a nonlinear structure.

- The approach, as reported in this chapter, is based on a multivariate statistical method and leads to an abstract mathematical model without a clear one-to-one mapping between the reduced model and the original structure. There is a trade-off between the robustness and accuracy of a POD feature space. The construction of a POD feature space is dependent on the responses obtained from experimental or numerical solutions. When this response data captures the dynamics of a nonlinear structure, the resulting POD feature space and the deduced model will effectively represent the original structure. This may be viewed as a strength in terms of effectiveness or as a weakness in terms of robustness to parameter variations. In this work, an average POM over a range of frequencies was used to form a POD feature space in which reduced models are reconstructed. Equation 3.37 implies a potential approach to improve reduced model. U and V are assumed to remain constant for a reduced model, while λ_i, the participation of POMs, can be changed to represent the response to new system parameters. Couplet et al. [141] suggested a calibration procedure for the coefficients of the reduced model that greatly improves model accuracy.

- In plasticity problems, the appearance of nonlinearities introduces high damping and energy is dissipated, which eliminates unexpected behaviours. Hence, this proposed method only considers nonlinear elastic problems. In future, materials may remain elastic over a bigger range than now.

- In this chapter, subharmonics were not considered to perform the parametric identification using harmonic balance method, although subharmonic oscillations are found to be a characteristic of dynamic behaviour of the cantilever [30]. When nonlinearities are strong, choices of subharmonic terms have influence on the identified parameters. Inappropriate selection of subharmonics can generate poor results. To avoid this, the key factor is to avoid noise contaminated subharmonics. The subharmonics of frequencies less than the excitation frequency might be selected to avoid noise.

6.10 Conclusion

A general method of constructing a reduced model of nonlinear dynamic structures is proposed. By considering relationship time histories, more nonlinearities can be modelled using this method, compared with the method proposed in the previous chapter. No information regarding the mass, damping and nonlinearity of the nonlinear structure is required. The use of HBM successfully makes the identification of all nonlinear systems possible.

The method was successfully applied to a highly nonlinear case of a cantilever with one side stop. The reduced SDOF model qualitatively captures dynamics of the original FEM model of this cantilever, over a range of parameters of interest. Quantitative comparisons using FFT spectra show that the reduced model predicts well the response of the original FEM model. The low order integrity plot using the reduced model offers a huge leverage factor on time saving over attempting this in full FEM models. Results show that this proposed method has a great potential to investigate global behaviours of realistic structures.

Chapter 7

Conclusions and Future Work

7.1 Conclusions

Vulnerability Study

1. A new POM-based method of assessing vulnerability of nonlinear structures (complementary to structural vulnerability theory) is proposed. This is based on the fact that changes in the global behaviour will cause detectable changes in the POMs. The sum of the weighted POMs, as a quantitative measure, helps to assess the effects of member failures on the global behaviour of the structure. Example studies show that the proposed method and the quantitative measure are suitable for the study of member failures, different external excitations and failure scenarios. The new vulnerability measure considering only the first POMs, provides an effective tool for identifying vulnerable structural members. This proposed method has the potential to help engineers to avoid vulnerable structural design.

Model Reduction

2. Two novel methods are proposed to construct efficient reduced models in a POD feature space. The simplicity and efficiency of the POD space makes it possible to qualitatively represent dynamics of highly nonlinear systems using the reduced models. Nonlinearities are considered in the form of a series of ordinary polynomial basis functions.

3. The method presented in Chapter 5, takes advantage of the orthogonal characteristic of POMs to uncouple the mass and damping terms of the reduced model. The

stiffness term is determined using results of nonlinear static analyses, using a commercial FEM package as the solver engine. This method overcomes the difficulties encountered using modal space viz. selection of modal modes and determination of the number of modal modes. This method is computationally efficient but is limited to geometric nonlinear problems and requires *a priori* knowledge of mass and damping matrices.

4. Examples using the above method show that even using only one POM, there is good correlation between the dynamic behaviour of the original system and that of the reduced model, although some information is lost due to the model reduction.

5. The method proposed in Chapter 6 utilises dynamic relationships between loads and responses. In this method, only response time histories are supposed to be known which can come from measurements on real structures or any numerical simulation. The use of HBM efficiently produces a reduced model and makes the identification of all nonlinear systems possible.

6. Dynamic analyses of the reduced model agree well with those derived from the original nonlinear system. Usually using only one POM, dynamics of the original system can be qualitatively captured. Quantitative comparisons using FFT spectra show that the reduced model predicts well the response of the original FEM model.

7. Since the POMs are derived from simulation or measurement data, the validity of the reduced model depends on the quality of the data. If the data sufficiently represents the dynamic behaviour of the structure over a parameter range, then the reduced model is valid for simulations within that parameter range. A new model could be created for parameters beyond the above range. A commercial FEM analysis will usually ensure that all necessary dynamic information is captured. FEM simulations are arranged as an external process. This is a significant attribute because it means that the power and versatility of commercial codes can be leveraged, greatly extending the range and type of problems that can be solved. Therefore, these two methods can be used in realistic structures with complicated geometry and complex nonlinearity.

Integrity Study

8. Examples show that averaging POMs is a feasible way to extend the validity of the POM for a parameter range of interest, and the resulting reduced models may be suitable for performing a parameter study.

9. The efficiency of reduced models provides potential solutions to the investigation of global behaviour of realistic structures with large DOF. POD-based reduced models make it very tractable to perform parameter studies. This may be very useful to ensure safety and robustness of nonlinear dynamic structures.

10. Parameter studies may be able to identify dependable regions in the parameter space of nonlinear systems. Dependable regions are those where the response of the system does not change significantly in comparison to the changes in loading and system parameters.

7.2 Future work

Some relevant areas of future work are as follows:

1. Further studies are needed to examine the applicability and generality of the proposed method in capturing global behaviour of nonlinear dynamic structures, including bifurcations. In particular, for unknown systems with strong nonlinearities, it is also necessary to extend the validity of POD-based reduced models under varying initial conditions. This will make the constructed reduced models robust. The goal is to build a SDOF reduced model for the first POM, and make it applicable for general initial conditions by adding a constraint. This is inspired by Nonlinear normal modes [44]. For example, in Equation 5.12, z_1 is the dominant state variable in the POD feature space. The coupling between z_1 and z_2 can be implicitly considered by expressing z_2 as a function of z_1 and $\dot{z}_1$

$$z_2 = \sum_{i}^{3} \sum_{j}^{3} \alpha_{i,j} z_1^i \dot{z}_1^j$$

The constraint z_2 might enlarge the applicable domain of the reduced model constructed using z_1. This new model can be regarded as the added-constraint model.

2. POMs are used to examine the vulnerability of nonlinear dynamic structures. The high sensitivity of higher level POMs might influence the capability of the proposed vulnerability measure (see Equation 4.3). There are two relevant topics which might deserve further study:

   - Employing multiple load patterns might extend the capability of higher level POMs, since POMs contain information associated with loadings.
   - Kernel POD is a new development of POD and its basic idea is to transform the raw response data into a feature space with the same dimensions via a nonlinear transformation operator, and then conduct a POD analysis in the feature space. However, the selection of the nonlinear transformation operator is still an unsolved problem (for example, see [142]).

3. A SVD-based least-squares technique was employed in this thesis. There are other interesting techniques that can be used, for example:

   - The use of Tikhonov regularisation in [143] provides an alternative.
   - An adaptive HBM devised by Maple [144] could be introduced to determine the number of frequencies for performing parametric identification in which a small number of frequencies are used and more frequency terms are augmented. By doing so, the difference between reduced models and the original system could be decreased.

4. The stability of reduced models over the parameter space of interest can become a problem. There are two potential ways to overcome this problem:

   - Kerschen et al. [35] stressed that nonlinear system identification requires an accurate characterisation of the nonlinearity present in a system, before any parameter estimation can be attempted. Therefore, an assumed model with reliable physical insight is essential (for example, see [6]). However, in most cases, the physical insights are not always available.

- Kernel POD provides a new feature space whose basis is nonlinear rather than linear as in the case of POD. This new feature space might represent the characteristics of the nonlinearities of the original model more accurately. It can be integrated with the proposed methods, although it might be difficult to find a proper nonlinear transformation.

5. In order to make the proposed method more practical for real structures with large DOF, there are three issues that require further study:

   - To explore the potential of utilising response time histories of several nodes in nonlinear systems to construct a reduced model with reasonable accuracy.
   - To define the range of initial conditions and parameters over which the reduced model can be used with acceptable accuracy.
   - Following the idea of substructuring, to apply the method locally to a part of a complex structure which contains highly nonlinear dynamics.

   Some clues might be found in [91], [141] and [145]. In order to improve the robustness of a POD feature space, Lieu and Farhat [92] introduced an interpolation technique to produce a set of global POMs between two proper orthogonal decomposition subspaces, then generated a new proper orthogonal decomposition basis through an orthogonal transformation based on the interpolated subspace angles.

6. Effectiveness of POD-based model reduction approaches in the presence of higher modes and nonlinearities need further investigation.

Bibliography

[1] A. H. Nayfeh and H. N. Arafat. *Structural Dynamics 2000: Current Status and Future Directions*, chapter An Overview of Nonlinear System Dynamics. Research Studies Press, 2001.

[2] H. Krawinkler. Importance of good nonlinear analysis. *Structural Design of Tall and Special Buildings*, 15(5):515–531, December 2006.

[3] A. L. Hale and L. Meirovitch. A general substructure synthesis method for the dynamic simulation of complex structures. *Journal of Sound and Vibration*, 69(2):309–326, 1980.

[4] G. Rega and H. Troger. Dimension reduction of dynamical systems: Methods, models, applications. *Nonlinear Dynamics*, 41(1-3):1–15, August 2005.

[5] R. Qiao and N. R. Aluru. Transient analysis of electro-osmotic transport by a reduced-order modelling approach. *International Journal for Numerical Methods in Engineering*, 56(7):1023–1050, February 2003.

[6] S. Lall, P. Krysl, and J. E. Marsden. Structure-preserving model reduction for mechanical systems. *Physica D*, 184(1-4):304–318, October 2003.

[7] M. Paz. Dynamic condensation. *AIAA Journal*, 22(5):724–727, 1984.

[8] W. C. Hurty, J. D. Collins, and G. C. Hart. Dynamic analysis of large structures by modal synthesis techniques. *Computers and Structures*, 1:535–563, 1971.

[9] L. Meirovitch. *Computational Methods in Structural Dynamics*. Kluwer Academic Publishers, 1980.

[10] R. R. Arnold, R. l. Citerley, M. Chargin, and D. Galant. Application of ritz vectors for dynamic analysis of large structures. *Computers and Structures*, 21(3):461–467, 1985.

[11] J. M. T. Thompson and H. B.Stewart. *Nonlinear Dynamics and Chaos (Second Edition).* John Wiley and Sons, LTD, 2002.

[12] F. Ehrich and H. N. Abramson. *Harris' Shock and Vibration Handbook*, chapter Nonlinear Vibration. McGraw-Hill, 2002.

[13] F. C. Moon. *Chaotic and Fractal Dynamics-an Introduction for Applied Scientists and Engineers.* John Wiley and Sons, LTD, 1992.

[14] L. N. Virgin. *Introduction to Experimental Nonlinear Dynamics.* Cambridge University Press, 2000.

[15] O. Oddbjornsson, N.A. Alexander, C.A. Taylor, and R. Sigbjornsson. Computational analysis of precast concrete frames with post-tensioned tendons. In B. H. V. Topping, editor, *Proceedings of the Eleventh International Conference on Civil, Structural and Environmental Engineering Computing*, 2007.

[16] D. J. Wagg. Periodic and chaotic dynamics in an asymmetric elastoplastic oscillator. *Chaos Solitons and Fractals*, 16(5):779–786, June 2003.

[17] J. M. Aguirregabiria. *Dynamics Solver Release 1.7 Manual.* 2007.

[18] P. Dallard, A. Fitzpatrick, A. Flint, S. Le Bourva, A. Low, R. R. Smith, and Wilford. The london millennium footbridge. *The Structural Engineer*, 79:17–35, 2001.

[19] K. J. Bathe. *Finite Element Procedures.* Prentice Hall, New York, 1996.

[20] C. M. Harris and A. G. Piersol, editors. *Harris' Shock and Vibration Handbook.* McGraw-Hill Professional, 5 edition, 2001.

[21] D. Vamvatsikos and C. A. Cornell. Incremental dynamic analysis. *Earthquake Engineering & Structural Dynamics*, 31(3):491–514, March 2002.

[22] B. Poddar, F. C. Moon, and S. Mukherjee. Chaotic motion of an elastic-plastic beam. *Journal of Applied Mechanics-Transactions of The ASME*, 55(1):185–189, March 1988.

[23] G. Rega. Non-linearity, bifurcation and chaos in the finite dynamics of different cable models. *Chaos Solitons and Fractals*, 7(10):1507–&, October 1996.

[24] M. S. Soliman and P. B. Goncalves. Chaotic behavior resulting in transient and steady state instabilities of pressure-loaded shallow spherical shells. *Journal of Sound and Vibration*, 259(3):497–512, January 2003.

[25] J. M. T. Thompson and M. S. Soliman. Fractal control boundaries of driven oscillators and their relevance to safe engineering design. *Proceedings of The Royal Society of London Series A-Mathematical Physical and Engineering Sciences*, 428(1874):1–13, March 1990.

[26] S. J. Hogan. On the dynamics of rigid-block motion under harmonic forcing. *Proceedings of The Royal Society of London Series A-Mathematical Physical and Engineering Sciences*, 425(1869):441–476, October 1989.

[27] J. Agarwal, D. I. Blockley, and N. J. Woodman. Qualitative analysis of non-linear dynamical systems. *Computer Methods in Applied Mechanics and Engineering*, 145(1-2):135–145, June 1997.

[28] J. Y. Lee, P. S. Symonds, and G. Borino. Chaotic responses of a 2-degree-of-freedom elastic-plastic beam model to short pulse loading. *Journal of Applied Mechanics-Transactions of The Asme*, 59(4):711–721, December 1992.

[29] R. I. K. Moorthy, A. Kakodkar, H. R. Srirangarajan, and S. Suryanarayan. Finite-element simulation of chaotic vibrations of a beam with nonlinear boundary-conditions. *Computers & Structures*, 49(4):589–596, November 1993.

[30] F. C. Moon and S. W. Shaw. Chaotic vibrations of a beam with non-linear boundary conditions. *International Journal of Non-Linear Mechanics*, 18(6):465–477, 1983.

[31] P. Krysl, S. Lall, and J. E. Marsden. Dimensional model reduction in non-linear finite element dynamics of solids and structures. *International Journal for Numerical Methods in Engineering*, 51(4):479–504, June 2001.

[32] G. Kerschen, J. C. Golinval, A. F. Vakakis, and L. A. Bergman. The method of proper orthogonal decomposition for dynamical characterization and order reduction of mechanical systems: An overview. *Nonlinear Dynamics*, 41(1-3):147–169, August 2005.

[33] J. Agarwal, D. Blockley, and N. Woodman. Vulnerability of structural systems. *Structural Safety*, 25(3):263–286, 2003.

[34] A. H. Nayfeh and P. F. Pai. *Linear and Nonlinear Structural Mechanics*. John Wiley and Sons, INC., 2004.

[35] G. Kerschen, K. Worden, A. F. Vakakis, and J. C. Golinval. Past, present and future of nonlinear system identification in structural dynamics. *Mechanical Systems and Signal Processing*, 20(3):505–592, April 2006.

[36] K. Worden and G. R. Tomlinson. *Nonlinearity in Structural Dynamics–Detection, Identification and Modelling*. Institute of Physics Publishing, 2001.

[37] B. H. K. Lee, S. J. Price, and Y. S. Wong. Nonlinear aeroelastic analysis of airfoils: Bifurcation and chaos. *Progress In Aerospace Sciences*, 35(3):205–334, April 1999.

[38] A. H. Nayfeh. *Perturbation Methods*. Wiley, New York, 1973.

[39] J. J. Thomsen. *Vibrations and Stability–Advanced Theory, Analysis, and Tools (Second Edition)*. Springer, 2003.

[40] D. W. Jordan and P. Smith. *Nonlinear Ordinary Differential Equations–An Introduction to Dynamical Systems (Third Edition)*. Oxford University Press, 1999.

[41] K. Yasuda, S. Kawamura, and K. Watanabe. Identification of nonlinear multi-degree-of-freedom systems (presentation of an identification technique). *JSME International Journal Series III-Vibration Control Engineering Engineering for Industry*, 31(1):8–14, March 1988.

[42] K. Yasuda and S. Kawamura. A nonparametric identification technique for nonlinear vibratory-systems - proposition of the technique. *JSME International Journal Series III-Vibration Control Engineering Engineering for Industry*, 32(3):365–372, September 1989.

[43] R. M. Rosenberg. The normal modes of nonlinear n-degree-of-freedom systems. *Journal of Applied Mechanics*, 30:7–14, 1962.

[44] S. W. Shaw and C. Pierre. Nonlinear normal-modes and invariant-manifolds. *Journal of Sound and Vibration*, 150(1):170–173, October 1991.

[45] A. F. Vakakis. Non-linear normal modes (nnms) and their applications in vibration theory: An overview. *Mechanical Systems and Signal Processing*, 11(1):3–22, January 1997.

[46] A. K. Chopra. *Dynamics of Structures–Theory and Application to Earthquake Engineering.* Prentice Hall, New York, 2001.

[47] P. E. Rapp, T. I. Schmah, and A. I. Mees. Models of knowing and the investigation of dynamical systems. *Physica D-Nonlinear Phenomena*, 132(1-2):133–149, July 1999.

[48] A. C. Antoulas. An overview of approximation methods for large-scale dynamical systems. *Annual Reviews In Control*, 29(2):181–190, 2005.

[49] D. J. Lucia, P. S. Beran, and W. A. Silva. Reduced-order modeling: New approaches for computational physics. *Progress In Aerospace Sciences*, 40(1-2):51–117, February 2004.

[50] A. Steindl and H. Troger. Methods for dimension reduction and their application in nonlinear dynamics. *International Journal of Solids and Structures*, 38(10-13):2131–2147, March 2001.

[51] H. Kim and M. Cho. Improvement of reduction method combined with sub-domain scheme in large-scale problem. *International Journal for Numerical Methods in Engineering*, 70(2):206–251, April 2007.

[52] Z. Q. Qu. *Model Order Reduction Techniques with Applications in Finite Element Analysis.* Springer, 2004.

[53] R. J. Guyan. Reduction of stiffness and mass matrices. *AIAA Journal*, 3, 1965.

[54] V. N. Shah and M. Raymund. Analytical selection of masters for the reduced eigenvalue problem. *International Journal for Numerical Methods in Engineering*, 18(1):89–98, 1982.

[55] N. Bouhaddi and R. fillod. A method for selecting master dof in dynamic substructuring using the guyan condensation method. *Computers and Structures*, 45(5-6):941–946, December 1992.

[56] P. Apiwattanalunggarn, S. Shaw, and C. Pierre. Component mode synthesis using nonlinear normal modes. *Nonlinear Dynamics*, 41(1-3):17–46, August 2005.

[57] P. Seshu. Substructuring and component mode synthesis. *Shock and Vibration*, 4(3):199–210, 1997.

[58] T. D. Burton and W. Rhee. On the reduction of nonlinear structural dynamics models. *Journal of Vibration and Control*, 6(4):531–556, May 2000.

[59] S. Benfratello and G. Muscolino. Mode-superposition correction method for deterministic and stochastic analysis of structural systems. *Computers and Structures*, 79(26-28):2471–2480, October 2001.

[60] M. I. McEwan, J. R. Wright, J. E. Cooper, and A. Y. T. Leung. A combined modal/finite element analysis technique for the dynamic response of a non-linear beam to harmonic excitation. *Journal of Sound and Vibration*, 243(4):601–624, June 2001.

[61] J. J. Hollkamp, R. W. Gordon, and S. M. Spottswood. Nonlinear modal models for sonic fatigue response prediction: a comparison of methods. *Journal of Sound and Vibration*, 284(3-5):1145–1163, June 2005.

[62] A. Przekop and S. A. Rizzi. Nonlinear reduced order random response analysis of structures with shallow curvature. *AIAA Journal*, 44(8):1767–1778, August 2006.

[63] A. Przekop and S. A. Rizzi. A reduced order method for predicting high cycle fatigue of nonlinear structures. *Computers and Structures*, 84(24-25):1606–1618, September 2006.

[64] A. Przekop and S. A. Rizzi. Dynamic snap-through of thin-walled structures by a reduced-order method. *AIAA Journal*, 45:2510–2519, 2007.

[65] A. A. Muravyov and S. A. Rizzi. Determination of nonlinear stiffness with application to random vibration of geometrically nonlinear structures. *Computers and Structures*, 81(15):1513–1523, July 2003.

[66] P. J. Attar and E. H. Dowell. A reduced order system id approach to the modelling of nonlinear structural behavior in aeroelasticity. *Journal of Fluids and Structures*, 21(5-7):531–542, December 2005.

[67] M. F. Platten, J. R. Wright, G. Dimitriadis, and J. E. Cooper. Identification of multi-degree of freedom non-linear systems using an extended modal space model. *Mechanical Systems and Signal Processing*, 2008. in Press.

[68] H. Sohn and K. H. Law. Extraction of ritz vectors from vibration test data. *Mechanical Systems and Signal Processing*, 15(1):213–226, January 2001.

[69] C. Chatfield and A. J. Collins. *Introduction to Multivariate Analysis*. Chapman and Hall, London, 1980.

[70] J. V. Stone. *Independent Component Analysis :A Tutorial Introduction*. MIT Press, Cambridge, 2004.

[71] R. Ghanem and F. Romeo. A wavelet-based approach for model and parameter identification of non-linear systems. *International Journal of Non-Linear Mechanics*, 36(5):835–859, July 2001.

[72] V. Lenaerts, G. Kerschen, and J. C. Golinval. Identification of a continuous structure with a geometrical non-linearity. part ii: Proper orthogonal decomposition. *Journal of Sound and Vibration*, 262(4):907–919, May 2003.

[73] H. Kanta and T. Schreiber. *Nonlinear Time Series Analysis.* Cambridge University Press, 1997.

[74] E. H. Dowell and K. C. Hall. Modeling of fluid-structure interaction. *Annual Review of Fluid Mechanics*, 33:445–490, 2001.

[75] K. Willcox and J. Peraire. Balanced model reduction via the proper orthogonal decomposition. *AIAA Journal*, 40(11):2323–2330, November 2002.

[76] S. Lall, J. E. Marsden, and S. Glavaski. A subspace approach to balanced truncation for model reduction of nonlinear control systems. *International Journal of Robust and Nonlinear Control*, 12(6):519–535, May 2002.

[77] A. H. Nayfeh, M. I. Younis, and E. M. Abdel-Rahman. Reduced-order models for mems applications. *Nonlinear Dynamics*, 41(1-3):211–236, August 2005.

[78] M. Meyer and H. G. Matthies. Efficient model reduction in non-linear dynamics using the karhunen-loeve expansion and dual-weighted-rresidual methods. *Computational Mechanics*, 31(1-2):179–191, May 2003.

[79] S. R. Idelsohn and A. Cardona. A reduction method for nonlinear structural dynamic analysis. *Computer Methods in Applied Mechanics and Engineering*, 49(3):253–279, 1985.

[80] K. Eriksson, D. Estep, P. Hansbo, and C. Johnson. *Computational Differential Equations.* Cambridge University Press, 1996.

[81] A. K. Noor. Recent advances in reduction methods for non-linear problems. *Computers and Structures*, 13(1-3):31–44, 1981.

[82] A. K. Noor. Recent advances and applications of reduction methods. *Applied Mechanics Review*, 47:125–145, 1994.

[83] K. K. Phoon, H. W. Huang, and S. T. Quek. Comparison between karhunen-loeve and wavelet expansions for simulation of gaussian processes. *Computers & Structures*, 82(13-14):985–991, May 2004.

[84] Y. C. Liang, H. P. Lee, S. P. Lim, W. Z. Lin, K. H. Lee, and C. G. Wu. Proper orthogonal decomposition and its applications - part i: Theory. *Journal of Sound and Vibration*, 252(3):527–544, May 2002.

[85] C. G. Wu, Y. C. Liang, W. Z. Lin, H. P. Lee, and S. P. Lim. A note on equivalence of proper orthogonal decomposition methods. *Journal of Sound and Vibration*, 265(5):1103–1110, August 2003.

[86] P. Holmes. *Turbulence, Coherent Structures, Dynamical Systems and Symmetry*. Cambridge University Press, 1998.

[87] P. Glosmann and E. Kreuzer. Nonlinear system analysis with karhunen-loeve transform. *Nonlinear Dynamics*, 41(1-3):111–128, August 2005.

[88] L. Sirovich. Turbulence and the dynamics of coherent structures .1. coherent structures. *Quarterly of Applied Mathematics*, 45(3):561–571, October 1987.

[89] L. Sirovich. Turbulence and the dynamics of coherent structures .2. symmetries and transformations. *Quarterly of Applied Mathematics*, 45(3):573–582, October 1987.

[90] L. Sirovich. Turbulence and the dynamics of coherent structures .3. dynamics and scaling. *Quarterly of Applied Mathematics*, 45(3):583–590, October 1987.

[91] M. Rathinam and L. R. Petzold. A new look at proper orthogonal decomposition. *SIAM Journal on Numerical Analysis*, 41(5):1893–1925, 2003.

[92] T. Lieu and C. Farhat. Adaptation of aeroelastic reduced-order models and application to an f-16 configuration. *AIAA Journal*, 45(6):1244–1257, June 2007.

[93] M. F. A. Azeez and A. F. Vakakis. Proper orthogonal decomposition (pod) of a class of vibroimpact oscillations. *Journal of Sound and Vibration*, 240(5):859–889, March 2001.

[94] B. F. Feeny and R. Kappagantu. On the physical interpretation of proper orthogonal modes in vibrations. *Journal of Sound and Vibration*, 211(4):607–616, April 1998.

[95] G. Kerschen and J. C. Golinval. Physical interpretation of the proper orthogonal modes using the singular value decomposition. *Journal of Sound and Vibration*, 249(5):849–865, January 2002.

[96] G. Kerschen, B. F. Feeny, and J. C. Golinval. On the exploitation of chaos to build reduced-order models. *Computer Methods in Applied Mechanics and Engineering*, 192(13-14):1785–1795, 2003.

[97] G. Solari, L. Carassale, and F. Tubino. Proper orthogonal decomposition in wind engineering. part 1: A state-of-the-art and some prospects. *Wind and Structures*, 10(2):153–176, March 2007.

[98] L. Carassale, G. Solari, and F. Tubino. Proper orthogonal decomposition in wind engineering. part 2: Theoretical aspects and some applications. *Wind and Structures*, 10(2):177–208, March 2007.

[99] M. A. Aschheim, E. F. Black, and I. Cuesta. Theory of principal components analysis and applications to multistory frame buildings responding to seismic excitation. *Engineering Structures*, 24(8):1091–1103, August 2002.

[100] E. Gutierrez and J. M. Zaldivar. The application of karhunen-loeve, or principal component analysis method, to study the non-linear seismic response of structures. *Earthquake Engineering and Structural Dynamics*, 29(9):1261–1286, September 2000.

[101] V. Lenaerts, G. Kerschen, and J. C. Golinval. Proper orthogonal decomposition for model updating of non-linear mechanical systems. *Mechanical Systems and Signal Processing*, 15(1):31–43, January 2001.

[102] G. Kerschen and J. C. Golinval. A model updating strategy of non-linear vibrating structures. *International Journal for Numerical Methods in Engineering*, 60(13):2147–2164, August 2004.

[103] D. Chelidze and W. L. Zhou. Smooth orthogonal decomposition-based vibration mode identification. *Journal Of Sound and Vibration*, 292(3-5):461–473, May 2006.

[104] J. P. Thomas, E. H. Dowell, and K. C. Hall. Three-dimensional transonic aeroelasticity using proper orthogonal decomposition-based reduced-order models. *Journal of Aircraft*, 40(3):544–551, May 2003.

[105] E. A. Christensen, M. Brons, and J. N. Sorensen. Evaluation of proper orthogonal decomposition-based decomposition techniques applied to parameter-dependent nonturbulent flows. *SIAM Journal on Scientific Computing*, 21(4):1419–1434, April 2000.

[106] T. C. Allison, A. K. Miller, and D. J. Inman. Free-response simulation via the proper orthogonal decomposition. *AIAA Journal*, 45(10):2538–2543, October 2007.

[107] R. Sampaio and C. Soize. Remarks on the efficiency of pod for model reductioniin non-linear dynamics of continuous elastic systems. *International Journal for Numerical Methods in Engineering*, 72(1):22–45, October 2007.

[108] M. I. Friswell and J. E. Mottershead. *Finite Element Model Updating in Structural Dynamics*. Kluwer Academic Publishers, 1995.

[109] M. Thothadri, R. A. Casas, F. C. Moon, R. D'Andrea, and C. R. Johnson. Nonlinear system identification of multi-degree-of-freedom systems. *Nonlinear Dynamics*, 32(3):307–322, May 2003.

[110] S. F. Masri and T. K. Caughey. Nonparametric identification technique for nonlinear dynamic problems. *Journal of Applied Mechanics-Transactions of the ASME*, 46(2):433–447, 1979.

[111] S. F. Masri, G. A. Bekey, H. Sassi, and T. K. Caughey. Nonparametric identification Of a class of non-linear multidegree dynamic-systems. *Earthquake Engineering and Structural Dynamics*, 10(1):1–30, 1982.

[112] M. A. Alhadid and J. R. Wright. Developments in the force-state mapping technique for non-linear systems and the extension to the location of non-linear elements in a lumped-parameter system. *Mechanical Systems and Signal Processing*, 3(3):269–290, July 1989.

[113] N. E. Sanchez and A. H. Nayfeh. Global behavior of a biased non-linear oscillator under external and parametric excitations. *Journal Of Sound and Vibration*, 207(2):137–149, October 1997.

[114] SCOSS. Standing committee on structural safety reports. Technical report, 1997, 1999, 2001, 2003.

[115] IStructE. Safety in tall buildings and other buildings with large occupancy. Technical report, Institution of Structural Engineers, London, 2002.

[116] A. Low. Designing for the consequences of hazards–an overview of the proceedings. In *IABSE Henderson Colloquium*, Cambridge, 2004.

[117] Z. Lu, Y. Yu, N. J. Woodman, and D. Blockley. A theory of structural vulnerability. *The Structural Engineer*, 77:17–24, 1999.

[118] J. Agarwal, D. Blockley, and N. Woodman. Vulnerability of 3-dimensional trusses. *Structural Safety*, 23(3):203–220, 2001.

[119] S. W. Doebling, C. R. Farrar, and M. B. Prime. A summary review of vibration-based damage identification methods. *The Shock and Vibration Digest*, 30(2):91–105, 1998.

[120] F. Lanata and A. Del Grosso. Damage detection and localization for continuous static monitoring of structures using a proper orthogonal decomposition of signals. *Smart Materials & Structures*, 15(6):1811–1829, December 2006.

[121] U. Galvanetto and G. Violaris. Numerical investigation of a new damage detection method based on proper orthogonal decomposition. *Mechanical Systems and Signal Processing*, 21(3):1346–1361, April 2007.

[122] J. Agarwal. Managing structural risks. In G.I. Augusti, G. Schueller and M. Ciampoli, editors, *Proceedings of ICOSSAR*, 2005.

[123] X. Wu. *Vulnerability Analysis of Structural Systems*. PhD thesis, University of Bristol, 1991.

[124] Y. Yu. *Analysis of Structural Vulnerability.* PhD thesis, University of Bristol, 1997.

[125] J. C. England. *Structural Vulnerability and Hazard Potential.* PhD thesis, University of Bristol, 2005.

[126] Z. Lu. *Structural Vulnerability Analysis.* PhD thesis, University of Bristol, 1998.

[127] J. Agarwal and G. N. Liu. Vulnerability and integrity of structural systems. In J. Kanda, T. Takada, and H. Furuta, editors, *Applications of Statistics and Probability in Civil Engineering, Proceedings of ICASP 10.* Taylor & Francis, July 2007.

[128] O. S. Salawu. Detection of structural damage through changes in frequency: a review. *Engineering Structures*, 19(9):718–723, September 1997.

[129] C. R. Farrar and S. W. Doebling. An overview of modal-based damage identification methods. In *EUROMECH 365 International Workshop: DAMAS 97, Structural Damage Assessment Using Advanced Signal Processing Procedures*, Sheffield, U.K., 1997.

[130] J. T. Kim, Y. S. Ryu, H. M. Cho, and N. Stubbs. Damage identification in beam-type structures: frequency-based method vs mode-shape-based method. *Engineering Structures*, 25(1):57–67, January 2003.

[131] C. Sansour, J. Sansour, and P. Wriggers. A finite element approach to the chaotic motion of geometrically exact rods undergoing in-plane deformations. *Nonlinear Dynamics*, 11(2):189–212, October 1996.

[132] R. Fotouhi. Dynamic analysis of very flexible beams. *Journal of Sound and Vibration*, 305(3):521–533, August 2007.

[133] ANSYS Inc. *ANSYS Release 10 Manual.* 2007.

[134] C. M. Richards and R. Singh. Feasibility of identifying non-linear vibratory systems consisting of unknown polynomial forms. *Journal of Sound and Vibration*, 220(3):413–450, February 1999.

[135] Y. Shi and C. Mei. A finite element time domain modal formulation for large amplitude free vibrations of beams and plates. *Journal Of Sound and Vibration*, 193(2):453–464, June 1996.

[136] Mathworks Inc. *MATLAB Release 7 Manual*. 2005.

[137] C. M. Yuan and B. F. Feeny. Parametric identification of chaotic systems. *Journal of Vibration and Control*, 4(4):405–426, July 1998.

[138] Y Liang and B.F. Feeny. Parametric identification of chaotic systems via a long-period harmonic balance. pages 1339 – 1345, Long Beach, CA, United States, 2005.

[139] M. A. Trindade, C. Wolter, and R. Sampaio. Karhunen-loeve decomposition of coupled axial/bending vibrations of beams subject to impacts. *Journal of Sound and Vibration*, 279(3-5):1015–1036, January 2005.

[140] K. Worden. Data-processing and experiment design for the restoring force surface method .1. integration and differentiation of measured time data. *Mechanical Systems And Signal Processing*, 4(4):295–319, July 1990.

[141] M. Couplet, C. Basdevant, and P. Sagaut. Calibrated reduced-order pod-galerkin system for fluid flow modelling. *Journal of Computational Physics*, 207(1):192–220, July 2005.

[142] Q. B. He, F. R. Kong, and R. Q. Yan. Subspace-based gearbox condition monitoring by kernel principal component analysis. *Mechanical Systems and Signal Processing*, 21(4):1755–1772, May 2007.

[143] M. Khalil, S. Adhikari, and A. Sarkar. Linear system identification using proper orthogonal decomposition. *Mechanical Systems and Signal Processing*, 21(8):3123 – 3145, 2007.

[144] R. C. Maple, P. I. King, P. D. Orkwis, and J. M. Wolff. Adaptive harmonic balance method for nonlinear time-periodic flows. *Journal of Computational Physics*, 193(2):620–641, January 2004.

[145] C. Homescu, L. R. Petzold, and R. Serban. Error estimation for reduced-order models of dynamical systems. *SIAM Review*, 49(2):277–299, June 2007.